MASTER

The virtual engine
design of a dynamic automotive transmission test rig

Scheepers, B.T.M.

Award date:
2003

Technische Universiteit Eindhoven, The Netherlands

The Virtual Engine

Design of a dynamic automotive transmission test rig

ing. B.T.M. Scheepers

Reportnumber: DCT-2003/26

Committee:
Prof. Ir. N.J.J. Liebrand (supervisor)
Dr. Ir. W.J.A.E.M. Post (coach)
Prof. dr. ir. J.J. Kok
Dr. ir. L.M.T. Somers

Technische Universiteit Eindhoven
Department of Mechanical Engineering
Section Control Systems Technology, Dr. Hub van Doorne Chair
P.O. Box 513
5600 MB, Eindhoven
The Netherlands

Eindhoven, May 12, 2003

Preface

During the last period of my study Mechanical Engineering at the Technische Universiteit Eindhoven, I have specialized myself in Automotive Engineering Science. This report is the result of the graduation project. Together with a presentation, the report is the closure of the graduation project and the study.

During the project I had the possibility to use the knowledge and experience of several people. I would like to use this opportunity to thank them. At first professor N. Liebrand for supervising and dr. ir. W. Post for coaching me during the graduation project. Furthermore Mr. J. de Vries and Mr. R. van den Bogaert for helping me realizing the prototype test rig. Finally, I would like to thank my colleague students for the inspiring three o'clock coffee conversations.

Summary

The increased demands for comfort and reliability in modern vehicles require well-developed solutions. The characteristics of the vehicle powertrain are a major criterium in this regard. It is important that the entire powertrain is designed optimally with respect to durability, dynamics, vibrations and acoustics under the most extreme conditions. To be sure the designed transmission satisfies the demands, testing complete transmissions and transmission parts is necessary. More and more durability tests are being performed on test rigs instead of testing in prototype vehicles. The development time decreases and testing can be done at lower costs. For creating reliable test results the test rig has to load the transmission in the same way the vehicle does. The motor part of the test rig has to simulate the behaviour of the combustion engine. The torque generated by the combustion engines is not constant. The torque is dynamic due to the intermittent combustion and accelerating / decelerating of the reciprocating parts. In the ideal situation, the motor part of the test rig is able to simulate a wide range of combustion engines. The motor part represents a virtual engine. Because electric motors and combustion engines aren't suitable for driving such test rigs, a prototype test rig driven by a hydraulic motor has been developed, build and tested. The specifications of the test rig were based on the properties of a VW Bora equipped with a 1.6L 4 cylinder 4-stroke petrol combustion engine. The emphasis of the design was put on simulating the dynamic engine torque. If the combustion engine is operated at a speed of 6000 $[rpm]$, the frequency of the dynamic torque will be 200 $[Hz]$.

The oil pressure in the supply pipe to the hydraulic motor is related to the motor torque. Dynamic torque is generated by dynamic pressure. A proportional directional control valve is mounted in a parallel branche to the hydraulic motor. If the valve opens, an amount of oil leaves the main flow and the pressure and consequently the torque will decrease. If the valve closes again, the pressure and torque will increase. A model has been developed for predicting the transfer function H_{mh} of the mechanical and hydraulic system (input = valve spool position, output = dynamic torque difference). The results of the simulation indicated that the designed configuration wouldn't be able to generate the desired torque amplitudes. Though, the rig has been build for investigating the dynamic hydraulic system. The designed rig consists of a mechanical, hydraulic and data acquisition / control part.

The motor torque generated with a non activated valve was not not constant. A torque ripple is caused by the 11 pistons in the motor. The torque ripple also results in vibrating of the mechanical part in its eigenfrequency. Unfortunately, the torque amplitude at the eigenfrequency is much larger than the dynamic torque that can be generated by the valve.

The measured transfer function of the proportional directional controlled valve (input = desired spool position, output = actual spool position) doesn't completely correspond to the transfer function presented by the manufacturer. The measured transfer function H_{mh} corresponds quite well to the calculated transfer function. As predicted, the realized prototype test rig is not able to generate the desired torque amplitudes.

The prototype can be improved in several ways. Tuning the hydraulic system is one of the possibilities. If the length of the supply pipe is variable, the frequency corresponding to the maximum impedance (maximum stiffness) of the hydraulic system can be changed. If the valve spool frequency equals this frequency, the generated torque amplitude is maximum.

Because simulating dynamic combustion engine torque is a topical subject, different companies and a university are studying this subject as well. All realized configurations are based on a different principle. The developers all claim that the rigs are able to generate the desired dynamic torque. Unfortunately no bode plots are present, so it's unknown what magnitudes of torque can be reached at specific frequencies.

Samenvatting

De toegenomen eisen voor comfort en betrouwbaarheid van moderne voertuigen vereist vergaande ontwikkelingen. De karakteristieken van de transmissie zijn wat dit betreft een belangrijk criterium. Het is belangrijk dat de hele transmissie optimaal ontworpen wordt betreffende duurzaamheid, dynamica, trillingen en geluidsproductie onder de meest extreme omstandigheden. Het is nodig de hele transmissie en delen ervan te testen om er zeker van te zijn dat de transmissie aan de gestelde eisen voldoet. Steeds meer duurzaamheidtesten worden uitgevoerd op testopstellingen in plaats van het testen in prototype voertuigen. De ontwikkelingstijd wordt korter en het testen wordt goedkoper. Noodzakelijk voor het creeren van betrouwbare testresultaten is een testopstelling die transmissie op dezelfde manier belasten als het voertuig doet. Het aandrijfgedeelte van de testopstelling moet het gedrag van de verbrandingsmotor simuleren. Een eigenschap van verbrandingsmotoren is de rimpeling van het gegenereerde koppel. Dit wordt veroorzaakt door de periodieke verbrandingen en het versnellen en vertragen van de op en neer gaande onderdelen. In de ideale situatie is het aandrijfgedeelte van de testopstelling in staat een reeks verbrandingsmotoren te simuleren. Het aandrijfgedeelte is een virtuele verbrandingsmotor. Omdat elektromotoren en verbrandingsmotoren niet geschikt zijn voor het aandrijven van zo'n testopstelling is een prototype testopstelling, aangedreven door een hydromotor, ontworpen, gebouwd en getest. De specificaties van de opstelling zijn gebaseerd op de eigenschappen van een VW Bora uitgerust met een 1,6L 4 cilinder 4-takt benzine verbrandingsmotor. De nadruk van het ontwerp is gelegd op het simuleren van het dynamisch motor koppel. Als de verbrandingsmotor met 6000 $[omw/min]$ draait is de frequentie van het dynamisch koppel 200 $[Hz]$.

De oliedruk in de aanvoerpijp naar de hydromotor is gerelateerd aan het motorkoppel. Dynamisch koppel wordt gegenereerd door dynamische druk. Een proportionele regelklep is gemonteerd in tak parallel aan de motor. Als de klep opent verlaat een hoeveelheid olie de hoofdstroom zodat de druk en het koppel dalen. Als de klep weer sluit zullen de druk en het koppel weer stijgen. Een model is ontwikkeld om de overdrachtsfunctie $[H_{mh}]$ van het mechanisch en hydraulisch systeem (input is de klep positie, output is het dynamische koppel verschil) te voorspellen. De resultaten van het model gaven aan dat het ontwerp niet de gewenste koppelamplitudes zou kunnen genereren. Desondanks is de opstelling gebouwd om het dynamisch hydraulisch systeem te kunnen onderzoeken. De opstelling bestaat uit een mechanisch, hydraulisch en data-acquisitie / regelsysteem.

Het gegenereerde koppel is niet constant als de klep gesloten is. Een koppelrimpel wordt veroorzaakt door de 11 zuigers in de motor. De koppelrimpel zorgt ervoor dat het mechanisch systeem in zijn eigenfrequentie begint te trillen. Helaas is de koppel amplitude veroorzaakt door de eigenfrequentie groter dan het dynamisch koppel gegenereerd door de klep.

De gemeten overdrachtsfunctie van de proportionele klep (input is gewenste klepstand, output is de werkelijke klepstand) komt niet geheel overeen met de overdrachtsfunctie zoals de leverancier die geeft. De gemeten H_{mh} komt goed overeen met de met het model berekende overdracht. Zoals voorspeld is het prototype niet in staat de gewenste koppel amplitudes te genereren.

Het prototype kan op verschillende manieren verbeterd worden. Tuning is een van de mogelijkheden. Als de lengte van de aanvoerbuis variabel wordt gemaakt kan de frequentie waarbij de impedantie van het hydraulisch systeem maximaal is (maximale stijfheid) veranderd worden. Als de frequentie van de klep overeenkomt met deze frequentie is de gegenereerde koppelamplitude maximaal.

Omdat het simuleren van het dynamisch koppelverloop van verbrandingsmotoren een actueel onderwerp is onderzoeken verschillende bedrijven en een universiteit dit onderwerp ook. Alle gerealiseerde opstellingen zijn gebaseerd op een ander principe. De ontwerpers claimen dat hun opstelling in staat is de gewenste koppel amplitudes genereren. Helaas zijn er geen Bode plaatjes voorhanden zodat het onbekend is welke koppelamplitudes bij bepaalde frequenties gehaald kunnen worden.

Contents

Chapter 1

Introduction

The increased demands for comfort and reliability in modern vehicles require well-developed solutions. The characteristics of the vehicle powertrain are a major criterium in this regard. It is important that the entire powertrain is designed optimally with respect to durability, dynamics, vibrations and acoustics under extreme conditions. Components such as the clutch, the torque converter and the differential gear must be able to withstand high dynamic loads over the entire life cycle. To be sure the designed transmission satisfies the demands, testing is necessary. During the development of the transmission, different tests are performed:

Component testing: Component testing is carried out at the early stage of the transmission development on a test rig. Individual subsystems (with their specific function) or parts are tested. These tests are kept as simple as possible for determining functional information about the components. Also durability tests can be performed. Influences from the environment, like when the component is part of a large system, are excluded.

Testing complete transmissions: During these tests on a rig, the engineer investigates the cooperation of the individual subsystems and parts. Properties like temperature behaviour, efficiency, vibration and noise emission are investigated. Durability tests are also part of test rig tests.

Vehicle testing: During the last part of the testing and development phase the transmission is mounted in a vehicle so real life situations can be investigated. The performance and reliability of the transmission is determined under various conditions.

Nowadays, the development of vehicles (and also transmissions) has to satisfy some contradictory demands:

- Development times have to decrease.
- Development costs have to decrease.
- The product has to be better.

For decreasing development time, different vehicle parts (e.g. engine, suspension, transmission) are developed at the same time. Development costs will decrease if the number of prototypes vehicles and the total test period are to be decreased. Major changes shouldn't have to be made during the vehicle test stage of the development. This is possible if the behaviour, performance and the cooperation of the individual parts and subsystems are conform the design criteria.

For transmissions more and more durability tests are performed on a test rig instead of testing the transmission in a prototype vehicle on a track or on public roads. To be able to predict the behaviour of the mounted transmission, the preceding tests have to be realistic. During the tests the transmission has to be loaded similar to the vehicle tests. Substituting the vehicle test into a dynamic test rig tests is called as: "Road to Rig" [1]. The road to rig principle can be applied to component tests (testing subsystems like the CVT variator) and the complete transmission tests. The load on the transmission depends on several factors. All of these factors have to be taken into account when performing "Road to Rig" tests. The factors are:

Engine: The engine causes loads acting on the transmission by enforcing torque. The heat generated by the engine can influence the transmission performance.

Driver: The driver influence can be divided into two phases: a shifting phase and a non shifting phase. When shifting, the driver loads the transmission by operating the clutch (torque variations on the transmission due to clutching and declutching behaviour), throttle and gearlever (shift forces). During non shifting phase the driver influences the transmission load by the way of operating the throttle and brake.

Vehicle: Transmission load depends on the drive train concept (front / rear wheel driven), vehicle class and payload.

Environment: Driving in mountainous environments (use of gear 1-3) causes different wear than driving on motorways (high speeds, use of the overdrive). On slippery roads the transmission is loaded in a different way than when driving on smooth roads. Imagine the transmission load when the wheels suddenly reach traction after slipping.

The drive motor is one of the most important parts of the rig. It has to load the transmission and simulate the vehicle engine as realistically as possible. At first sight, using a combustion engine seems to be the easiest way of powering a test rig. The advantages and disadvantages of this approach are:

\+ **Exact copy of reality:** If the combustion engine used on the test rig is identical to the engine mounted in the vehicle, the load on the transmission caused by the engine is realistic. The tests performed on the rig may give the same results as the tests performed during a vehicle test. This test is very reliable.

\- **Expensive:** The corresponding engine has to be mounted for every transmission tested on the rig. This requires a lot of effort due to the necessary cooling, exhaust pipes, fuel supply, connection to the operating room etc. That's why most times only a single engine is used for testing a range of transmissions.

\- **Engine not always available:** Because of parallel development of vehicle components, it may happen that the transmission has to be tested while the engine is not yet available.

\- **Safety:** When running 24 hours a day, safety provisions with regard to fuel supply are required.

Because of the disadvantages of the combustion engine, nowadays most test rigs are equipped with an electric motor for driving the transmission. The advantages and disadvantages of an electric motor used as power supplier are discussed below.

+ **Simulating of all combustion engines may be possible:** The electric motor is able to simulate the engine map (torque and motor speed).

+ **Easy to control:** By using frequency converters it is easy to control the electric motor concerning speed and torque.

+ **Energy recovery:** Recovering brake energy is possible when the brake is an electric generator. The electric motor converts electrical energy in rotational mechanical energy, the brake reverses the conversion. The electric brake power can be presented to the motor by using frequency converters. Only the power losses have to be compensated.

+ **Reliable:** An electric motor is very reliable. Only few maintenance is necessary.

- **Not an exact copy of the reality:** This is the only disadvantage of using an electric motor. There is a major difference between the combustion engine (reality) and the electric motor concerning the torque-inertia ratio (abbr.: TI-ratio). The TI-ratio of the engine is much smaller than the TI-ratio of a comparable electric AC motor. Figure 1.1 shows the engine map of an 1.6 $[L]$ combustion engine and an 81 $[kW]$ electric motor. The inertia of the combustion engine is 0.1 $[kgm^2]$. At a rotational speed of 3500 $[rpm]$, the torque is at its maximum: 155 $[Nm]$ so the TI-ratio equals 1550 $[rad/s^2]$. At that speed, the e-motor torque is 225 $[Nm]$. Because the inertia of this motor is 0.5 $[kgm^2]$, the TI-ratio equals 450 $[rad/s^2]$.

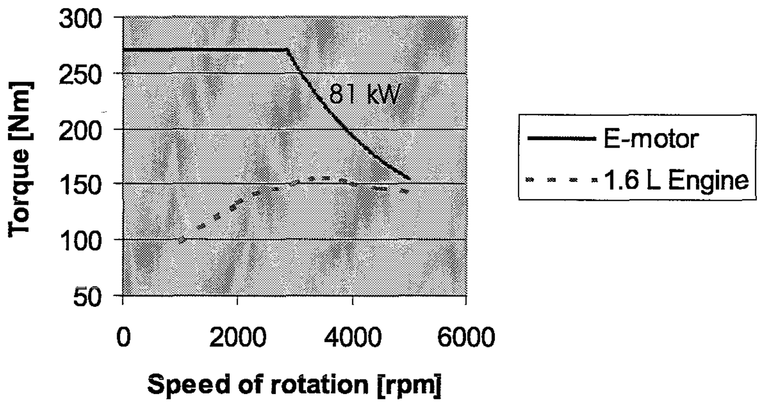

Figure 1.1: Engine map of an electric AC motor and a 1.6 $[L]$ combustion engine.

When running at constant speed, the electric motor can be used for simulating the engine because at all speeds the e-motor can generate more torque than the combustion engine. Some problems may occur when performing dynamic tests:

- **Accelerating:** For simulating an acceleration of the engine (e.g. kick down), the e-motor can not deliver enough torque for accelerating the inertia like the engine.

- **Torque behaviour:** Due to the intermittent combustion and the acceleration and deceleration of the reciprocating parts (e.g. pistons), the combustion engine doesn't generate a constant torque. The torque ripple may cause damage to the transmission parts. Figure 1.2 shows the torque generated by a 3 cylinder diesel engine. The dotted line indicates the mean torque. The torque is measured at the crank shaft. Because of the high rotor inertia, the electric motor is not able to simulate these highly dynamic torques.

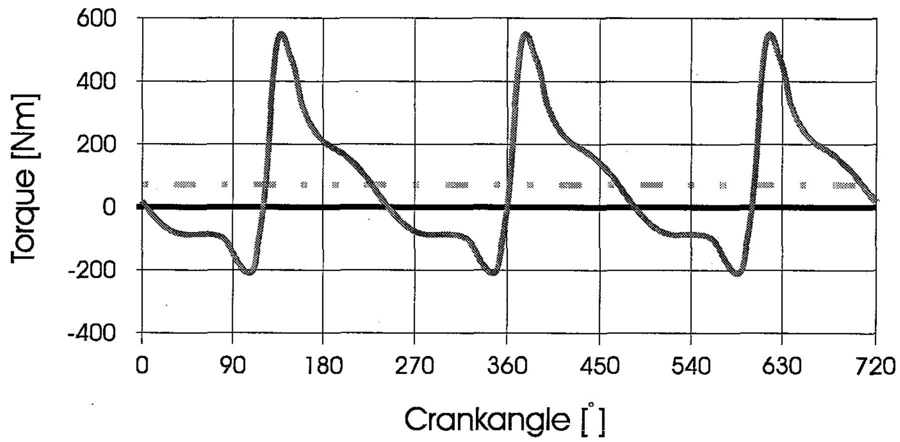

Figure 1.2: Torque generated by a 3 cylinder diesel engine at 2100 [rpm] and at 50% of full load.

The application of the combustion engine as well as the electric motor have disadvantages. Both are not suitable for loading a "Road to Rig" transmission test rig. Another solution has to be found for such dynamic application. A virtual engine has to be developed that is able to simulate a wide range of combustion engines. Applying a hydraulic motor might possible because of the favourable TI-ratio (up to 28600 [rad/s^2]). During this graduation project, the suitability of the use of a hydraulic motor for simulating combustion engines has been investigated. The introduction may be summarized by:

Problem definition: Electric motors and combustion engines aren't suitable for driving a "Road to Rig" transmission test rig.

Aim of the project: Investigate the suitability of a hydraulic motor for simulating combustion engines so the motor can be used as dynamic virtual engine for driving "Road to Rig" transmission test rigs.

For investigating the suitability, a prototype test rig has been developed. The emphasis was put on simulating the dynamic engine torque because developing a complete transmission test rig is not possible in the available time. The project target was investigating the dynamic performances of a hydraulic motor. That's why a prototype rig has been developed with parts available at Fluid Power Laboratory of the TU/e. The rig design has been based on the specifications of a VW Bora because a lot of information of this vehicle is available at the university. The vehicle has been examined accurately during the ZI-project at the TU/e [4] [6]. Another reason for choosing this car is the engine map. The hydraulic motors available at the Fluid Power Laboratory of the TU/e are able to generate enough power for simulating the Bora engine.

This report describes the following subjects. At first, the specifications of the rig (based on the VW Bora properties) are determined. A Matlab model has been developed for calculating the dynamic torque on the transmission in all working conditions. Chapter 3 describes the design of the rig. The chosen mechanical, hydraulic and control system are explained. The rig has been build and was tested. The test results can be found in chapter 4. Chapter 5 discusses the possibilities of increasing the performance of the test rig. In chapter 6, other dynamic test rigs that should to be able to simulate the dynamic engine torque are described. Finally, some conclusions and recommendations are expressed in chapter 7.

Chapter 2

Specifications of the test rig

Before developing a new transmission test rig, the demands to satisfy have to be known. For performing "Road to Rig" tests, the rig has to load the transmission in exactly the same way the vehicle does. The engine and vehicle load the transmission in a dynamic way. The project focusses on simulating the dynamic torque behaviour of the combustion engine. That's why the specifications will be only functional. Other demands like dimensions and user interface are not taken into account.
When specifying the rig, the properties of a VW Bora, equipped with a 1.6 $[L]$ petrol engine and CVT transmission are taken as the starting point. Because "Road to Rig" tests can be performed on the complete transmission and on the variator part (component testing), some parameters have to be specified twice. The specifications are split up into static and dynamic parts.

Static properties: The static properties of the rig are prescribed by the engine map and vehicle properties. The drive unit has to be able to generate the torques and rotational speeds the engine does. Figure 2.1 shows the engine map of the Bora. The brake unit has to load the transmission and to simulate the vehicle inertia.

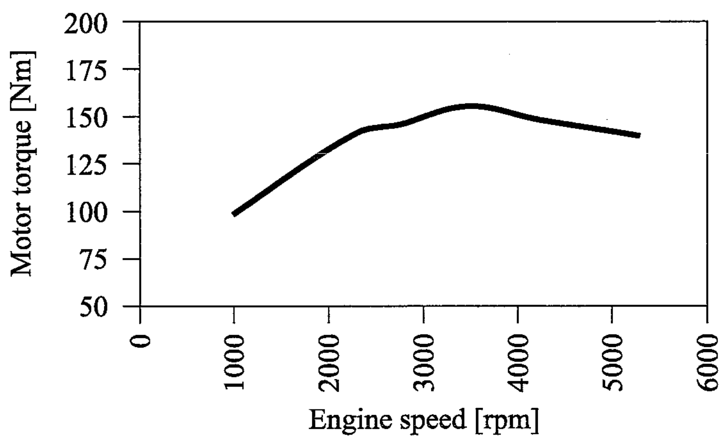

Figure 2.1: Engine map of the 1.6 $[L]$ 4 stroke VW Bora petrol engine

Because of the absence of a final reduction, the specifications of the variator brake unit differ from the brake unit applied when a complete transmissions has to be tested.

drive unit

Power:	max.	75	$[kW]$
Speed of rotation:	min.	1000	$[rpm]$
	max.	6000	$[rpm]$
Torque:	max.	155	$[Nm]$
Inertia		0.1	$[kgm^2]$

brake unit variator

Brakepower:	min.	75	$[kW]$
Speed of rotation:	min.	416	$[rpm]$
	max.	7992	$[rpm]$
Braking torque:	max.	368	$[Nm]$
Inertia		6	$[kgm^2]$

brake unit complete transmission

Brakepower:	min.	75	$[kW]$
Speed of rotation:	min.	88	$[rpm]$
	max.	1700	$[rpm]$
Braking torque:	max.	1730	$[Nm]$
Inertia		132	$[kgm^2]$

Dynamic properties: The dynamic properties concern the dynamic engine torque. The torque acting on the crank shaft T_e is generated by gas pressure in the cylinder T_p and the acceleration and deceleration of the reciprocating parts T_i. The resultant torque on the crankshaft T_e is calculated by adding T_p and T_i.

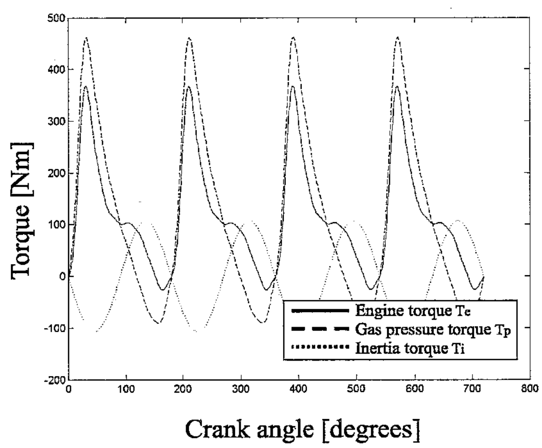

Figure 2.2: Dynamic torque acting on the crankshaft. $T_e = T_p + T_i$

Figure 2.2 shows the torques acting on the crankshaft at 2500 $[rpm]$ and 115 $[Nm]$. It is difficult to specify the demands concerning the dynamic torque because the dynamic torque behaviour is different in all working conditions.

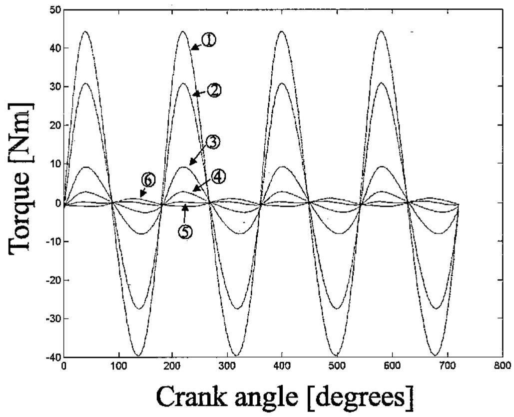

Figure 2.3: Dynamic torque acting on the transmission at several speeds and maximum torque

The dynamic torque depends on several variables. A Matlab program has been developed for calculating the torque acting on the transmission and variator in all possible working conditions (engine speed, engine torque, transmission ratio etc.). Appendix A details the calculation method. The specifications have to be based on the most demanding situations for the rig (high torque amplitudes and high frequencies). These situations occur if the CVT ratio is maximum (overdrive = 2.15) and the nominal engine torque is at its maximum. Figure 2.3 shows the calculated dynamic part of the engine torque acting on the transmission at several speeds and maximum torque. Only the dynamic part is shown, the nominal torque is omitted. The operating conditions can be found in table 2.1.

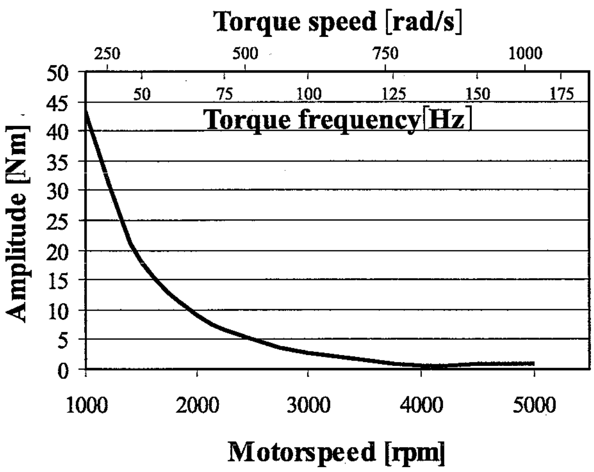

Figure 2.4: Dynamic torque amplitudes.

Figure 2.4 shows the dynamic torque amplitude depending on the engine speed (the corresponding torque frequency and speed are shown as well). The torque frequency is twice the engine frequency. Because the maximum engine speed is 6000 $[rpm]$, the maximum torque frequency is 200 $[Hz]$. Figure 2.4 is the starting point for designing the dynamic transmission test rig. The hydraulic motor has to be able to generate these torque amplitudes at corresponding frequencies.

Number	*Speed* $[rpm]$	*Nominal Torque* $[Nm]$	*Torque frequency* $[Hz]$	*Torque amplitude* $[Nm]$
1	1000	100	33	44
2	1194	115	40	31
3	2000	135	67	9
4	3000	150	100	2.8
5	4000	150	133	0.6
6	5000	145	167	1

Table 2.1: Operating conditions of figure 2.3 and 2.4.

Chapter 3

Design of the prototype test rig

The test rig can be developed now the specifications are known. This chapter describes the development of the mechanical, hydraulic and data acquisition / control system. As announced in the introduction, the emphasis of the design is put on simulating the fluctuating torque generated by the engine. A prototype rig will be designed for researching the feasibility of a hydraulically driven transmission test rig. Omitting the transmission won't change the rig performance but makes the rig much more uncomplicated. That's why no transmission is mounted in the prototype rig. The parts are chosen and dimensioned according to the specs of the VW Bora. Only parts available in the Fluid Power Laboratory of the TU/e are used.

3.1 Mechanical part

The motor part represents the combustion engine (torque / inertia). The brake part of the rig has to simulate the vehicle (vehicle inertia and load). In this section the chosen motor and brake part are discussed.

3.1.1 Engine simulation

The output shaft of the hydraulic motor part drives the transmission. Different motor configurations may be possible. In case of a single hydraulic motor, the motor has to generate the combined nominal and dynamic torque. In case of multiple motors, the functions of generating torque can be split. The first motor generates the nominal torque, the second one adds the dynamic torque part.

Combining multiple motors needs special attention. Several configurations are possible, see figure 3.1. In all configurations in the figure the left motor generates the nominal torque and the right motor the dynamic torque. Just connecting all motors to a rigid shaft won't satisfy (picture A). The added torque fluctuations would not reach the transmission due to the high total inertia. The inertia's have to be uncoupled. There are several ways to do this.

Spring: By mounting a torsional spring between the two motors, the inertia's are uncoupled. Both motors rotate at almost the same speed and support on the fixed world. The first motor generates the nominal torque, the second the dynamic torque fluctuations (picture B).

Planetary gear set: A planetary gear set has three shafts. When connecting both motors and the transmission to a separate shaft, the inertia's are split. Both motors support on the fixed world. The first motor rotates and generates the nominal torque. The second motor only has to rotate over a small angle, just enough to compensate the angle caused by the dynamic torque. Unlike the previous solution, the second motor has to withstand a part of the nominal torque continuously due to the planetary gear set construction (picture C).

Special motor: The first motor supports the generated torque on the fixed world. If the second motor supports the torque on the shaft of the first motor, the inertia's are uncoupled. The first motor rotates at constant speed and generates the nominal torque. The complete second motor rotates at the same speed the first motor does. Again, the angle of rotation between the input and output shaft of the second motor may be very small. The second motor has to withstand the nominal torque continuously (picture D).

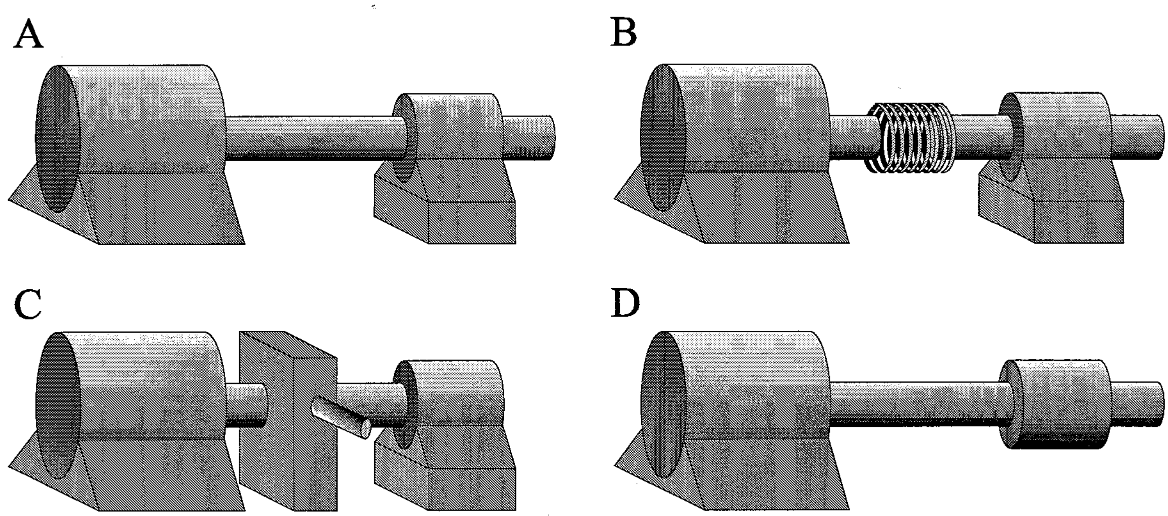

Figure 3.1: Different ways to connect two motors. A: rigid, B: spring, C: planetary set, D: special motor

Using multiple motors is complex but practicable. Unfortunately, an actuator as applied in configuration C and D of figure 3.1 is not present in the fluid power laboratory. Because of the complexity of using multiple motors, only one hydraulic motor will drive the prototype test rig. Also with this configuration, researching the feasibility of hydraulically driven dynamic test rig is possible. If the results are positive, designing a rig with multiple motors can be done in a later stadium. More specific information about the chosen hydraulic motor can be found in section 3.2.2.

3.1.2 Vehicle simulation

The brake part has to simulate the vehicle. This comes down to simulating the load (air drag, climbing resistance etc.) and vehicle inertia. The load is applied by a hydraulic pump that converts the rotating mechanical energy in hydraulic energy. In section 3.2.2 more info concerning the chosen hydraulic pump can be found.

The vehicle inertia is composed of rotating wheels and a translating vehicle and will be simulated by a flywheel on the brake shaft. The flywheel keeps the speed almost constant in case of dynamic motor torque. Because no transmission is applied, the flywheel speed equals the motor speed. The flywheel inertia has to be adapted to this situation and has to become 5.97 $[kgm^2]$. It equals the inertia of the flywheel in case of testing the CVT variator as subsystem (chapter 2). The inertia of the only suitable flywheel is 2.3 $[kgm^2]$. In this situation (focussing on the torque fluctuations) the inertia satisfies. The speed will stay almost constant. When braking on the engine has to be simulated, the inertia of this flywheel is too low.

3.1.3 Complete mechanical layout

Finally, the mechanical part of the test rig consists of a hydraulic motor, flywheel and hydraulic brake (figure 3.2 shows the final mechanical layout). For measuring the generated motor torque, a torque transducer in mounted between the motor and the flywheel. The rig simulates the vehicle the most if the connection between the transmission and the flywheel is established by the original drive shafts. If a variator is tested, there is no final gear and the shaft stiffness has to become 280 $[Nm/rad]$. In the final layout, all shafts are relatively stiff. The torque transducer is the most flexible part.

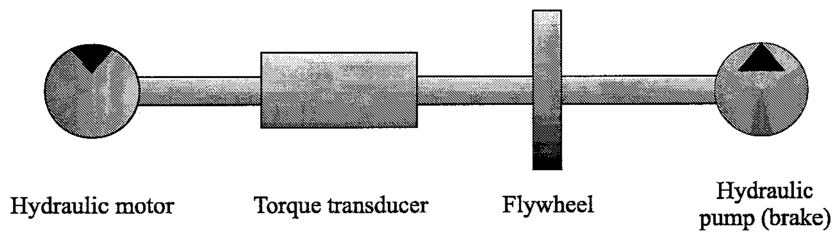

Figure 3.2: Schematic representation of the final mechanical layout

3.2 Hydraulic part

The hydraulic part of the test rig is discussed in this section. At first, different configurations that might satisfy the demands are presented. The best option is chosen and all parts of the rig are discussed. Finally, the properties of the rig are predicted by a developed Matlab Simulink model. An introduction in fluid power can be found in appendix B.

3.2.1 Possible hydraulic configurations

In this subsection three different hydraulic system configurations are discussed that might be able to generate the desired dynamic torque. Also for the hydraulic part, only parts available in the Fluid Power Laboratory of the TU/e can be used. Figure 3.3 shows three possible hydraulic configurations. The pump and motor part are identical in all situations. In the hydraulic motor, oil pressure is converted into motor torque. The oil flow determines the motor speed. The desired dynamic torque has to be generated by fluctuating the oil pressure by the conductive part. Modulation of the oil pressure as fast (frequency) and as much (amplitude) as possible is the goal of the design.

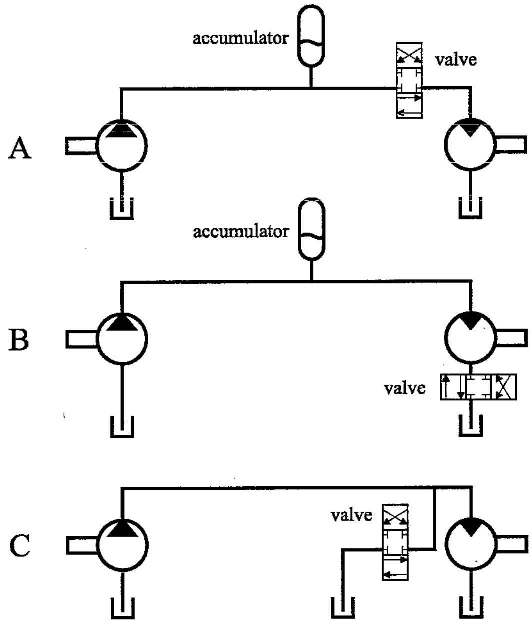

Figure 3.3: Possible hydraulic configurations

The parts used:

Throttle valve: In these situations, the valve is used to control a flow rate. The valve acts like a variable hydraulic resistance. The flow through the valve depends on the pressure difference over the valve and the resistance of the passageways. The resistance depends on the flow area that can be changed by means of a solenoid. More about the applied valve in the next section.

Accumulator: The hydraulic accumulator is a device for storing energy in the form of hydraulic fluid under pressure. Most time the accumulator comprises of a steel bottle containing a flexible bag charged with nitrogen. If the pressure rises, the oil flows in the accumulator. Pressure decrease causes the gas to expand forcing the fluid back out into the circuit.

Description of the hydraulic configurations of figure 3.3:

Configuration A: In this design, the valve is mounted in the main flow close to the motor. If the valve closes, the flow through the valve decreases. Because of the flywheel, the motor speed, and so the flow through the motor stays constant. As a result, the pressure in the pipe before the motor decreases. Due to the decreased pressure, the motor torque drops as well. If the valve opens again, the flow and pressure increase. The accumulator assures almost constant pressure in the pipe between the pump and valve.

Configuration B: Like configuration A, also in this design the valve is placed in series with the main oil flow. The only difference is the position of the valve. The valve is mounted on the discharge side, instead of the pressure side of the pipe. Closing the valve results in a pressure rise at the discharge side. The pressure difference between the pressure and discharge side of the motor decreases, consequently the motor torque will drop.

Configuration C: In this case, the valve is placed in a parallel branch. If the valve opens, an amount of oil will leave the main flow. The oil will expand and the pressure will drop. When the valves closes again, the oil is compressed and the pressure will increase. In contrast to configuration A and B, the hydraulic system should be as stiff as possible. If an amount of oil leaves the main flow, the pressure should drop as much as possible. That's why no accumulator is mounted.

All configurations may satisfy the demands. Which one will be the best suited? Each layout has advantages and disadvantages. If the flow through the valve in layout A remains low for a too long period, the pressure decreases too much. Due to the energy stored in the flywheel, the motor starts acting like a pump. The pressure decreases even more. The system becomes uncontrollable. Due to the low pressure, cavitation may arise in the motor. This can never take place in layout B. The main disadvantage of layout A and B is the position of the valve in the main flow. The valve has to be large sized. The larger the valve, the slower the response will become. A smaller valve satisfies for configuration C. Only small valves are available in the Fluid Power Lab. It seemed that configuration C is the best for the purpose. That's why this layout is taken as a basis for the further hydraulic design.

3.2.2 Complete hydraulic layout

Now the basic layout has been chosen, the individual parts have to be sized. The demands specified in the previous chapter have to be taken into account. Figure 3.4 shows the complete layout of the hydraulic system. The torque transducer and flywheel will be mounted between drive motor F10-39 and brake pump F11-58 as described in the previous subsection. Specification of the chosen parts:

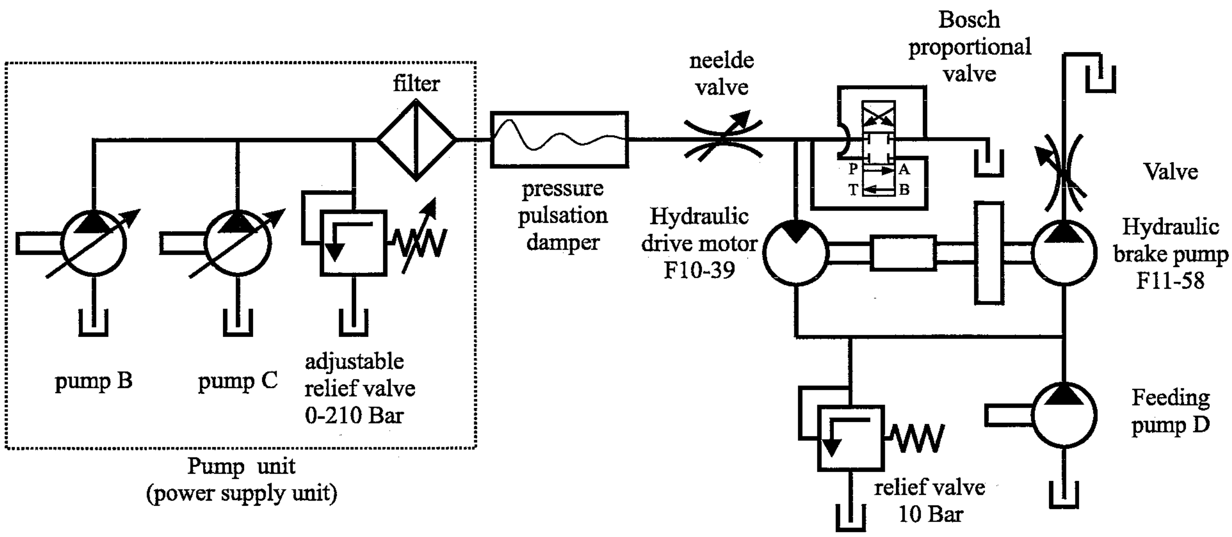

Figure 3.4: Complete hydraulic layout

Hydraulic motor / pump unit combination: The performance of the drive motor (F10-39) depends on the motor itself and the pump unit that supplies the oil flow. Appendix C shows available hydraulic motors and pumps in the fluid power laboratory. The motors and pumps are fixed displacement machines. The maximum power of the Bora engine that has to be simulated is 75 $[KW]$. Pump B and C supply the power for the hydraulic motor. The pumps are similar and generate 31.5 $[KW]$ (90 $[L/min]$ at 210 $[Bar]$). A valve combines both flows. The maximum pressure remains 210 $[Bar]$, the flow is doubled. The resulting pump power (63 $[KW]$) still doesn't correspond to the engine power (75 $[KW]$) but is high enough to test the system. Now an appropriate motor has to be selected. The mechanical working conditions of the hydraulic motor have to correspond to the engine map of the Bora engine. Figure 3.5 shows the working conditions of the available hydraulic motors supplied by the combined flow of pumps B + C. The engine map of the Bora is plotted as well. The last part of the hydraulic motor number code corresponds to the displacement in $[cm^3/rev]$. Operating motor models F11-10, F11-19 and F11-39 in the light gray area (high motor speeds) is only allowed for a short time. It is clear that the mechanical work area of motor F10-39 corresponds the best to the engine map of the Bora. That's why this motor has been selected. The TI-ratio of the hydraulic motor (28603 $[rad/s^2]$) is much more than the TI-ratio of the Bora engine (1550 $[rad/s^2]$). The combined oil flow supplied by pump B and C can be adjusted between 0 and 180 $[L/min]$ each by changing the swash plate angle. The maximum pressure in the supply line is controlled by a relief valve. The pressure can be adjusted between 0 and 210 $[Bar]$. By controlling the flow and maximum pressure, the pump characteristic can be adjusted (figure B.2).

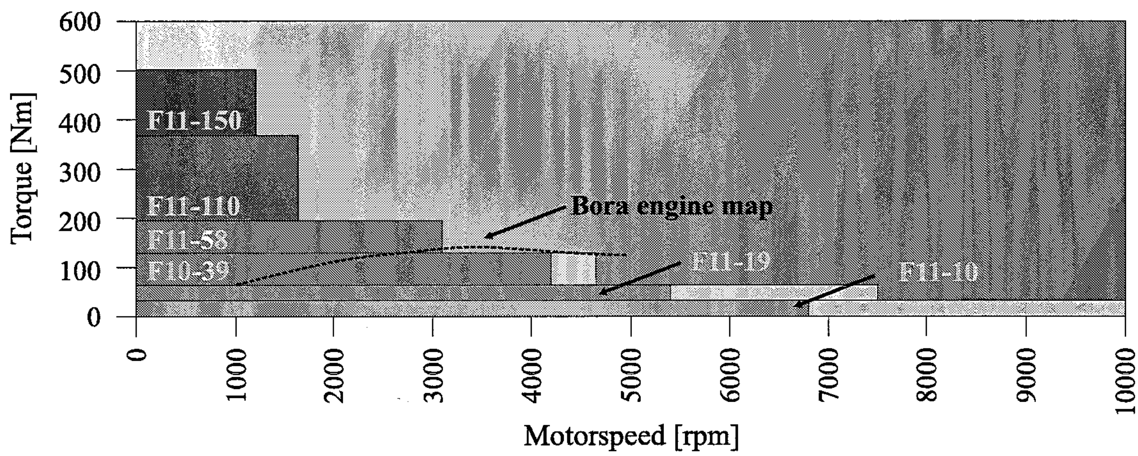

Figure 3.5: Engine map of the Bora engine and the working conditions of the available hydraulic motors supplied by pumps B+C

Filter: After the pumps, a filter is mounted for filtering out the oil contamination.

Pressure pulsation damper: Due to the finite number of pistons in the pumps of the power supply unit, the oil flow is not constant. This causes a pressure ripple. The ripple is damped out by the pressure pulsation damper.

Hydraulic brake: The hydraulic brake consists of a hydraulic pump (F11-58) and a variable resistance (Fig 3.4). In fact, the brake pump is the same kind machine as the motor used. The only difference will be the direction of the energy flow. The machine is now used as a pump instead of a motor.

A smaller model (F11-19) or a larger model (F11-58) has to be chosen because only one F11-39 motor / pump is available. Applying the F11-19 model will result in a too high oil pressures (430 [Bar]) at maximum motor torque (129 [Nm]). That's why the F11-58 model of pump is used. However, the maximum allowed speed of the brake is limited to 4500 [rpm], about 150 [rpm] lower than the maximum motor speed.

The flow to the brake is supplied by both the hydraulic motor (discharge side) and pump D of the power supply unit (max 100 [L/min] at 10 [Bar]). Because the flow from the discharge side of the motor is smaller than the desired flow for feeding the brake pump, pump D is necessary. A pressure relief valve sets the feeding pressure at a constant value of 10 [Bar] to prevent cavitation.

The mechanical energy transmitted to the brake pump is converted into oil flow resulting in a pressure due to the resistance. The pressure causes brake torque and can be adjusted by the variable resistance. Actually, the resistance consists of three different sized valves mounted in parallel. By opening or closing the valves, the resistance can be adjusted so the load characteristic changes (figure B.2).

Proportional directional valve: The proportional valve is the most important part of the rig. The valve is responsible for generating the desired dynamic torque. The chosen valve (Bosch PL-NG 6) has the largest bandwith of the available valves in the laboratory. The data sheet can be found in appendix D. The valve is a small system consisting of the actual valve (mechanical part) and an electronic part (actuation and position control).

The valve has four connections ports: P, T, A and B (see appendix). For normal use, the first two ports have to be connected to the **P**ump and **T**ank. A and B have to be connected to the supply and discharge of the controlled part (cylinder or motor). Because the valve can reverse the connection from port P and T to ports A and B, the cylinder and motor can move in two directions. In neutral position, the valve is closed. In normal position, port P is connected to port A and port T is connected to port B. In reverse position, port P is connected to port B and port T is connected to port A.

Unfortunately, the size of the valve is small, the nominal flow through is only 4 [L/min] at a pressure difference of 35 [Bar] per port. Because no return flow is necessary (only a flow from the high-pressure pipe to the reservoir), a external connection can be made between port T-A and P-B. Now the flow through the valve is doubled. Figure 3.4 shows the valve with all external connections used. The distance between the valve and motor will increase due to the external connections.

In this report, the spool position is indicated by dimensionless variable u [$-$]. If the spool is in neutral position, $u = 0$. If the valve is completely opened in normal position / reverse position, $u = +1$ respectively $u =$ -1. u_d represents the desired spool position, u_a represents the actual spool position.

The electronic part of the valve consist of a internal amplifier, and controller. The desired spool position is presented to the electronic part as a voltage between -10 and +10 [V] (corresponds to u between -1 and +1). The electronics activate and solenoid that puts the spool in the right position. An internal sensor measures the actual position of the spool continuously. The position is fed back to the internal control system.

Needle valve: An extra valve is mounted close to the proportional valve, between the pulsation damper and the valve connection. The valve improves the dynamic behaviour of the system. The partially closed valve (resistance) is a barrier for the pressure drop. When the proportional valve opens, only in the pipe between neelde valve and the motor the pressure decreases. When the needle valve would be omitted, the pressure in the entire supply pipe drops. In that case, the pressure drop would not be that high. More about the influence of the needle valve in section 3.2.3 and 4.2.2.

Hydraulic medium: The hydraulic fluid in the system is Mobil DTE-25 hydraulic oil. The fluid properties for modeling the system (next section) are the density ρ $[kg/m^3$, the bulk modules β $[Pa]$ and the dynamic viscosity μ $[Ns/m^2]$. These properties depend on the temperature and pressure (figure 3.6).

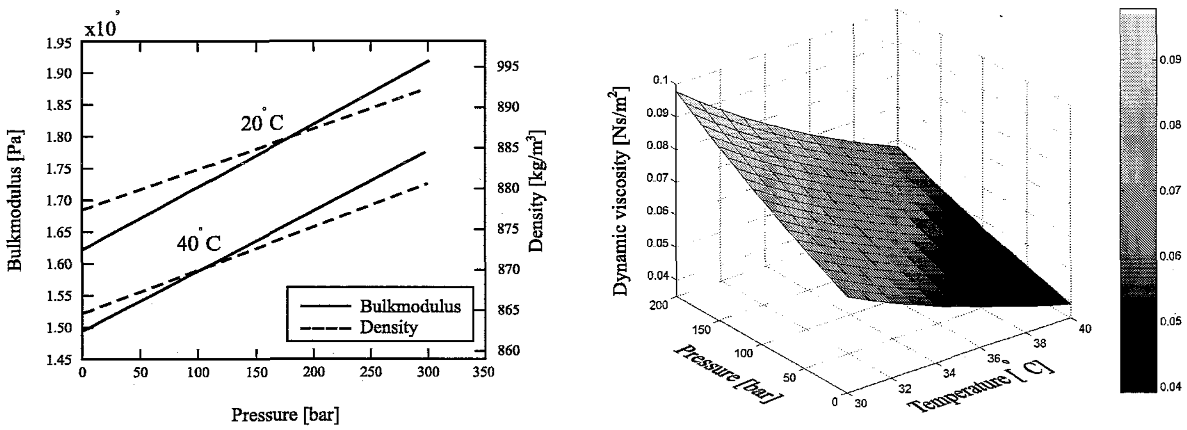

Figure 3.6: Oilproperties: bulk modulus, density and dynamic viscosity

The bulk modulus of the oil is comparable with the E-modulus of steel. The bulk modulus represents the oil stiffness:

$$\beta = V\frac{dp}{dV} \tag{3.1}$$

3.2.3 Modeling the hydraulic parts and systems

Before building the test rig, a dynamic Matlab Simulink model has been made in order to predict the properties of the system. The transfer functions from the real spool position to the corresponding motor torque have to be calculated. The corresponding Bode plots show the torque amplitudes that can be reached.

Mathematical descriptions

For modeling the system, mathematical descriptions of all parts have to be known.

hydraulic pump unit / drive motor / brake pump: Because the hydraulic pump and motor are the same kind of machine, the same formula's can be used [21].

$$T = \frac{V_d}{2\pi} p \tag{3.2}$$

$$\omega = \frac{2\pi}{V} q \tag{3.3}$$

where V_d $[m^3/rev]$ is the displacement of the machine. The flow is represented by q $[m^3/s]$, the torque by T $[Nm]$. The efficiency is assumed 100%. The pump flow and motor torque are assumed constant. The influence of the pistons is not taken into account.

Proportional valve: The flow through the valve depends on the nominal flow q_{nom} $[m^3/s]$ (depends on the valve geometry), the pressure difference over the ports of the valve Δp $[Bar]$ and the spool position u (-1 to +1).

$$q = |u| q_{nom} \sqrt{\frac{\Delta p}{35}} \tag{3.4}$$

q_{nom} of the Bosch valve equals 4 $[L/min]$. Because all ports are connected, the nominal flow is doubled.

Oil: Under dynamic conditions, the oil in the pipe (with length L and internal diameter D) acts like a spring (fluid capacity) and as an inertia (fluid inductance). Due to friction, there is also resistance. The corresponding formula's for these effects are:

Fluid capacity:

$$q_{in} - q_{out} = C \frac{dp}{dt} \quad with \quad C = \frac{\pi D^2 L}{4\beta} \tag{3.5}$$

The formula relates the incoming and outgoing flow rates with the time rate of change of the pressure in the pipe. C is the capacity of the oil volume.

Fluid inductance:

$$p_a - p_b = I \frac{dq}{dt} \quad with \quad I = \frac{4L\rho}{\pi D^2} \tag{3.6}$$

p_a and p_b are the pressures at the beginning and at the end of the pipe. I is the inductance of the oil volume. Actually, the formula is the application of Newton's second low of motion to the hydraulic system.

Fluid resistance:

$$p_a - p_b = Rq \quad with \quad R = \frac{128\mu L}{\pi D^4} \tag{3.7}$$

R is the resistance of the pipe. Assuming the flow to be laminar this linear formula may be used.

A model of the system can be made now the mathematical descriptions of all parts are known. The pressure and flow are variables in all formulas. These variables will be used to link the individual parts. A library that contains all occurring parts has been made in Matlab Simulink. Besides the hydraulic parts described in the previous section, also the mechanical parts like inertia and stiffness are modeled. The used formulas can be found in figure A.9. Sometimes, two or more library blocks have to be made from the same part. For example, in some situations the pressure is the input of the capacity block. In other situations the flow is the input. In this case formula 3.5 has to be rewritten from a differential to an integral form with an initial pressure. Because a pipe may be modeled as a combination of capacity, inductance and resistance, a special library block is made that contains all these effects. Figure 3.7 shows the contents of the pipe block.

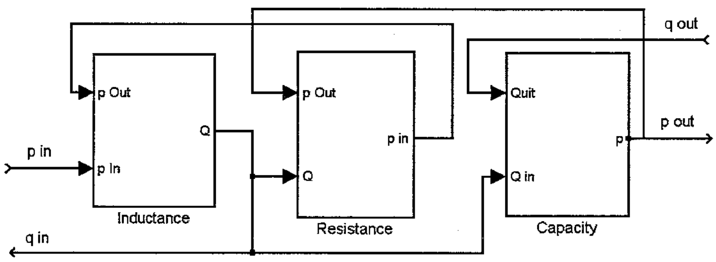

Figure 3.7: Contents of the Simulink pipe block.

Modeling the rig

Figure 3.8 shows the simplified model. The complete Simulink model can be found in appendix E. Some remarks concerning the modeled parts:

- **Part 2** represents the filter, modeled as a capacity.
- **Part 3, 4 and 6** represent the pipes, modeled as a combination of inductance, capacity and resistance part.
- **Part 5:** represents the pressure pulsation damper. The pulsation damper is modeled as a pipe. The special dynamic behaviour (damping out pressure pulses) is not taken into account.
- **Part 7:** represents the resistance caused by the needle valve.
- **Part 8:** represents the capacity of the oil in the motor and in the short pipe between the needle valve and motor.
- **Part 10:** represents the inertia of the motor, axle and torque transducer.
- **Part 11:** represents the stiffness of the torque transducer.
- **Part 12:** represents flywheel inertia.

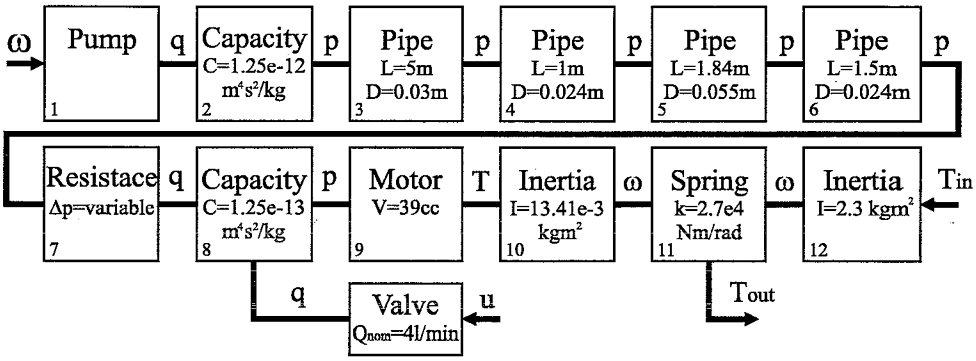

Figure 3.8: Simplified hydraulic model.

The input parameters of the model are the pump speed ω, the brake torque T_{in} and the spool position u of the proportional valve. The pump speed, and thus the flow to the filter is assumed constant. Because of the high flywheel inertia, the brake system dynamics are assumed not to have any influence on the performance of the rig. That's the reason why the brake system is modeled as a constant torque on the flywheel. Resistance due to pipe bends is not modeled. The input parameter of the transfer function is the real spool position u. The motor torque T_{out} is the output parameter of the function. ω and T_{in} are constant during each simulation.
As can be seen in figure 3.6, the oil properties depend on the oil temperature and pressure. The temperature is assumed constant during the simulation because the temperature of the oil in the reservoir is kept constant by a heater/cooler at 35 $[^oC]$. In this case the oil properties only depend on the nominal load (pressure).

Expected properties

The Simulink model has been used to predict the performance of the rig. The transfer functions of the mechanical and hydraulic system H_{mh} have been calculated. Input is the actual valve spool, output is the motor torque. From this analysis it was found that the motor speed doesn't influence the transfer functions. Several simulations have been performed to determine the influence of the load torque. The transfer has been calculated at 25, 50, 75, 100 and 125 $[Nm]$. The needle valve was opened completely. Figure 3.9 shows the corresponding Bode plots.
In the figure, are peaks are visible at four frequencies. Increasing the load results in higher magnitudes of the transfer function. This is due to the higher pressure resulting in higher flow rates through the proportional valve. Higher flow through the valve causes higher pressure differences and thus higher torque amplitudes.

Figure 3.10 shows the influence of the pressure difference over the needle valve on the transfer function. The nominal load was set to 50 $[Nm]$ during the simulations. The needle valve was set corresponding to the following pressure differences over the valve: Δp = 0, 5, 10, 15, 35, 55, 75 and 95 $[Bar]$. Larger pressure differences causes higher magnitudes in the Bode plot. Small pressure differences effect the increase of the magnitude significantly. The effect at high pressure differences is smaller.

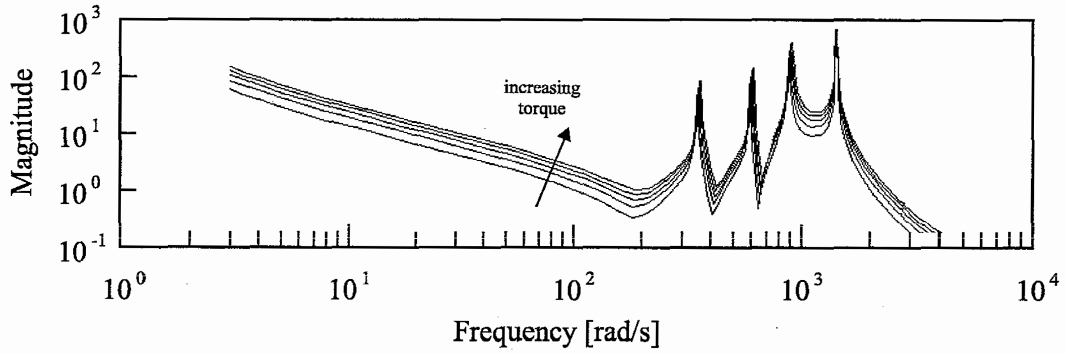

Figure 3.9: Bode plots of the calculated transfer functions H_{mh} at different loads.

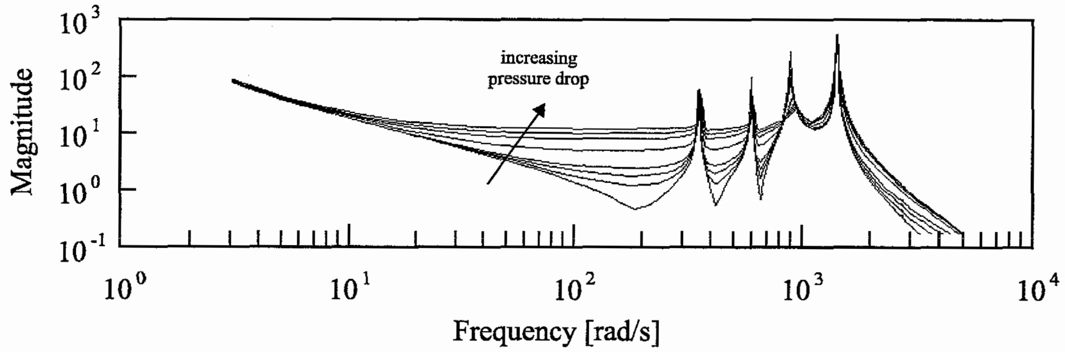

Figure 3.10: Influence of the pressure difference over the needle valve on the Bode plot.

Unfortunately, the magnitude of the transfer seems to be too low. In combination with Bode plot of the proportional valve (appendix D), the desired torque amplitudes can not be generated. Causing a pressure drop by the needle valve improves the magnitude, but the effect will not be enough. Nevertheless, the rig is realized for investigating dynamic hydraulic systems. The simulations have to be validated (section 4.2.2). In a later stadium the rig can be improved. The hydraulic system has to be optimized and better chosen parts have to be applied (chapter 5).

3.3 Data acquisition and control system

For determining the properties of the rig (e.g. transfer functions as described in the previous section), a data acquisition system will be necessary. The system has to be able to measure and log different variables. Furthermore, the system has to present the desired spool position to the valve electronics. Actually, the designed system is not a control system! It is an open loop system that prescribes the desired valve spool position to the valve electronics. The valve electronics control the spool position (feedback).

The complete data acquisition and control system consists of the following parts:

Sensors: The following variables will be measured by the sensors:

- Motor torque

- Oil pressure at the supply side of the motor
- Motor speed
- Valve spool position

Actuator: In this case, the spool position is the only actuated variable. Motorspeed and load will be adjusted manually.

TU/e DACS/1: The DACS (**D**ata **A**cquisition and **C**ontrol **S**ystem) acts as the interface between the digital laptop and the analog sensors / actuator. Only the a analog - digital converters are used.

Voltage dividers / amplifiers: The input / output voltages of sensor, actuators and the TU/e DACS system use specific ranges. Because the ranges don't always correspond, some voltages have to be decreased by voltage dividers, others have to be increased by amplifiers.

Laptop with Simulink software: The heart of the data acquisition system is the laptop, equipped with Simulink Matlab 6.1 software.

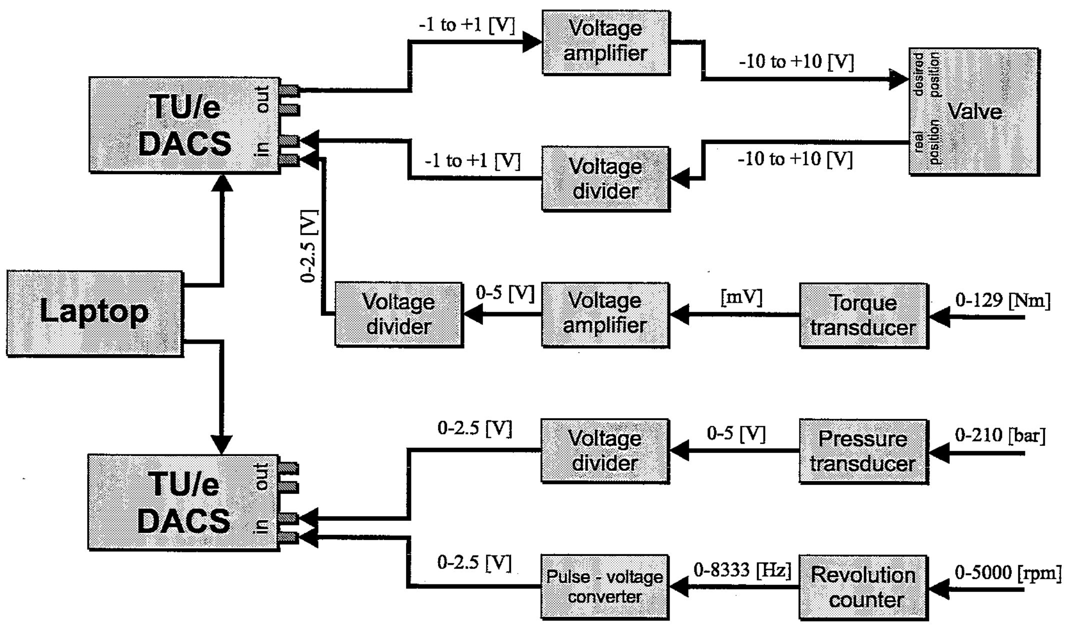

Figure 3.11: Schematic overview of the data acquisition system

Figure 3.11 shows a schematic representation of the data acquisition and control system. In appendix F, the complete system is discussed.

3.4 Realized prototype test rig

The mechanical and hydraulic design as well as the data acquisition and control system are realized in the fluid power laboratory. Figure 3.12 shows the realized data acquisition / control part and the prototype test rig. The arrows point to the locations of the parts.

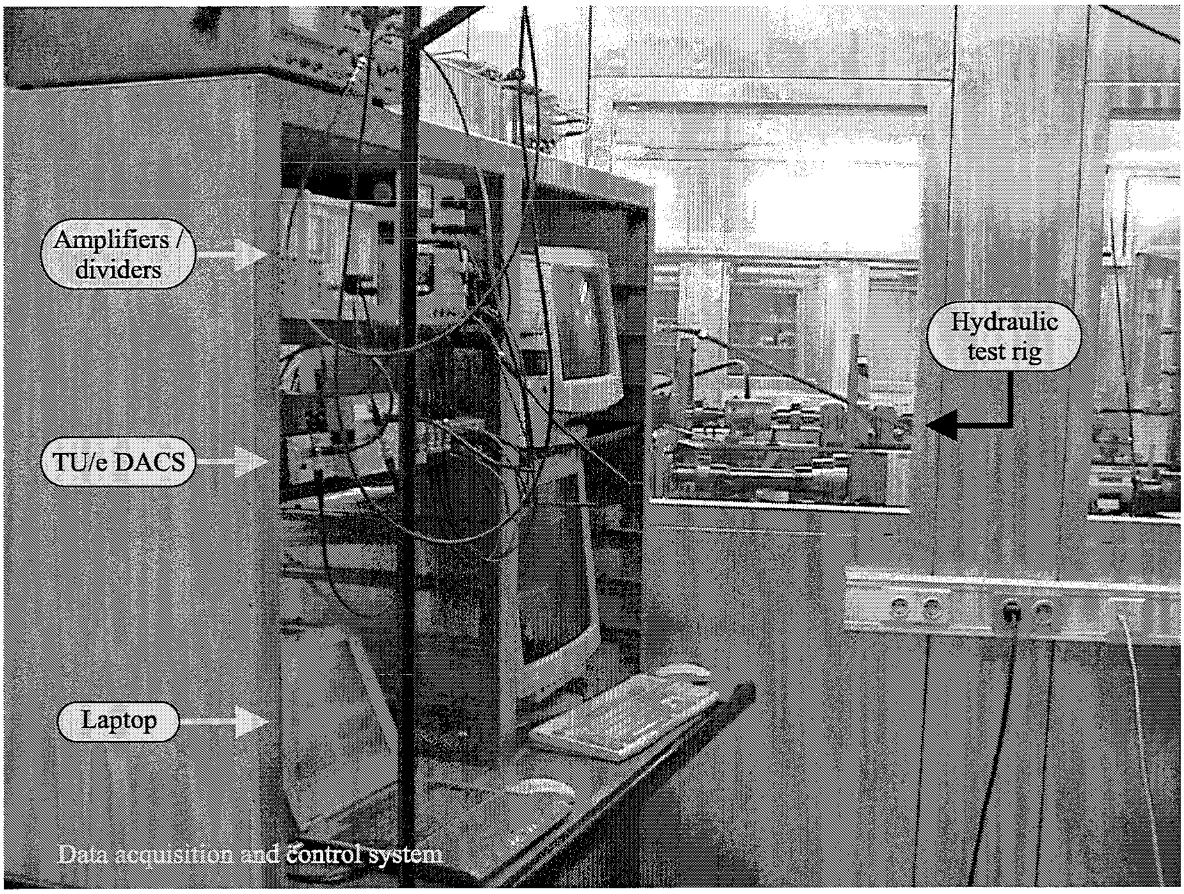

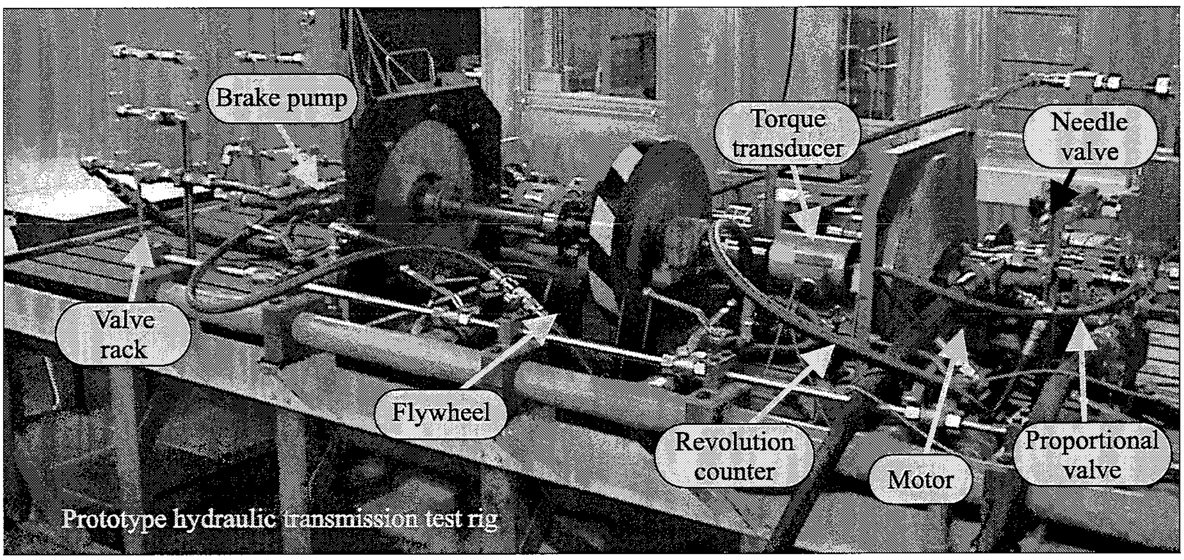

Figure 3.12: Realized data acquisition / control part and the prototype hydraulic test rig.

Chapter 4

Test results

For determining the properties of the test rig, a number of measurements have been performed. At first the motor torque was measured while the valve was closed. Then, the transfer functions of the valve, the hydraulic / mechanical system, and the complete system have been determined under different conditions. Finally, the maximum torque amplitude that can be generated by the test rig has been compared to the desired torque amplitudes. The results of the measurements are described in the following sections.

4.1 Stationary torque

The torque generated by the motor in case of a closed proportional valve is called the stationary torque. In the ideal situation, the torque is constant. However, the used hydro motor is a positive displacement machine containing 11 pistons. It was expected that the stationary torque is not constant due to the influence of the pistons. The torque consists of ripple added to the nominal torque. The ripple amplitude depends on the nominal torque and the number of pistons. Low amplitudes are achieved at low nominal torque and a high number of pistons. The ripple frequency depends on the motor speed and number of pistons. High frequencies are the result of high motor speeds and a high number of pistons.

A non-constant stationary torque is inevitable because of the motor properties. The presence of the ripple is acceptable if the amplitude of the ripple is much smaller than the amplitude of the dynamic torque fluctuation generated by the proportional valve. The larger the difference in frequency between the ripple and dynamic torque, the better the effects can be identified. Because the hydraulic motor contains 11 pistons, the ripple frequency will be 11 times the motor speed. A 4 stroke 4 cylinder engine generates 2 torque pulses per revolution. The frequency of the dynamic torque will be 2 times the motor speed. The torque frequency generated by the hydraulic motor will always be a factor 5.5 times larger.

To investigate the effects, some measurements were done. The nominal motor torque was set to 20 $[Nm]$ and was measured during a period of 1 second (sample rate = 1600 $[Hz]$. To be ascertain that the torque ripple caused by the pistons can be recognized, the motor speed was kept low (600 and 1200 $[rpm]$). Figure 4.1 shows the results. Because the nominal torque is the same, the amplitude of the torque ripple is to be expected the same. Unfortunately, this is not the case. When zooming in on the signals, the fluctuation caused by the pistons can't

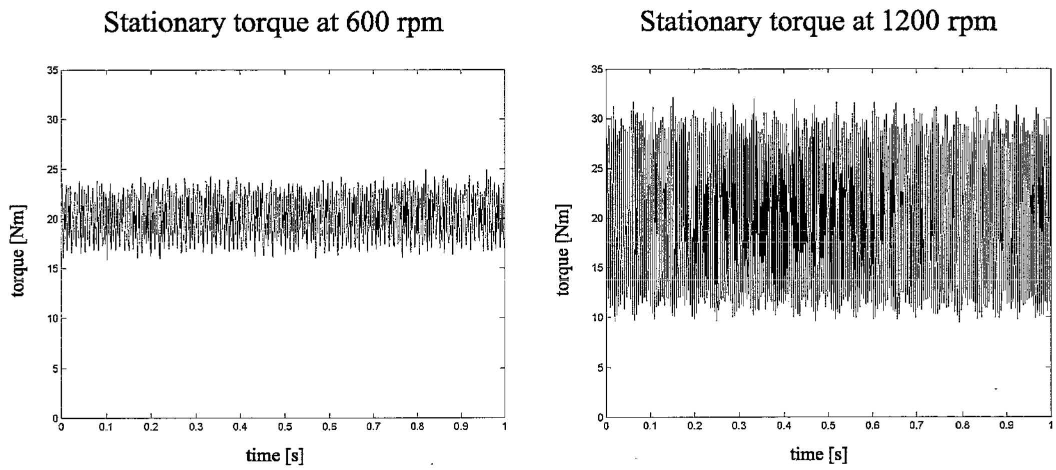

Figure 4.1: Time signal of the stationary motor torque. Nominal torque: 20 $[Nm]$

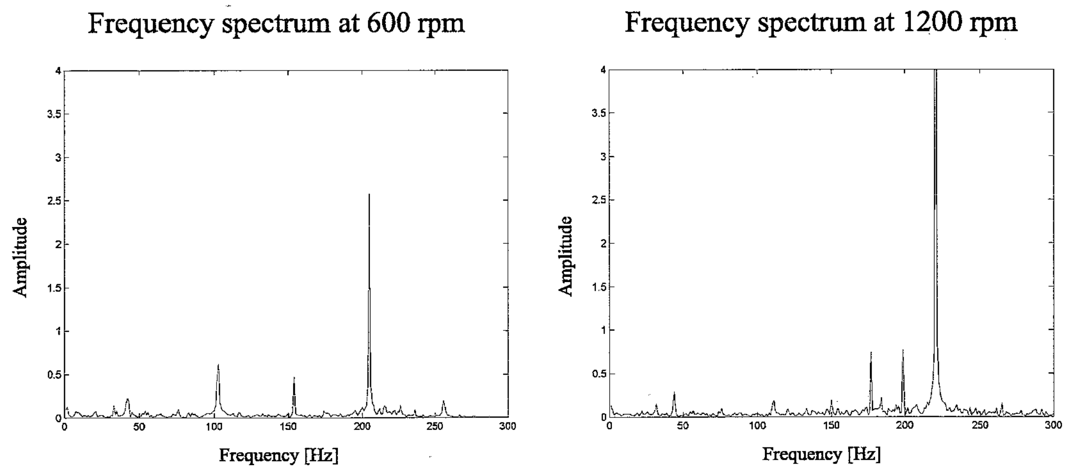

Figure 4.2: Frequency spectrum of the stationary motor torque. Nominal torque: 20 $[Nm]$

be recognized. The torque signal appears to be noise. It is not possible to give a sensible explanation for this behaviour. The time domain seems not to be the most suitable way of analyzing the origin of the torque fluctuations. That's why a fourier analysis has been performed. The torque signal was split in a series of sine signals with specific frequencies and amplitudes.

Figure 4.2 shows the resulting frequency spectra of the time signals of figure 4.1. When taking a closer look to the left picture of the figure, three peaks can be recognized. Only the peak at 110 $[Hz]$ is expected as it is caused by the hydraulic motor (number of pistons times the rotational speed). When the speed is doubled (right picture of figure 4.2), the peaks at 110 and 155 $[Hz]$ disappear. The amplitude of the right peak (now at 220 $[Hz]$) has become much larger. The peak at about 220 $[Hz]$ was expected (hydraulic motor). It seems like there's an eigenfrequency at about 220 $[Hz]$. In the right picture, the frequency of the motor torque ripple equals the eigenfrequency; the system is in resonance.

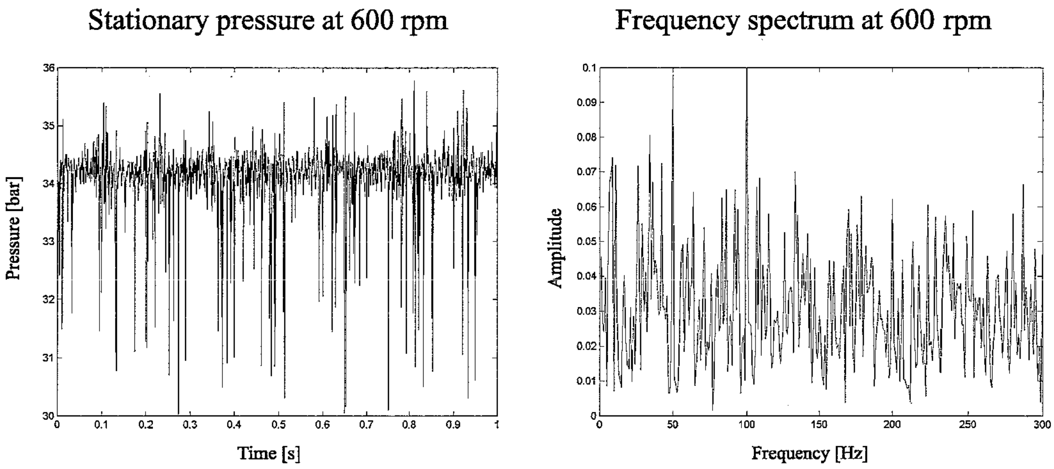

Figure 4.3: Motor pressure difference at stationary torque. Left: time signal of the pressure Right: frequency spectrum. Nominal torque: 20 $[Nm]$

The model described in the previous chapter already predicted the presence of an eigenfrequency at 225 $[Hz]$ (1419 $[rad/s]$ in figure 3.9). The eigenfrequency can be a result of the hydraulic and / or the mechanical system. When the resonance is due to the hydraulic system, a peak at about 220 $[Hz]$ should have to be visible in the frequency spectrum of the pressure. Figure 4.3 shows the pressure at a nominal torque of 20 $[Nm]$. The left picture shows the time signal of the pressure difference over the hydraulic motor. The pressure is more constant than the measured torque (figure 4.1). When inspecting the frequency spectrum (right figure), no distinct peaks are visible. This proves the absence of eigenfrequencies in the hydraulic system in this part of the frequency spectrum.

Because the eigenfrequency is not caused by the hydraulic system, it must be caused by the mechanical system. Because the flywheel has such a high inertia compared to the other parts, it may be interpreted as rigid. The torque transducer is the most elastic part. The other shafts are much stiffer. The torque transducer is the dominant spring of the system. The mass-spring system that causes the eigenfrequency consists of the next parts:

inertia:

- Hydro motor J=$4.51 \cdot 10^{-3}$ $[kgm^2]$
- Shafts and couplings between motor and torque transducer J=$8.4 \cdot 10^{-3}$ $[kgm^2]$
- Half of torque transducer J=$0.5 \cdot 10^{-3}$ $[kgm^2]$

spring:

- Torque transducer k=$2.7 \cdot 10^4$ $[Nm/rad]$

The eigenfrequency can be calculated on basis of a single spring / mass system:

$$f = \sqrt{\frac{k}{J_{tot}}} \cdot \frac{1}{2\pi} = \sqrt{\frac{2.7 \cdot 10^4}{13.41 \cdot 10^{-3}}} \cdot \frac{1}{2\pi} = 225[Hz] \tag{4.1}$$

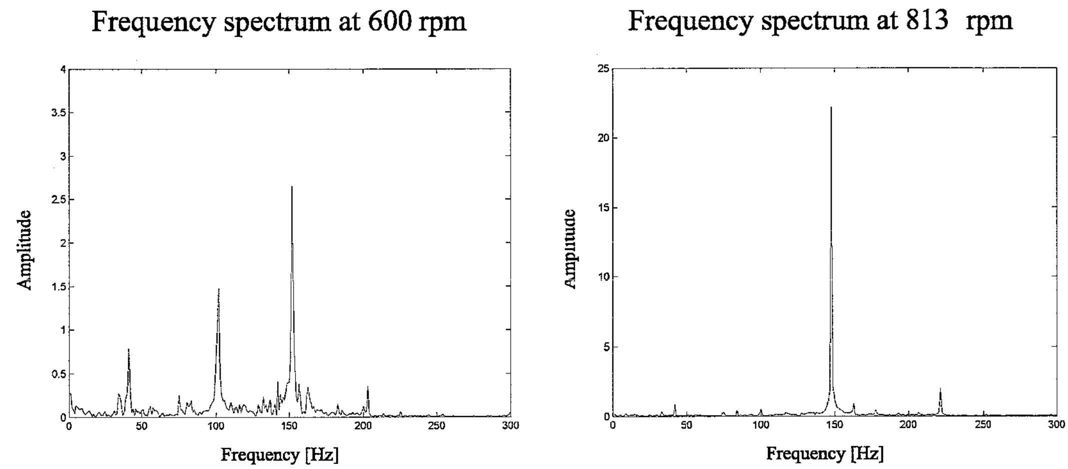

Figure 4.4: Frequency Spectrum with weak torque axis. Nominal torque: 20 $[Nm]$

The calculated eigenfrequency is close to the eigenfrequency found in figure 4.2. To confirm this result, the torque axis has been replaced by a less stiffer one (k=$1.18{\cdot}10^4[Nm/rad]$). The eigenfrequency is expected to decrease. According to 4.1 the resulting eigenfrequency will be 149 $[Hz]$. Some measurements were performed. The nominal torque was 20 $[Nm]$, the rotational speeds were 600 and 813 $[rpm]$. The motor speed of 813 $[rpm]$ was chosen on purpose for bringing the system in resonance. The frequency of the torque ripple caused by the pistons equals 149 $[Hz]$. In the left picture of figure 4.4 the peak at 110 $[Hz]$ is caused by the motor pistons, the peak at 150 $[Hz]$ is caused by the eigenfrequency of the less stiffer torque transducer. This corresponds well to the calculation. Compare the left picture of figure 4.2 with the left picture of figure 4.4. It's noticeable that the decreased stiffness of the torque transducer shifts the eigenfrequency from about 220 $[Hz]$ to 149 $[Hz]$. In the right plot of figure 4.4 the frequency of the motor torque fluctuations equals the eigenfrequency of the system; the system is in resonance. Note that the y-axes of figure 4.4 have different scales.

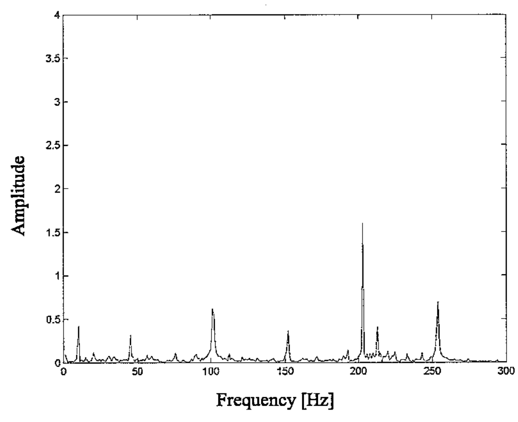

Figure 4.5: Frequency Spectrum of the torque generated by the proportional valve. Sine frequency: 10 $[Hz]$, Nominal torque: 20 $[Nm]$, Motorspeed: 600 $[rpm]$

As mentioned before, the effect on the system is acceptable if the torque amplitude caused by the motor pistons is much smaller than the torque fluctuation caused by the proportional valve. Unfortunately the torque ripple caused by the motor introduces mechanical vibrations. Figure 4.5 shows the torque frequency spectrum in case the valve is activated at 10 $[Hz]$. It's clear that the amplitude of the torque vibration caused by the proportional valve (10 $[Hz]$) is dominated by the other amplitudes. This is not acceptable! In chapter 5 it is discussed how this problem can be tackled.

4.2 Transfer functions

This section describes the determined transfer functions. At first the transfer functions of the valve H_v are described. The desired spool position u_d is the input signal, the actual spool position u_a is the output signal. For the transfer function of the mechanical and hydraulic system H_{hm}, the actual spool position is the input signal. The resulting motor torque difference is output signal. Finally, the transfer function of the complete system H_c is discussed (input = desired spool function, output = motor torque difference). Figure 4.6 is an overview of the transfer functions.

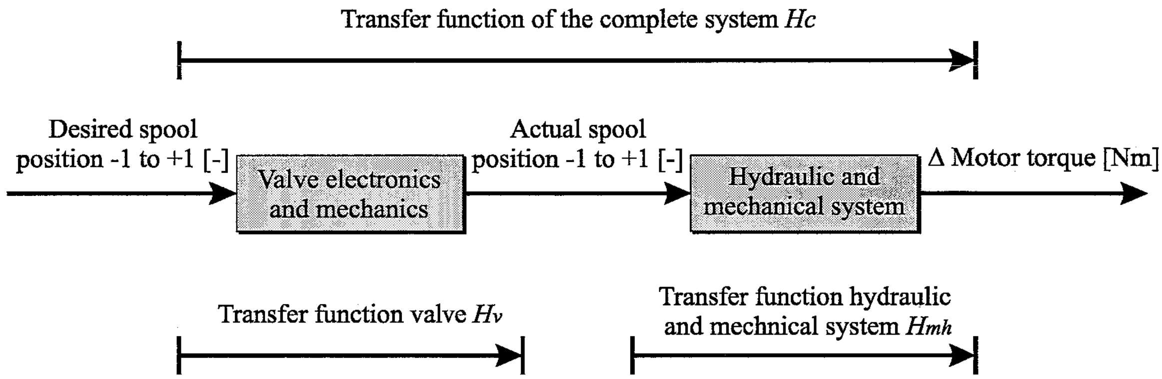

Figure 4.6: Transfer functions in the test rig

During all tests, the input signal of the valve electronics was a sine sweep voltage. At the beginning, the sine frequency was 0. The frequency was changed linearly till 250 $[Hz]$ was reached after 25 seconds. The sample rate was 1600 $[Hz]$. In this way, the size of the data file is kept low (measuring only takes 25 seconds) whereas the complete frequency range is measured. The data was processed by Matlab routines. The "ETFE" function computed the Empirical Transfer Function Estimate. The estimate was used to generate the Bode plots.

4.2.1 Transfer function of the proportional valve

The bode plot of the valve is already known (brochure Bosch). Nevertheless, it is important to determine the Bode plot of the valve again. The presented plot can deviate from the real bode plot for several reasons. The presented plot is the average of a large series of valves. Due to production tolerances the plots may differ from each other. Furthermore, the operating circumstances in the test rig can deviate from the circumstance at Bosch. When the Bode plots are determined, the performances of the valve as when mounted in the test rig are known. Finally, the data-acquisition system can be tested.

Like the bode plot presented by Bosch, two different input amplitudes were used: ± 100 % (u_d = ± 1 [−]) and ± 5 % (u_d = ± 0.05 [−]). The desired position (prescribed) and actual spool position were measured.

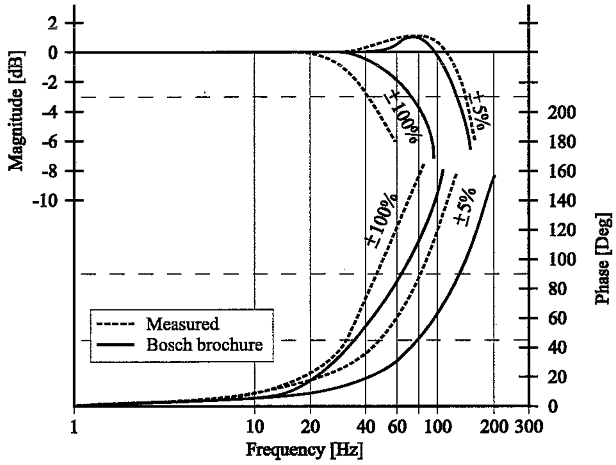

Figure 4.7: Bode plot hydraulic valve. Amplitude ratio and phase shift

Figure 4.7 shows the results. The solid lines represent the plots as presented by Bosch, the dotted lines the measured ones. It is clear that the plots don't match exactly. At low amplitudes (5%) the magnitude is a bit higher than the presented one. At 100 % amplitude, the magnitude decreases at a lower frequency than the presented one; the valve performs worse. The real phase shift is much higher than expected.

4.2.2 Transfer function of the hydraulic and mechanical system

To get a good impression of the performance of the mechanical and hydraulic part of the test rig, transfer functions at several points spread over the working conditions of the motor were measured. During these tests, the desired spool position u_d was $0.5 + 0.5sin(\omega t)$. The spool operates between the neutral and maximum normal position (u between 0 and 1). In this case, the actual in stead of the desired valve spool position was taken as input. In this way the influence (transfer function) of the valve is excluded. Only the hydraulic and mechanical part is investigated.
The theoretical work area of the motor is bounded by a torque of 0 - 129 $[Nm]$ and a motor speed 0 - 4200 $[rpm]$. This is visualized as the dark gray area in figure 4.8. The torque is limited by the maximum pump pressure difference (210 $[bar]$), the motor speed is limited by the allowable motor speed presented by the manufacturer. The light gray area represents the real work area. As can be seen, the light gray area is smaller than the dark one with respect to the torque. The theoretical torque can't be reached.
This is due to friction in the pipes and fittings. This concerns especially the discharge pipe of the motor that is also the supply pipe to the brake. At high motor speeds (high flows), the pressure in the pipe increases. The pressure difference over the motor and consequently also the maximum motor torque decreases. The pipe diameter is dimensioned too small.

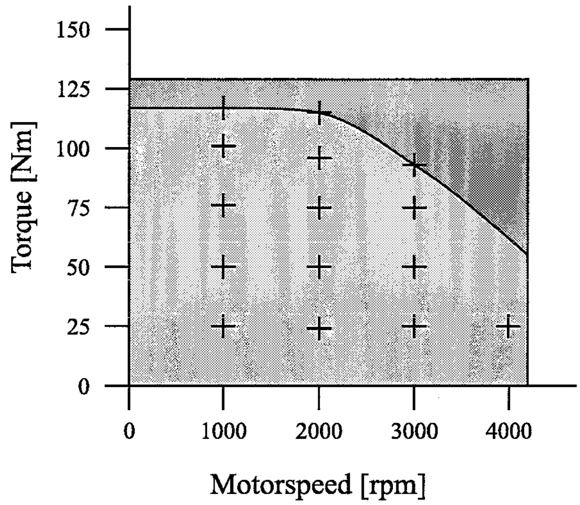

Figure 4.8: Map of working conditions of the hydraulic motor. Dark gray = theoretical. Light gray = real

Several measurements have been performed for determining the influence of the motor speed and average torque on the transfer function. The other parameters are kept constant during the measurements. The crosses in figure 4.8 represent the measuring points.
After making Bode plots of all measurements, it was found that motor speed doesn't influence the transfer function. However, increasing the torque results in higher magnitudes in the Bode plots. The results can be seen in figure 4.9. Only the measurements at 1000 $[rpm]$ are shown because the speed doesn't influence the bode plot.

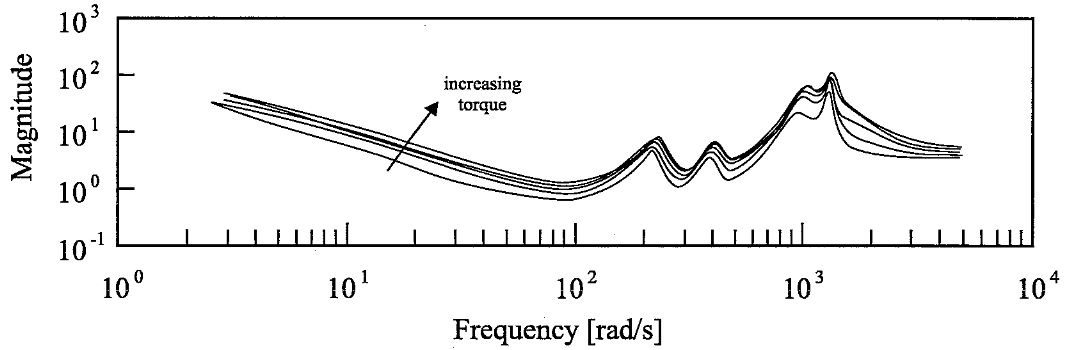

Figure 4.9: Bode plots hydraulic and mechanical system. Motorspeed = 1000 $[rpm]$
Torque = 25, 50 , 75, 100 and 117 $[Nm]$

The figure shows four peaks. The highest one at the right is caused by the eigenfrequency of mechanical parts (subsection 4.1). The other peaks are caused by the eigenfrequencies of the hydraulic system. Because of the low spool response at frequencies above 150 $[Hz]$, the reliability of the information in the Bode plot above the frequency of 940 $[rad/s]$ is doubtful.

Influence of the needle valve on the transfer function

Some measurements were done to investigate the influence of the partly closed needle valve on the bode plot of the hydraulic / mechanical system. The motor speed and motor torque were kept constant at 1000 [*rpm*] and 50 [*Nm*]. A pressure drop over the valve is caused when the needle valve is partly closed. The pressure drop is the only variable during these measurements. The valve is set corresponding to the following pressure drops: $\Delta p = 0$, 5, 10, 15, 35, 55, 75 and 95 [*bar*]. Figure 4.10 shows the resulting Bode plots of the transfer functions.

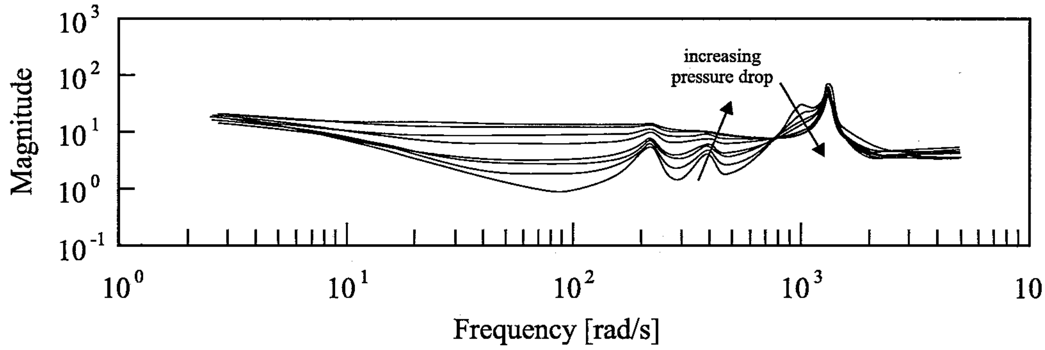

Figure 4.10: Influence of the pressure drop over the needle valve on the Bode plot of the hydraulic / mechanical system. Motorspeed = 1000 [*rpm*] Torque = 50 [*Nm*]

When inspecting the figure, it is clear that a partially closed valve has a positive influence on the behaviour of the hydraulic system. At low pressure drops, the dips between the peaks caused by the hydraulic system disappear. From $\Delta p = 35$ [*bar*] the magnitude increases at all frequencies between 30 and 800 [*rad/s*]. Small pressure drops have most influence. The peak caused by the mechanical system is unaffected because the mechanical system hasn't changed.

The disadvantage of using the valve is the loss of energy due to the pressure drop. In this test, 95 [*bar*] was necessary to generate 50 [*Nm*]. When increasing the magnitude by creating 95 [*bar*] pressure drop over the needle valve, 50% of the used energy was wasted!

Comparison with model

Figures 3.9 and 3.10 are the predictions of figure 4.9 and figure 4.10. At first sight, the model predicts the transfer functions quite well. The predicted as well as the measured Bode plots show four eigenfrequencies. Also the influence of the increasing nominal torque and the pressure drop over the needle valve corresponds. Although there are some differences. The eigenfrequencies as a result of the hydraulic system don't correspond with the reality. The differences can be caused by the special dynamic behaviour of the pressure pulsation damper that is not modeled. Furthermore, the modeled pipe lengths don't exactly match the real pipe lengths. In the measured Bode plots, the peaks at the eigenfrequencies are much lower than the peaks in the Bode plots of the modeled system. The real system is more damped than the modeled system. The modeled resistance is apparently to low.

4.2.3 Transfer function of the complete system

The final measurements involved the transfer function of the complete system H_c. The bode plots of the complete system were determined from the most favourable bode plots of figure 4.9 and 4.10. In this case, the desired valve spool position was taken as input. In this way the influence (transfer function) of the valve was taken into account. Again, the presented desired spool position u_d was $0.5 + 0.5sin(\omega t)$. Figure 4.11 shows the results. The corresponding working conditions were:

plot 1:	motor speed = 1000 $[rpm]$	nominal torque = 50 $[Nm]$	Δ p valve = 95 $[Bar]$
plot 2:	motor speed = 1000 $[rpm]$	nominal torque = 117 $[Nm]$	Δ p valve = 0 $[Bar]$

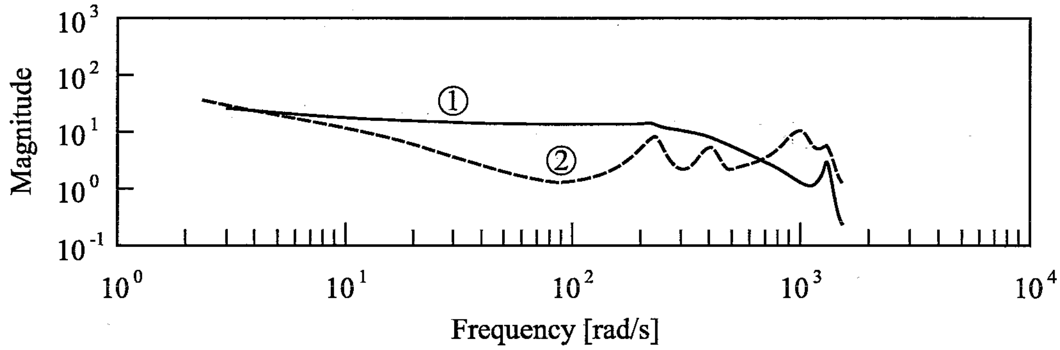

Figure 4.11: Bode plots of the complete system at most favourable working conditions.

The influence of the valve transfer on the Bode plot of the complete system is visible at higher frequencies. Compared to figure 4.9 and 4.10, the magnitudes decrease.

4.2.4 Dynamic performance

Graph 3 of figure 4.12 shows the motor torque amplitudes the test rig should have to generate according to the specifications (figure 2.4). Graph 1 and 2 represent the torque amplitudes the rig can generate in the working conditions corresponding to figure 4.11.

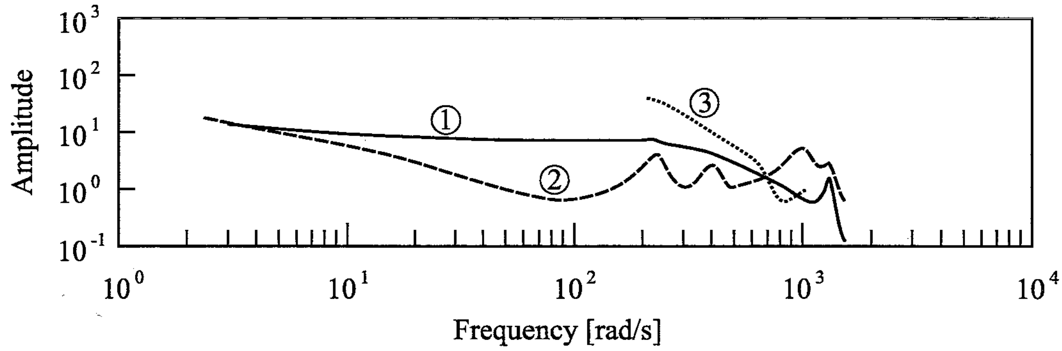

Figure 4.12: Desired and real dynamic torque amplitudes.

Unfortunately, the prototype rig does not satisfy the demands concerning the dynamic torque. The desired torque amplitudes can not be generated over the complete frequency range. Chapter 5 describes in what ways the performance of the test rig can be improved.

4.3 Conclusions

Several test have been performed to determine a number of properties of the test rig. The most important conclusions from these tests are:

- The torsional vibration caused by the eigenfrequency of the mechanical system has a larger amplitude than the torque caused by the proportional valve.
- The measured bode plot of the proportional valve doesn't exactly match the plot presented by the manufacturer.
- The motorspeed doesn't influence the Bode plot of the mechanical and hydraulic system. Higher nominal torques lead to higher magnitudes in the bode plot.
- The partly closed needle valve increases the magnitude of the Bode significantly.
- With the prototype test rig, the desired dynamic torque amplitudes can't be generated.
- The developed model corresponds quite well to the reality. Although some differences appeared.

Chapter 5

Improving the prototype configuration

The realized prototype transmission test rig has been build for investigating the suitability of a hydraulic motor for simulating combustion engines. Only parts available in the fluid power laboratory of the university were used for the prototype test rig. After investigating especially the dynamic hydraulic properties, it was clear that adjustments are necessary for satisfying the demands. Some parts need to be replaced by parts that have other properties or higher qualities. Furthermore, the hydraulic system has to be improved. Tuning of the pipe system is necessary for increasing the dynamic torque amplitudes.

5.1 Improvements

If the decision is made to go on with this configuration, the following improvements have to be considered. These improvements are necessary for increasing the amplitude of the dynamic torque signal caused by the proportional valve.

- **Mechanical system:** The eigenfrequency of the mechanical system has to be increased to prevent the system from vibrating at its eigenfrequency due to the torque ripple caused by the motor pistons. Increasing the eigenfrequency can be realized by increasing the stiffness and decreasing the inertia of the mechanical system. Another advantage of decreasing the mass of the parts mounted beween the motor and transmission is the lower damping of the dynamic torque signal caused by the valve. The following parts need attention:
  - The current used torque transducer (range = 500 $[Nm]$, k = $2.7 \cdot 10^4$ $[Nm/rad]$, J=$1 \cdot 10^{-3}$ $[kgm^2]$) should be replaced by a stiffer one like a HBM torque flange T10F (range = 200 $[Nm]$, k = $115 \cdot 10^4$ $[Nm/rad]$, J = $3{,}4 \cdot 10^{-3}$ $[kgm^2]$).
  - The inertia of the joints motor-torque transducer and torque transducer- transmission has to be reduced. The use of light weight lamination couplings improves the performance.
- **Hydraulic system:** The major problem of the current hydraulic system is the low pressure drop caused by the proportional valve. The current hydraulic system can be compared with a rubber hose filled with compressed air. A hole is made in the hose by

a needle. Pressure fluctuation is created by opening and closing the hole with a finger. The pressure fluctuation will be limited. If the pressure fluctuation can be increased, the amplitude of the torque vibration will increase as well. There are several ways to realize this:

- The magnitude at low nominal torque is low (figure 4.9). This is due to the low flow through the proportional valve at low pressure difference over the valve (figure 5.1A). Increasing the amplitude at low torque can be realized by connecting the valve to a high pressure source in stead of the tank (figure 5.1B). The pressure over the valve and consequently the flow through the valve is higher. In this situation, the flow is to the system. In stead of a small pressure drop in the pipe, a large pressure increase is generated. The pressure difference over the valve (Δp in the figure) should be as high as possible.

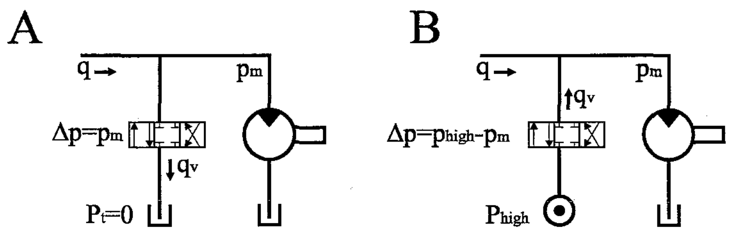

Figure 5.1: Pressure difference over the valve

- The capacity C of the oil volume in the pipe system should be decreased. With the same flow through the proportional valve, the pressure will decrease more. The capacity can be decreased in several ways:
  * Get rid of all the air in the oil system. The bulk modulus of air is much smaller than the bulk modulus of oil so a small amount of air in the pipes increases the capacity of the system with a large amount.
  * Decreasing the pipe volume. By placing the pumps as close as possible to the hydraulic motor, the minimum capacity is reached.
- The applied proportional valve is not ideal. The flow is only 4 $[L/min]$ per port at a pressure difference of 35 $[Bar]$. Furthermore, the bandwith is too small for this application (figure 4.7). A better choice would be Moog servovalve D765. Not only the bandwith but also the nominal flow is much larger (38 $[l/min]$). Using only one connection satisfies because the nominal flow is that high. The valve can be positioned closer to the motor resulting is a smaller oil capacity. More info about this valve can be found in appendix I.
- Tuning of the pipe system. The performance of the rig can be improved by choosing the right hydraulic lay out (pipe length and diameter). More about tuning the pipe system in section 5.2.

- **Other improvements:**
  - In the current configuration, the brake energy is converted to heat. The efficiency of the test rig is very low. However, the energy may be recovered by presenting the brake flow to the motor. The brake energy will be reused by the motor. The

motor and pump pressure have to correspond. That's why the motor or brake pump has to be equipped with an adjustable swash plate. Only the energy losses in the transmission, hydraulic motor and pump have to be added to the system.

- The diameter of the pipe between the motor discharge and brake supply has to be enlarged. The friction and consequently the pressure decreases, especially at high flows. Higher maximum torque at high motor speed can be reached.

5.2 Introduction of tuning the hydraulic system

The performance of the test rig can be increased by choosing the right hydraulic layout: the hydraulic system has to be tuned. Different ways of tuning are possible. In this section is discussed how tuning based on the impedances-frequency relation of the pipe can be performed. This section does not pretend to be complete, it is just an introduction of the possibilities of tuning. For understanding the tuning principle, the dynamic behaviour of the hydraulic system has to be investigated. The dynamic behaviour of the basic hydraulic components can be found in appendix G.

5.2.1 Modeling the pipe impedance

Consider the pipe section section shown in figure 5.2(a) of length L and diameter D. The section can offer resistance impedance X_R, inductive impedance X_I and capacitive impedance X_C.

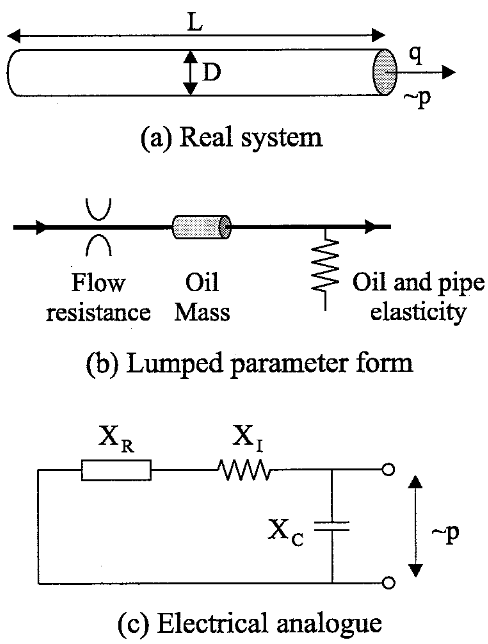

Figure 5.2: Lumped model and electrical analogue of a pipe section [16]

The left end of the pipe is connected to the pumps. The right end is connected to capacity at the side of the hydraulic motor (part 9 in figure 3.8). The pump pressure is presumed constant. The pressure at the motor side is sine shaped due to proportional valve. Figure

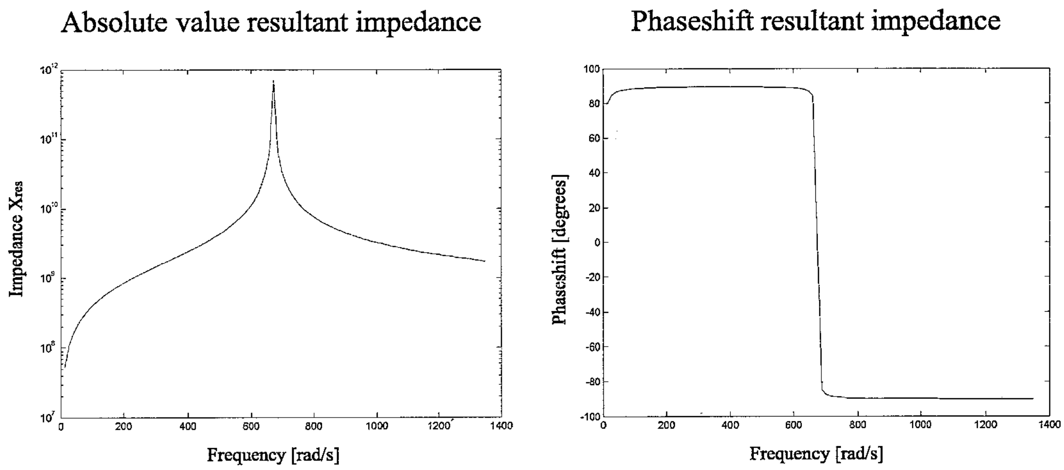

Figure 5.3: Absolute value (left) and phase shift (right) of the resultant impedance

5.2(b) shows the lumped parameter form of the pipe section. Figure 5.2(c) is the electrical analogue of the pipe. The basic relationship between the pressure and flow rate is:

$$p = X \cdot q \tag{5.1}$$

X represents the impedance of the hydraulic system. Due to the fluctuating pressure, the flow fluctuates as well. If the impedance of the complete pipe is known, the flow can be calculated using formula 5.1. The resultant impedance X_{res} can be calculated using the standard network formulas:

$$X_{res} = \frac{1}{\frac{1}{X_C} + \frac{1}{X_I + X_R}} = \frac{1}{Cj\omega + \frac{1}{Lj\omega + R}} \tag{5.2}$$

The value of X_{res} is complex and dependent on the the frequency of the pressure fluctuations. Suppose the pipe shown in figure 5.2 has the following parameters: $L = 2[m]$ and $D = 0.024[m]$. The oil properties can be found in figure 3.6. After using formula 3.5, 3.6 and 3.7: C=5.7·10^{-13}, I=3.9·10^{6} R=9.8·10^{6}. Figure 5.3 shows the absolute value and phase shift of X_{res}. At 670 $[Hz]$ the absolute value of the impedance is very large. This results in a very low dynamic flow. **This situation is very favourable!!** If the pressure drops in case the proportional valve opens, the flow from the pipe will stay constant because of the high impedance. This also happens if the needle valve is closed partially. The stationary flow only feels the resistance caused by X_R. The dynamic flow also feels X_C and X_I. For optimal performance, the stationary resistance should be very low and the dynamic resistance should be very high. Unfortunately, only at a single frequency the impedance is very high. This frequency might be adjusted by changing the pipe dimensions: tuning the hydraulic system.

5.2.2 Tuning the hydraulic system

At first the cause of the impedance peak has to be determined. In this example, at higher frequencies X_R is much smaller than X_I. That's why X_R will be neglected during further calculations. From figure 5.2(c), it is clear that the pressure over the capacity is equal to the pressure over the inductance. This is visualized in figure 5.4 by the pressure vector on the real axis. The corresponding flow through the capacity q_C and inductance q_I are visualized by the vectors on the imaginary axis (opposite direction). The smallest impedance (largest flow) dominates the situation, X_I in the figure. The system behaves like it's an inductance. A special situation appears if $X_C = X_I$.

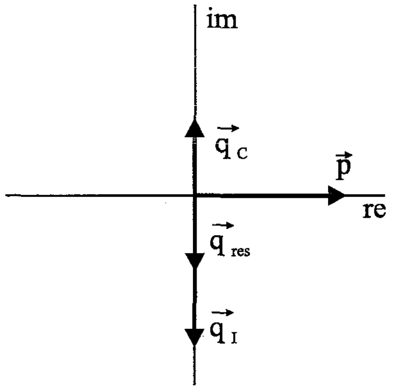

Figure 5.4: Complex presentation of the flow and pressure relation

The resultant flow q_{res} becomes zero and the resultant impedance X_{res} infinitely large. This desired situation only appears at a specific frequency: the resonance frequency $\omega_{resonace}$. The resonance frequency can be calculated in the next way:

$$X_I = X_C \quad \rightarrow \quad \omega I = \frac{1}{\omega C}$$

$$\omega_{resonance} = \frac{1}{\sqrt{IC}} \tag{5.3}$$

Combining formula 3.5, 3.6 and 5.5 results in:

$$\omega_{resonance} = \frac{1}{\sqrt{\frac{\rho L}{\frac{\pi}{4}D^2}\frac{\frac{\pi}{4}D^2 L}{\beta}}} = \frac{\sqrt{\beta}}{L\sqrt{\rho}} \tag{5.4}$$

Because bulk modulus β and density ρ are oil properties, the resonance frequency can only be adjusted by changing the pipe length. It's remarkable that the diameter of the pipe doesn't influence the frequency. For adjusting $\omega_{resonance}$, the length of the pipe should have to be continuously variable like a slide trombone. The larger the length, the lower the resonance frequency. The highest required resonance frequency of 200 $[Hz]$ (equals $\omega = 1256$ $[rad/s]$) prescribes the basic pipe length of L=1.07 $[m]$. This is the maximum length of the pipe between the pumps and hydraulic motor. Figure 5.5A shows the influence of the pipe length on the resonance frequency.

If applying the slide trombone principle isn't possible, another way of tuning can be used. The pipe length is kept constant. An extra continuously variable volume (like a hydro cylinder) is added at the motor side of the pipe. This volume acts like a capacity that is added to the pipe capacity. Large extra capacity causes low resonance frequencies, because:

$$\omega_{resonance} = \frac{1}{\sqrt{I(C_{pipe} + C_{extra})}} = \frac{1}{\sqrt{\frac{\rho L^2}{\beta} + \frac{\rho L C_{extra}}{\frac{\pi}{4}D^2}}} \tag{5.5}$$

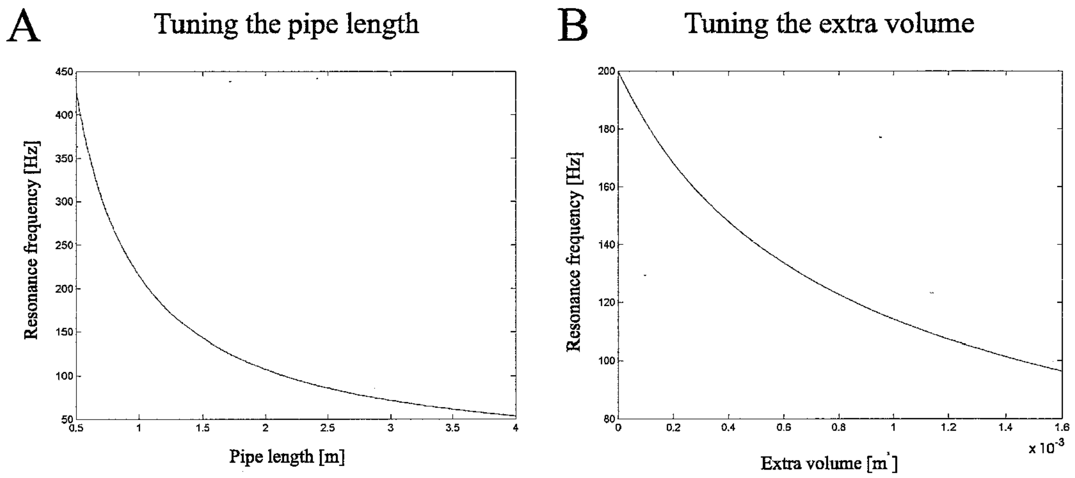

Figure 5.5: Influence of changing the pipe length (picture A) and adding extra volume (picture B) on the resonance frequency.

Figure 5.5B shows the influence of the addition of extra volume on the resonance frequency (L=1.07[m], D=0.024[m]). Adding only a small volume decreases the resonance frequency very much. According to formula 5.5, the frequency decrease also depends on the pipe length and diameter. For achieving $\omega_{resonance} = 200$ [Hz], also in this situation the maximum pipe length is 1.07 [m].

In all situations, the pipe diameter shouldn't be too small because X_R is assumed much smaller than X_I.

5.2.3 Considerations

Tuning the hydraulic system as described before hasn't been tested yet. Before tuning the test rig, some more research has to be done. Improving the model is the first step. Until now, a lumped model has been used. In other words, all resistances, capacities and inductances are concentrated (fig 5.2). This doesn't correspond to the reality. Actually, the pipe should have to be split in a number of small pipe sections (a kind of finite element model). The impedances are divided over the whole length of the pipe. Furthermore the model has to be extended. It has to be possible to determine the effect of pressure waves in the pipe. Then also other ways of tuning the hydraulic system can be studied. Applying the Helmholz principle might be possible.

5.3 Properties improved design

A much higher torque amplitude could be realized in case the improvements discussed in this chapter are applied to the rig. To verify these assumptions, a model has been made based on the model discussed in section 3.2.3. Blocks 2-7 of the original model (figure 3.8) have been omitted. The nominal flow of the valve has increased to 38 [L/min] and the stiffness of the torque transducer (block 11) has become $115 \cdot 10^4$ [Nm/rad]. The value of the inertia of block 10 has become $6.21 \cdot 10^{-3}$ [kgm^2] due to the reduced inertia of the shaft between the hydraulic motor and torque transducer. Graph 1 in figure 5.6 shows the corresponding Bode plot of the mechanical and hydraulic system in case the nominal torque is 50 $[Nm]$. The eigenfrequency of the mechanical system increased and is consequently not visible in the figure. Graph 2 represents the Bode plot of the original design. It is clear that the performance of the improved design has increased drastically.

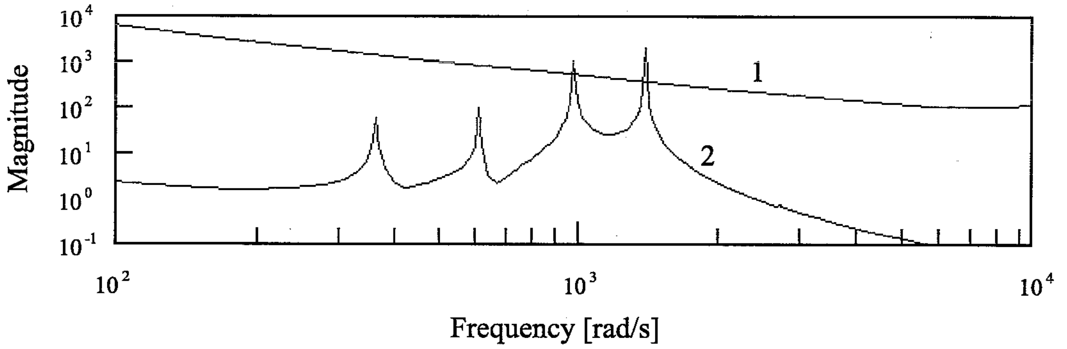

Figure 5.6: Bode plot of mechanical and hydraulic system of the improved design (1) and the original design (2). Nominal torque equals 50 $[Nm]$

The use of a servovalve with large bandwith and high nominal flow instead of the small proportional valve is important. Due to the high flow, the use of the reverse connection is not necessary. The valve can be mounted closer to the hydraulic motor. The capacity of the oil volume in the pipe decreases and performance improves.

Chapter 6

Other dynamic test rigs

Because simulating dynamic torque generated by the combustion engine is a topical subject, different companies and a university are studying this subject as well. During the graduation period, some information of these rigs is gathered. Unfortunately the amount of information is not that extensive. In this chapter three different approaches of designing a dynamic test rig are discussed.

It is difficult to predict the performance of a specific rig concerning the simulation of dynamic engine torque. Not only the motor inertia and torque, but also the other parts (e.g. transmission and brake) influence the dynamic torque behaviour. In this chapter the suitability of the motor that drives the rig is based on the TI-ratio: the ability of the motor to accelerate itself. For simulating an engine, the motor must have a TI-ratio that is equal or higher than the engine that has to be simulated. The TI-ratio of the Bora engine is 1550 $[rad/s^2]$.

6.1 Schenck Dynas3 220 ULI

Schenck is a German company specialized in mechatronics. They are very experienced in developing and building test rigs. The rig designed for simulating combustion engines (Dynas3 220 ULI) is equipped with a 220 $[kW]$, 380 $[Nm]$ electric motor. Compared to other e-motors that generate this power, the rotor inertia of the Dynas motor is very low, only 0.11 $[kgm^2]$. The TI-ratio of this motor is 3455 $[kgm^2]$. Special water and air cooling is necessary because of the high heat development. The feasible torque amplitudes and frequencies are unknown.

6.2 Rostock multiple electric motors resonance test rig

Instead of one electric motor, the test rig developed by the Rostock University is equipped with multiple motors in series. Figure 6.1 shows the working principle.
The torque that has to be generated is divided over the motors. The main (induction) motor is low dynamic due to high inertia and generates a constant mean torque. The small servo motor is high dynamic and can only generate lower (compared with the main motor) torques. The servo motor is able to change quickly the generated torque from positive into negative. The arrows in the figure represent the magnitude and direction of the torque. The main motor and servo-motor are connected by means of a torsion spring. This spring gives the servo-motor a degree of freedom in rotational direction. It enforces the torque but not the

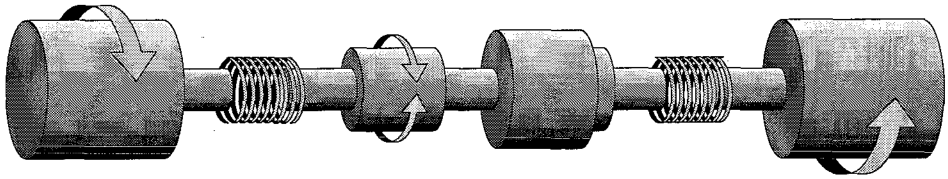

Figure 6.1: Test rig equipped with multiple electric motors. [20]

rotation. The inertia's of both motors are uncoupled. The servo-motor is connected with the transmission (rigid) and executes the prescribed rotation. The transmission is loaded by an electric brake, also connected by means of a spring. The servo-motor and transmission resonate at certain test frequencies due to the applied springs. The eigenfrequencies of the system are used to obtain the required amplitudes.

some motor properties:

Servo motor:	T=200	$[Nm]$	J=0.058	$[kgm^2]$	$TI - ratio = 3448$	$[rad/s^2]$
Induction motor:	T=610	$[Nm]$	J=1.93	$[kgm^2]$	$TI - ratio = 316$	$[rad/s^2]$

The TI-ratio of the servo motor should be high enough to simulate a combustion engine. The servo motor is specially developed for this application and is equipped with water cooling. The TI-ratio of the total system is 407 $[rad/s^2]$. This is a factor 3.7 less than the TI-ratio of the combustion engine. The motors will not be able to accelerate as fast as a combustion engine will do.
The developed rig is still not able to simulate the dynamic engine torques. This is due to the frequency modulator. This part is not able to cope with the necessary high currents for powering the servo motor.

6.3 MTS Spinning Torsion Actuator

MTS is an American company specialized in mechanical testing and simulation equipment. They also developed a transmission test rig that is able to simulate the engine torque vibrations. Like the Rostock University design, also this rig is equipped with two motors. A large motor for generating the nominal torque and a smaller actuator for adding the torque fluctuations. Figure 6.2 is a schematic representation of the MTS test rig. Instead of a small low inertia electric motor, the MTS design is equipped with a hydraulic actuator. The reaction torque of the actuator acts on the electric motor instead of the fixed world. A flywheel for simulating the vehicle inertia is mounted between the transmission and the brake motor.
The most interesting part of the rig is the spinning torque actuator. It's a dual vane type rotary actuator. The maximum rotation angle is 100 degrees. This small angle is large enough because only the angular differences between the drive motor and the transmission have to be

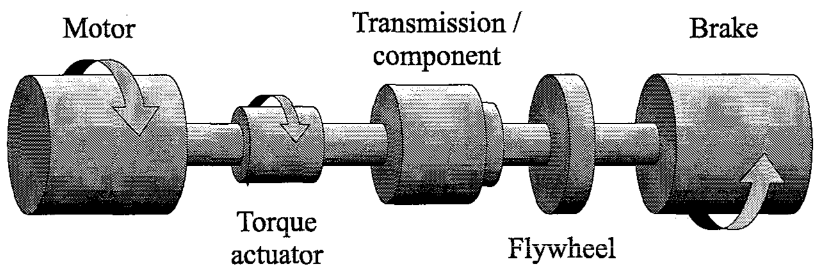

Figure 6.2: MTS test rig equipped with a hydraulic spinning torque actuator. [26]

intercepted. The oil flows will be small because of the small rotating angles. The applied servo valve is small and has a large bandwith. The valve takes care of the high torque frequency. According to the brochure the frequency range is 20-850 $[Hz]$ (!!), the power range is 55-250 $[kW]$. The generated torque amplitude is not known.

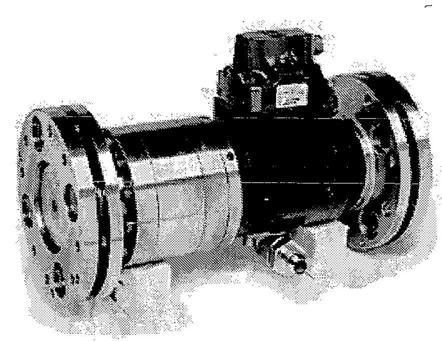

Figure 6.3: MTS spinning torque actuator [25]

Figure 6.3 shows the MTS spinning actuator inclusive the high dynamic servo valve and oil connection. The actuator can also be used to update existing static test rigs. The actuator has to be mounted between the motor and transmission.

6.4 Conclusions

The developers of the test rigs described in the previous sections all claim that the rigs are able to simulate combustion engines. Unfortunately, not enough information is available to confirm if these assertions are true.

Due to the high TI-ratio, the Schenck design should be able to satisfy some of the demands. The TI-ratio of the Rostock design is much too low. Engine torque simulation is, due to the applied springs, only possible at certain frequencies. The MTS spinning torque actuator seems to be the best solution to the problem. Especially because of the low flows, a valve with high bandwith can be applied that might be able to simulate the desired dynamic torque.

Unfortunately no bode plots of these rigs are present. So it's unknown what magnitudes of torque can be reached at specific frequencies.

Chapter 7

Conclusions and Recommendations

After designing, building and testing the prototype transmission test rig, at lot of knowledge is acquired concerning dynamic hydraulic systems. Some conclusions can be drawn and some recommendations can be made.

7.1 Conclusions

Despite of the high TI-ratio of the applied hydraulic motor, the prototype test rig seems not to be able to simulate all of the combustion engine properties. The demands are only partly satisfied.

Static properties: Due to high pressure drops in the pipes at high speeds, the desired maximum torque can not be reached. The maximum speed of the combustion engine can not be reached due to the limit of the maximum speed of the chosen hydraulic motor.

Dynamic properties: The desired torque amplitudes can not be reached over the desired frequency spectrum due to the small sized valve with limited bandwith in combination with a high capacity of the oil in the system.

The use of a fixed displacement axial piston motor is not ideal due to the generated torque ripple. The mechanical system of the prototype test rig resonates at its eigenfrequency. The torque amplitude at the eigenfrequency is much larger than the dynamic torque amplitude generated by the valve. Companies that develop dynamic test rigs don't use axial piston motors. Only vane type of rotary actuators that generate constant torque are applied.

The configuration can be improved in several ways. Creating pressure variations by the valve mounted in a parallel branche still seems to be a good starting point.

The magnitude of the Bode plot of the mechanical / hydraulic system increases due to the resistance of the needle valve. Unfortunately, the loss of energy is significant.

7.2 Recommendations

The mechanical configuration is not optimal. Only a single hydraulic motor is used for generating the nominal and dynamic torque. The use of a single motor results in some contradictory demands concerning the diameter of the supply pipe. For decreasing the pressure losses the diameter should be large enough. However, the dynamic torque amplitudes increase with decreasing capacity of the hydraulic system. The diameter of the pipe should be as small as possible.

Using multiple motors could solve this problem. Separating the motor functions should be investigated. Especially design C and D of figure 3.1 may be suitable solutions. The torque of the motor generating the rotation speed should be kept constant. Fixed displacement motors with pistons as used in the prototype cause dynamic torques and aren't therefore suitable. An electric motor could be a more appropriate choice. The motor generating the dynamic torque only has to rotate over a small rotation angle. A vane type of rotary actuator can be used. Because only small flows occur, a small sized valve with high bandwith can be applied.

Tuning the hydraulic system as described deserves special attention. It may improve the performances of the rig. However, some more investigations are necessary.

A transmission test rig equipped with a combustion engine will be available at the automotive laboratory soon. It is recommended to measure the dynamic engine torque on the transmission so the model as described in appendix A can be validated.

Symbols

greek	description	unit
α	crank angle measured from firing top	$[rad]$
β	bulk modulus	$[Pa]$
ϕ_n	phase angle for gas torque	$[rad]$
ω	speed of rotation	$[rad/s]$
$\omega_{resonace}$	resonance frequency	$[rad/s]$
θ	phase shift between successive firing / gradient	$[rad]$
ρ	density	$[kg/m^3]$
μ	dynamic viscosity	$[Ns/m^2]$

roman	description	unit
A	piston area	$[m^2]$
C	capacity of the oil volume	$[m^4s^2/kg]$
B	piston bore	$[m]$
D	diameter	$[m]$
c_{tc}	torsional damping torque converter	$[Nms/rad]$
c_v	air drag coefficient	$[kg/m]$
F_d	air drag on vehicle	$[N]$
F_g	hill climbing resistance	$[N]$
F_w	tire tractive force	$[N]$
g	gravity	$[m/s^2]$
H_c	transfer function of the complete system	$[N]$
H_{mh}	transfer function of the mechanical and hydraulic system	$[N]$
H_{pp}	transfer function of the primary pulley	$[-]$
H_{trm}	transfer function to the transmission	$[-]$
H_v	transfer function of the proportional valve	$[-]$
I	inductance of the oil volume	$[kg/m^4]$
J_e	engine + pump + impeller inertia	$[kgm^2]$
J_l	lockup inertia	$[kgm^2]$
J_p	inertia primary pulley + DNR carrier and planets	$[kgm^2]$
J_s	secundary pulley + final drive + differential	$[kgm^2]$
J_t	turbine + DNR sun gear inertia	$[kgm^2]$
J_{turb}	turbine inertia	$[kgm^2]$
J_w	inertia two wheels	$[kgm^2]$

k_d	torsional stiffness drive shaft	$[Nm/rad]$
k_l	torsional stiffness lockup spring clutch	$[Nm/rad]$
L	length pipe / connecting rod	$[m]$
m_R	mass reciprocating parts	$[kg]$
m_v	vehicle mass	$[kg]$
n	harmonic order	$[-]$
N_c	number of cylinders	$[-]$
q	flow	$[m^3/s]$
q_C	flow through the capacity	$[m^3/s]$
q_I	flow through the inductance	$[m^3/s]$
q_{nom}	nominal flow through the valve	$[m^3/s]$
q_{res}	resultant flow	$[m^3/s]$
r	compression ratio	$[-]$
R	distance crankshaft axis to center crankpin	$[m]$
R	resistance	$[kg/m^2s]$
R_{cvt}	CVT ratio	$[-]$
R_d	final reduction gear ratio	$[-]$
R_w	wheel radius	$[m]$
p	pressure	$[N/m^2]$
S	piston stroke	$[m]$
t	time	$[s]$
T	torque	$[Nm]$
T_e	total torque applied to the crankshaft	$[Nm]$
T_i	torque due to the movement of reciprocating parts	$[Nm]$
T_m	mean torque generated by the engine	$[Nm]$
T_p	torque due to gas pressure on the piston	$[Nm]$
T_{rf}	roll resistance torque both front wheels	$[Nm]$
T_{rr}	roll resistance torque both rear wheels	$[Nm]$
T_{trm}	torque acting on the transmission	$[Nm]$
u	dimensionless valve spool position	$[-]$
u_a	actual valve spool position	$[-]$
u_d	desired valve spool position	$[-]$
U_n	cosine coefficient for gas torque	$[-]$
v_v	vehicle speed	$[m/s]$
$\dot{v}_v$	vehicle acceleration	$[m/s^2]$
V	volume	$[m^3]$
V_d	displacement	$[m^3/rev]$
V_n	sine coefficient for gas torque	$[-]$
x	distance crankshaft axis to center piston pin	$[m]$
$\dot{x}$	piston speed	$[m/s]$
$\ddot{x}$	piston acceleration	$[m/s^2]$
x_r	non symmetric tire deformation	$[m]$
X_C	capacitive impedance	$[kg/m^4s]$
X_I	impedance impedance	$[kg/m^4s]$
X_R	resistance impedance	$[kg/m^2s]$

Bibliography

[1] Sciuto, M.; Hellmund, R.: *"Road to Rig" - Simulationskonzept an Powertrain-Prüfständen in der Getriebeerprobung*, ATZ Automobiltechnische Zeitschrift, 2001, vol 103 afl 4, blz. 298-307

[2] Spijker, E.: *Steering and control of a CVT based hybrid transmission for a passenger car*, Ph.D. thesis, Technische Universtiteit Eindhoven, 1994, ISBN 93-886-8173-5

[3] Taylor, C.F.: *The Internal-Combustion Engine in Theory and Practime*, volume II, Massachusetts Institute of Technology, 1968

[4] Serrarens, A.F.A.: *Coordinated Control of The Zero Inertia Powertrain*, Ph.D. thesis, Technische Universiteit Eindhoven, 2000, ISBN 90-586-2583-9

[5] Vroemen, B.G.: *Component Control of The Zero Inertia Powertrain*, Ph.D. thesis, Technische Universiteit Eindhoven, 2001, ISBN 90-380-2583-6

[6] van Druten, R.M.: *Transmission Design of The Zero Inertia Powertrain*, Ph.D. thesis, Technische Universiteit Eindhoven, 2001, ISBN 90-386-2603-7

[7] Kok, J.J.: *Regelen van Multivariabele Systemen*, Lecture notes, Technische Universiteit Eindhoven, 2001

[8] Gyan, P., Ginoux, S., Champoussin, J.C.: *Crankangle based torque estimation: mechanistic / stochastic*, SAE technical paper, 2000-01-0559, March 2000

[9] Mauer, F.: *Modeling and experimental validation of torsional crankshaft dynamics*, SAE technical paper, 940630, March 1994

[10] Azzoni, P., Minelli, G., Moro, D.: *Indicated and load torque estimation using crankshaft angular velocity measurement*, SAE technical paper, 1999-01-0543, March 1999

[11] Azzoni, P., Moro, D., Ponti, F.: *Engine and load torque estimation with application to electronic throttle control*, SAE technical paper, 980795, February 1998

[12] Porter, F.P.: *Harmonic Coefficients of Engine Torque Curves*, Journal of Applied Mechanics, 10, March 1943, A-33

[13] Talor, E.S., Morris: *Harmonic analysis of engine torque due to gas pressure*, Journal of Aeronautical Science, 3, 129, February 1936

[14] Watton, J.: *Fluid Power Systems*, School of Engineering, University of Wales, Prentice Hall, 1989, ISBN 0-13-323197-6

[15] Pinches, J.P., Ashby, J.G.: *Power Hydraulics*, Sheffield City Polytechnic UK, Prentice Hall, 1988, ISBN 0-13-687443-6

[16] McCloy, D., Martin, H.R.: *Control of Fluid Power*, Ulster Polytechnic, Ellis Horwood, 1980, ISBN 0-85312-135-4

[17] Walters, R.B.: *Hydraulic and Electro-hydraulic Control Systems*, Elsevier Applied Science, 1991, ISBN 1-85166-556-0

[18] Blackburn, J.F., Reethof, G., Shearer, J.L.: *Fluid Power Control*, The Technology Press of M.I.T., 1960, 59-6759

[19] Beckwith, T.G., Marangoni, R.D., Lienhard, J.H.: *Mechanical Measurements*, Addison-Wesley Publishing Company, 1993, ISBN 0-201-56947-7

[20] Falkenstein, J.; Hirschmann, K.H.: *Elektrischer Prüfstandsantrieb ersetzt Verbrennungsmotor*, Antriebstechnik 40, 2001, No. 9, blz. 70-72

[21] Post, W.: *Hydraulische Aandrijftechniek*, Lecture notes 4N630, Technische Universiteit Eindhoven, 1997

[22] Internet site Moog: www.Moog.com

[23] Catalogue Hottinger Baldwin Messtechnik 1999

[24] Catalogue Bosch Servo Solenoid Valves

[25] Catalogue MTS Model 217 Spinning Torque Actuator

[26] Catalogue MTS Virtual Engine Simulator

List of Figures

Appendix A

Transmission load

Before developing the hydraulic test rig, it has to be known what demands it has to satisfy. One of the demands concerns the dynamic torque acting on the transmission and variator. Due to the intermittent combustion and the acceleration and deceleration of the reciprocating parts, the torque on the crankshaft is not constant. The dynamic torque behaviour (torque at every crank angle at different engine loads and speeds) of the VW Bora in combination with the CVT transmission is not known yet. There are different ways to obtain the behaviour:

Measuring a map: when an engine is available, it is possible to measure the dynamic torque by mounting a torque sensor on the transmission shaft. The engine has to be mounted in a vehicle or on a test rig. The availability of an engine and transmission is a required. This way of obtaining the engine behaviour actually outpaces the target (designing a test rig without an combustion engine) because an engine still has to be used.

Measuring data from literature: In literature, a large amount of information can be found concerning combustion engines. It is expected that also measuring data of dynamic torque behaviour is available.

Formulate an algorithm: This way is expected to be difficult because the dynamic torque behaviour is dependent of numerous variables. If once an algorithm has been determined, it is very easy to simulate different type of engines under various conditions.

Because measuring the torque on a vehicle or engine test rig is not possible and the available information in literature wasn't satisfying ([8] [9] [10] [11]), the only way to determine the dynamic torque is by formulating algorithm.

A.1 Formulating an algorithm

The algorithm is primarily meant for determining the demands the rig has to satisfy concerning the dynamic torque. So an algorithm has to be formulated that is easy to use and is accurate enough. Accurate simulation programs like GT-Power (from Gamma Technologies) use a lot of parameters. The engine parts have to be modelled very accurately. These kind of programs won't be used because modelling engines so accurate is outside the scope of the project. Furthermore, the necessary accurate engine properties aren't known.
Instead of using a difficult simulation program, a simple model will be developed. The model uses basic formulas and consists of two parts: an engine model and a powertrain transfer

model. The engine model calculates the torque acting on the crankshaft. The powertrain transfer is used to calculate the torque transfer from the crankshaft to the transmission and CVT variator. Both models are programmed and coupled in MatLab.

A.1.1 Engine torque model

Torque on the crankshaft will be here classified as engine torque. It is caused by two sources. The first one is the gas pressure on the piston. The resulting torque on the crankshaft is called the gas pressure torque $T_{p(\alpha)}$. The second source that generates torque on the crankshaft is acceleration and deceleration of the reciprocating parts: the pistons and the connecting rods. It is called the inertia torque $T_{i(\alpha)}$. The parts accelerate and decelerate twice every rotation. When accelerating, the torque on the crankshaft is negative, when decelerating the torque is positive. The average torque is zero. If $T_{e(\alpha)}$ is denoted as the torque applied to the crankshaft by one of the cylinders at any given crank angle α (measured from firing top), then

$$T_{e(\alpha)} = T_{p(\alpha)} + T_{i(\alpha)} \tag{A.1}$$

In the next sections can be read how the gas pressure and inertia torques are determined. The whole model is based on VW Bora specifications. General properties of the engine:

Total cylinder volume:	1.6 $[l]$
Fuel	petrol
Cycles	4 stroke
Cylinders:	4 (in line)
Bore B:	76.5 $[mm]$
Stroke S:	86.9 $[mm]$
Compression ratio r:	10.3:1
Length connecting rod L:	165 $[mm]$
Mass piston	0.30 $[kg]$
Mass connecting rod	0.58 $[kg]$

The used indicator diagrams were calculated by TNO Automotive in Delft.

Gas pressure torque

The gas pressure torque $T_{p(\alpha)}$ acting on the crankshaft changes constantly because of the intermittent pressure on the piston and the dependency of the geometry (connecting rod / crank) on the crank angle. The instantaneous torque on the crank shaft due to gas pressure can be found by noting that, neglecting friction, the work done on the piston is equal to the work done on the crankshaft.

$$pdV = T_p d\alpha \tag{A.2}$$

where p is the pressure on the piston and V the cylinder volume. Since

$$dV = Adx \tag{A.3}$$

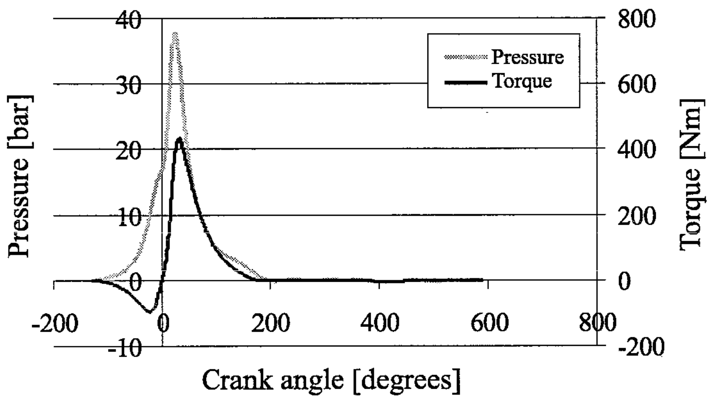

Figure A.1: Gas pressure versus crank angle. Average gas pressure torque is 29 $[Nm]$ per cylinder

where A represents the piston area and x the piston position, combining formula A.2 and A.3 gives:

$$T_p = p\frac{dV}{d\alpha} = pA\frac{dx}{d\alpha} = pA\frac{dx}{dt}\frac{dt}{d\alpha}$$

$$T_p = pA\frac{\dot{x}}{\omega} \tag{A.4}$$

The piston velocity is expressed by $\dot{x}$ $[m/s]$, the crankshaft speed by ω $[rad/s]$. The value of p has to be taken from the indicator diagram (plot of pressure versus crank angle). According to [3] (blz. 296), $\frac{\dot{x}}{\omega}$ can be approached by:

$$\frac{\dot{x}}{\omega} = R(sin\alpha + 0.5\frac{R}{L}sin(2\alpha)) \tag{A.5}$$

R represents half the stroke. Combining formula A.4 and A.5 gives

$$T_p = pAR(sin\alpha + 0.5\frac{R}{L}sin(2\alpha)) \tag{A.6}$$

Figure A.1 shows the indicator diagram and the resulting torque on the crank shaft. The Bora motor generates an average torque of 29 $[Nm]$ per cylinder.
Because the indicator diagram shows a periodic function (in theory every two rotations the same pattern), the instantaneous gas pressure torque for each cylinder may be expressed as a Fourier series. The representation of the gas pressure torque by sines and cosines is especially useful for the transfer.

$$T_{p(\alpha)} = T_m(1 + \sum_{n=\frac{1}{2},1,1\frac{1}{2},\ldots}^{n=\infty} U_n sin(n\alpha) + V_n cos(n\alpha)) \tag{A.7}$$

T_m represents the mean gas torque, n the harmonic order. Values of the coefficients U_n and V_n are plotted in figure A.2. Coefficients for various types of engines are available in literature [12].

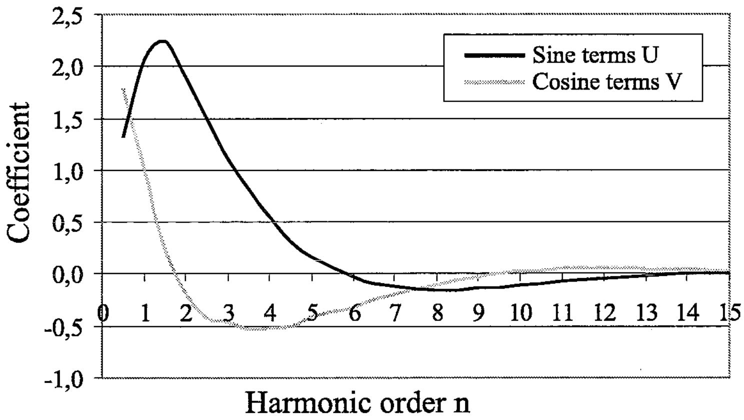

Figure A.2: Harmonic coefficients U and V of gas pressure torque (VW Bora engine).

According to [3] blz. 272, when changing the spark timing, compression ratio or fuel-air ratio, the coefficients don't change that much. Cycle-to-cycle variations will to some extent modify the torque coefficients. An exact prediction of engine-torque coefficients is not possible. In formula A.7, no engine speed variable can be found. According to [13], the gas-pressure torque only depends on T_m. The torque scales linearly with the mean load. This statement is acceptable when taking a look at figure A.3. The figure shows three gas pressure torque plots calculated from three indicator diagrams (different engine speeds and torques). The diagrams are almost linear multiplications (stretched) of each other.

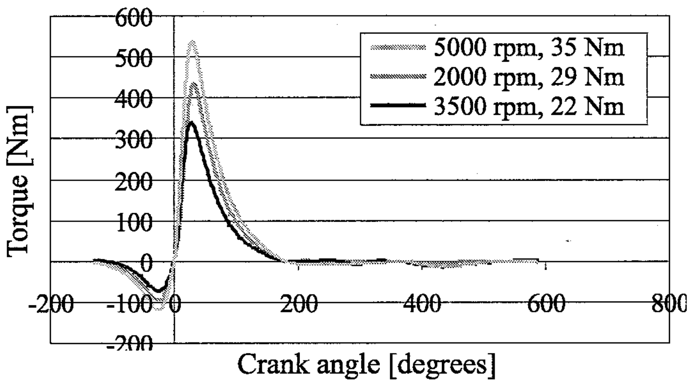

Figure A.3: Gas pressure torque for three different situations.

Figure A.2 shows the harmonic coefficients for a single-cylinder 4-cycle engine. The process of summing torque in a multi-cylinder engine is easy if all torques act on the same axis and firing is evenly spaced. It is assumed that the Bora engine satisfies these demands. Angle θ represents the crank angle between firing. $\theta = 4\pi/N_c$ for 4-cycle and $2\pi/N_c$ for 2-cycle engines. N_c represents the number of cylinders. An example of torque-vector addition can be seen in figure A.4.

In the figure, the angle between the successive numbers represents the phase angle between the cosines / sines of a specific order number. The phase shift is $n\theta$. This example illustrates the general principle that, with evenly spaced firing, the vectors add if $n\theta$ is a multiple of 2π

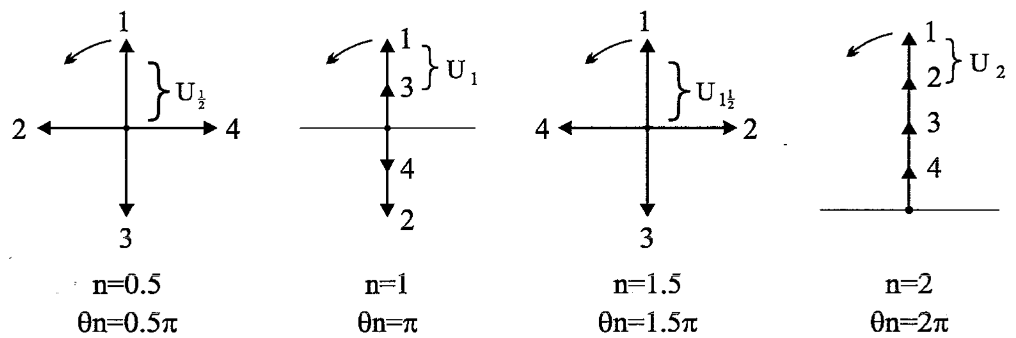

Figure A.4: Vectordiagram of torque output for 4-cylinder 4-cycle engine [3]

(the right picture). For other values of n, the coefficients cancel out. In general, for 4-stroke engines the vectors add when n is a multiple of $N_c/2$, for 2-stroke engines the vectors add when n is a multiple of N_c. All other coefficients cancel out. Table A.1 summaries these relations for various number of cylinders. Note that the arrangement of cylinders does not make any difference as long as the firing intervals are equal. Now it's clear that smooth engine operation is approached as the coefficients cancel out with increasing number of cylinders. For the Bora engine (4 cylinder 4 stroke), the lowest sine and cosine frequency is twice the engine frequency.

Number of cylinders	*Cycle*	*Orders appearing, n*
1	2	1, 2, 3, 4, etc.
1	4	$\frac{1}{2}$, 1, $1\frac{1}{2}$, 2, $2\frac{1}{2}$, etc.
2	2	2, 4, 6, 8, etc.
2	4	1, 2, 3, 4, etc.
3	2	3, 6, 9, etc.
3	4	$1\frac{1}{2}$, 3, $4\frac{1}{2}$, 6, $7\frac{1}{2}$, etc.
4	2	4, 8, 12, etc.
4	4	2, 4, 6, 8, etc.
5	2	5, 10, 15, etc.
5	4	$2\frac{1}{2}$, 5, $7\frac{1}{2}$, etc.
6	2	6, 12, 18, etc.
6	4	3, 6, 9, 12, etc.
etc.		

Table A.1: Orders of gas-pressure torque which appear in multi-cylinder engines with even firing and uniform indicator diagrams. [3]

Inertia torque

Except gas-pressure, also the reciprocating parts generate torque on the crankshaft because they accelerate and decelerate constantly. When accelerating, the torque on the crankshaft is negative, when decelerating the torque is positive. The reciprocating mass m_R consists of the piston mass and a part of the connecting rod. The connection rod makes a combined translating (piston side) and rotating movement (crank side). Only the translating mass part is part of m_R. The translating mass part can be determined by dividing the connecting rod mass in two pointmasses located at its ends. The sum of the two pointmasses equals the connecting rod mass. The center of gravity is preserved. The lumped mass at the piston side is the translating part. More detailed information: [3] pag. 266-268. The instantaneous inertia torque $T_{i(\alpha)}$ can be calculated by supposing that the change in kinetic energy of the reciprocating parts must be equal to the work done by the crankshaft on the connecting rod. This results in the next formula:

$$d(\frac{m_R}{2}\dot{x}^2) = -T_i d\alpha$$

$$\frac{d}{dt}(\frac{m_R}{2}\dot{x}^2) = m_R\dot{x}\ddot{x} = -T_i\frac{d\alpha}{dt} = -\omega T_i$$

$$T_i = -m_R\ddot{x}\frac{\dot{x}}{\omega} \tag{A.8}$$

$\alpha = 0$ corresponds to the top death center of the (if there are more then one, the first) cylinder. $\dot{x}$ and $\ddot{x}$ are the piston speed and acceleration. Substituting the formulas for $\dot{x}$ and $\ddot{x}$ ([3] pag. 264) approaches the next formula close:

$$T_i = m_R\omega^2 R^2(\frac{1}{4}\frac{R}{L}sin\omega t - \frac{1}{2}sin2\omega t - \frac{3}{4}\frac{R}{L}sin3\omega t) \tag{A.9}$$

In contrast with the gas pressure torque, the inertia torque is proportional to the square of the engine speed and is independent of the nominal torque. The torque on the crankshaft generated by the reciprocating parts of one cylinder can be calculated by using formula A.9. When the engine consists of more cylinders, the formula changes in:

$$T_i = m_R\omega^2 R^2[(\frac{1}{4}\frac{R}{L}(sin\omega t + sin(\omega t + \theta) + sin(\omega t + 2\theta).....)$$

$$-\frac{1}{2}(sin2\omega t + sin2(\omega t + \theta) + sin2(\omega t + 2\theta) + ...)$$

$$-\frac{3}{4}\frac{R}{L}(sin3\omega t + sin3(\omega t + \theta) + sin3(\omega t + 2\theta) + ...)] \tag{A.10}$$

Notice that the second order component is large and independent of R/L. By arranging the cylinders of a multi cylinder engine in a specific way, the resulting inertia torque cancels out. The average inertia torque is zero because the sinuses in formula A.9 don't have an offset. The lowest sine frequency is similar to the engine frequency.

Figure A.5 is the result of formula A.1, A.7 and A.10. It shows the gas pressure torque, inertia torque and the resulting torque on the crankshaft for the Bora engine running at 2500 [rpm] and 115 [Nm]. At low speeds and high nominal torque, the gas pressure torque rules. At high speeds and low nominal torques, the inertia torque rules.

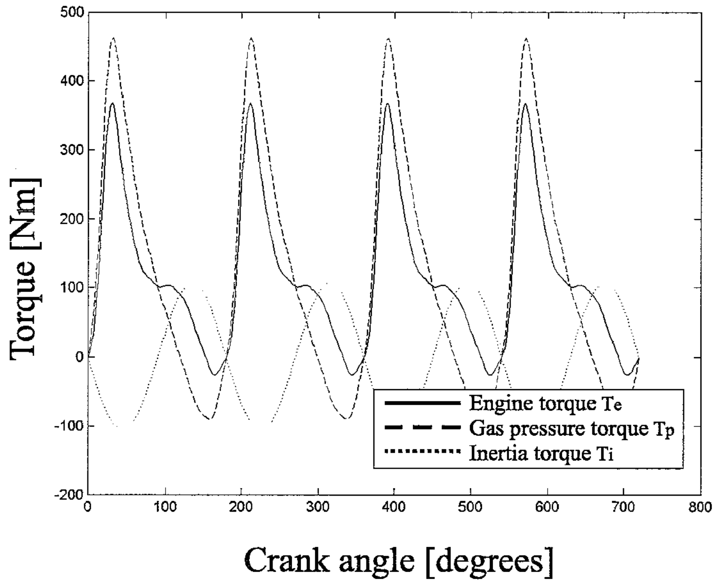

Figure A.5: Dynamic torque acting on the crankshaft. $T_e = T_p + T_i$

A.1.2 Powertrain transfer model

With the formula's presented in the previous section, the dynamic torque on the crankshaft can be calculated. However, the torques acting on the transmission and variator have to be known. The torque is transmitted by the powertrain. The corresponding transfer functions from the crankshaft to the transmission and variator will be determined in this section. In general, the term powertrain refers to the entire system necessary to propel the vehicle: from fuel tank to tire. In this report, the term is restricted to the parts that influence the transmission load. Because the vehicle body also influences the powertrain dynamics (e.g. inertia and interaction with environment), it is seen as a part of the powertrain.

VW Bora CVT powertrain

Figure A.6 shows the Bora powertrain. For simplicity, the powertrain is drawn without the vehicle body. The powertrain is not standard, it is equipped with a CVT (continuous variable transmission) developed by VDT. The powertrain consists of the following parts:

Engine: Generates the power that propels the vehicle. Loads the transmission.

Starter flywheel: An inertia coupled to the engine's crankshaft. Lets the engine run smoother. The starter motor is coupled to the flywheel.

Torque converter: A fluid coupling mounted between the engine and the transmission. Its purpose is transmitting and amplifying the engine torque during vehicle launch. When the engine reaches 950 rpm, a mechanical clutch (lock-up) closes. Then, the torque converter acts as a inertia-spring system with little damping.

Pump: A pump takes care of the oil flow and pressure necessary for operating the torque converter, DNR set and CVT.

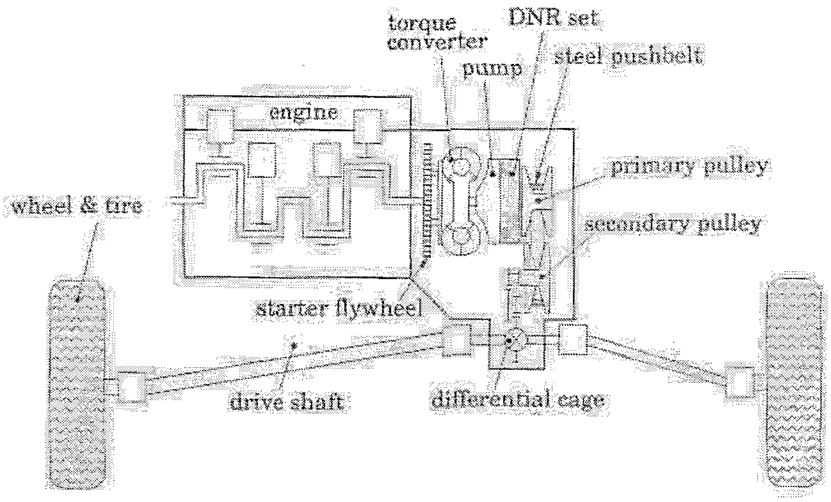

Figure A.6: CVT based powertrain [4]

DNR set: Planetary gear set for shifting between **D**rive-**N**eutral-**R**everse. For "D", the speed of the input shaft is equal to the speed of the output shaft. When driving in "R", the gear ratio equals -1.1

CVT: The **C**ontinuously **V**ariable **T**ransmission consists of a hydraulically controlled metal pushbelt variator. The diameter of the pulleys can change continuously. The possible range of the ratio is limited by the underdrive ratio (0.416) and overdrive ratio (2.15).

Final drive, differential and drive shafts: For reducing the speed and increasing the torque, two stages of gear sets (overall ratio 0.2127) are applied to the powertrain. The differential divides the torque between the two drive shafts. The drive shafts transmit the torque from the differential to the wheels. The shafts have low inertia and are relatively flexible.

Tires, vehicle and external interactions: Traction force causes slip between tires and road. The external load on the powertrain is determined by the roll resistance (tire deformation), hill grade, air drag and accelerating of the wheel inertia's and vehicle mass.

Modeling powertrain parts

For calculating the transfers, a model of the powertrain has to be developed. The powertrain will be reduced to basic mechanical components (inertia's, springs and dampers) and a tire model. Figure A.7 shows the Bora powertrain model. Explanation of the variables can be found in the table. As can be seen in figure A.7, some inertia's are represented by equivalent inertia's. Of course all parts have an inertia, spring and damper coefficient. Only (relatively) small spring and damper coefficient have impact on the system behaviour. Other coefficients are left out of the model.

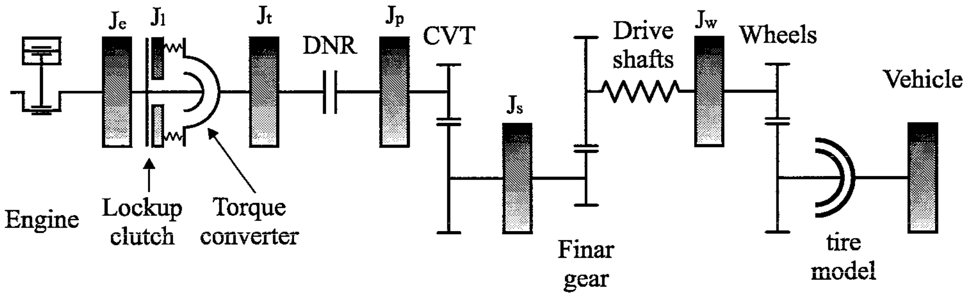

Figure A.7: powertrain model [4]

Variable	Description	Value	Unit
c_{tc}	torsional damping torque converter	1	$[Nms/rad]$
F_d	air drag on vehicle		$[N]$
F_g	hill climbing resistance		$[N]$
J_e	engine + flywheel + impeller inertia	0.156	$[kgm^2]$
J_l	lockup inertia	10-5	$[kgm^2]$
J_p	primary pulley + DNR carrier and planets	0.042	$[kgm^2]$
J_s	secundary pulley + final drive + differential	0.033	$[kgm^2]$
J_t	turbine + pump + DNR sun gear inertia	0.036	$[kgm^2]$
J_w	inertia two wheels	1.7	$[kgm^2]$
k_d	torsional stiffness drive shaft	6200	$[Nm/rad]$
k_l	torsional stiffness lockup spring clutch	1182	$[Nm/rad]$
m_v	vehicle mass	1364	$[kg]$
R_{cvt}	CVT ratio		$[-]$
R_d	final reduction gear ratio	0.2127	$[-]$
R_w	wheel radius	0.307	$[m]$
T_e	torque applied on the crankshaft		$[Nm]$
T_{rf}	roll resistance torque both front wheels		$[Nm]$
T_{rr}	roll resistance torque both rear wheels		$[Nm]$

The operating conditions that correspond to durability tests when dynamic torque is involved are applied to the model.

- vehicle is driving at constant speed
- torque converter is closed
- DNR set runs at "D", ratio = 1
- CVT runs at constant ratio

For simplifying the model, the powertrain efficiency is assumed 100%. Figure A.8 shows the Bora powertrain model split up in parts with corresponding inertia's, masses, speeds, forces and torques.

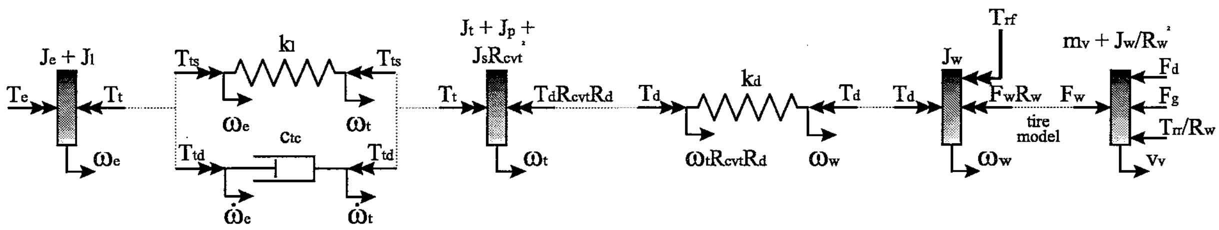

Figure A.8: Simplified powertrain model

Equations for all powertrain parts will be formulated. The basic equations of motion can be found in figure A.9. From left to right in the figure:

Engine, impeller:

$$\dot{\omega}_e = \frac{T_e - T_t}{J_e + J_l} \tag{A.11}$$

torque converter:

$$\dot{T}_{ts} = (\omega_e - \omega_t)k_l \tag{A.12}$$

$$\dot{T}_{td} = (\dot{\omega}_e - \dot{\omega}_t)c_{tc} \tag{A.13}$$

$$\dot{T}_t = \dot{T}_{ts} + \dot{T}_{td} \tag{A.14}$$

turbine, DNR set, variator, final drive:

$$\dot{\omega}_t = \frac{T_t - T_d R_{cvt} R_d}{J_t + J_p + J_s R_{cvt}^2} \tag{A.15}$$

shafts:

$$\dot{T}_d = (\omega_t R_{cvt} R_d - \omega_w)k_d \tag{A.16}$$

front wheels:

$$\dot{\omega}_w = \frac{T_d - F_w R_w - T_{rf}}{J_w} \tag{A.17}$$

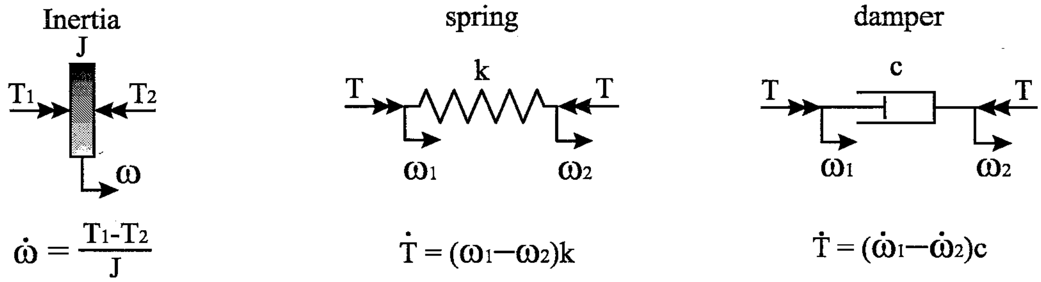

Figure A.9: Basic mechanical parts for modeling transmissions

The tire tractive force F_w can be calculated by using the next formula [4]:

$$F_w = b_w(1 - \frac{v_v}{R_w \omega_w}) m_{vf} g \cos\theta \tag{A.18}$$

F_w depends on the slip between the tire and the road, the total vehicle mass on the front wheels m_{vf} (800 [kg]), the gravity g and the slope θ. b_w = approximately 8.8 [-].

$$T_{rf} = x_r m_{vf} g \cos\theta \tag{A.19}$$

Roll resistance torque is caused by the non symmetric deformation of the tire at the contact interface with the road. The normal force from the road on the tire acts at a small lever $x_r \approx 0.004[m]$ away from the wheel center.

vehicle:

$$\dot{v}_v = \frac{F_w - F_d - F_g - T_{rr}/R_w}{mv + J_w/R_w^2} \tag{A.20}$$

air drag:

$$F_d = c_v v_v^2 \tag{A.21}$$

c_v represents the air drag coefficient $= 0.39$ $[kg/m]$

hill climbing resistance:

$$F_g = m_v g \sin\theta \tag{A.22}$$

Now the complete powertrain model is described by equations of motion, a transfer function can be formulated.

Transfer function

Because of the made assumptions, the model can be analyzed at specific discrete modes. The input of the system is the torque acting on the crankshaft as calculated in the previous section. The output is the torque acting on the transmission or variator.

The powertrain system can be described by a set of six nonlinear first order differential equations:

$$\dot{x}(t) = f(x(t), u(t)) \tag{A.23}$$

$\dot{x} = [\dot{\omega}_e, \dot{T}_t, \dot{\omega}_t, \dot{T}_d, \dot{\omega}_w, \dot{v}_v]^T$. The six differential equations can be found in the previous subsection. $\dot{T}_t$ can be derived by combining formula A.11, A.12, A.13 A.14, A.15:

$$\dot{T}_t = (\omega_e - \omega_t)k_l + (\frac{T_e - T_t}{J_e + J_l} - \frac{T_t - T_d R_{cvt} R_d}{J_t + J_p + J_s R_{cvt}^2}) c_{tc} \tag{A.24}$$

The external input vector only contains the engine torque: $u = [T_e]$. Because the differential equations are not linear, linearisation around a nominal trajectory is necessary. The perturbations δx and δu around the stationary state x_0 with input u_0 are assumed to be small enough to remain in close proximity of the equilibrium state x_0. Therefore the dynamics of these perturbations may be described as the first order approximation [7]:

$$\dot{\tilde{x}}(t) = \frac{\partial f}{\partial x}|_{\bar{x}(t),\bar{u}(t)} \tilde{x}(t) + \frac{\partial f}{\partial u}|_{\bar{x}(t),\bar{u}(t)} \tilde{u}(t) = A(t)\tilde{x}(t) + B(t)\tilde{u}(t) \tag{A.25}$$

The tilde above the variables indicates on small perturbations. The bars point to the nominal trajectory. The differentiation is partial. Matrix A(t) will be obtained in the next way:

$$A(t) = \frac{\partial f}{\partial x}|_{\bar{x}(t),\bar{u}(t)} = \begin{pmatrix} \frac{\partial f_1}{\partial x_1} & \frac{\partial f_1}{\partial x_2} & \cdots \\ \frac{\partial f_2}{\partial x_1} & \frac{\partial f_2}{\partial x_2} & \cdots \\ \vdots & \vdots & \ddots \end{pmatrix} \tag{A.26}$$

Matrix B(t) can be determined in a similar way (∂u in stead of ∂x). Because in this case the nominal trajectory is restricted to a stationary point (engine speed, cvt ratio and nominal engine torque are constant), the matrices will become constant:

$$A(t) = A, \quad B(t) = B \tag{A.27}$$

summarized:

$$\dot{\tilde{x}}(t) = A\tilde{x} + B\tilde{u} \tag{A.28}$$

in this case: $A(j,k)$ (matrix) and $B(j)$ (column) with $j = 1..6$ and $k = 1..6$. After linearisation:

$$\begin{array}{llll}
A(1,1) & = 0 & A(4,1..2) & = 0 \\
A(1,2) & = \frac{-1}{J_e+J_l} & A(4,3) & = k_d R_{cvt} R_d \\
A(1,3..6) & = 0 & A(4,4) & = 0 \\
A(2,1) & = k_l & A(4,5) & = -k_d \\
A(2,2) & = (\frac{-1}{J_e+J_l} - \frac{1}{J_t+J_p+J_s R_{cvt}^2})c_{tc} & A(4,6) & = 0 \\
A(2,3) & = -k_l & A(5,1..3) & = 0 \\
A(2,4) & = (\frac{R_{cvt} R_d}{J_t+J_p+J_s R_{cvt}^2})c_{tc} & A(5,4) & = \frac{1}{J_w} \\
A(2,5..6) & = 0 & A(5,5) & = \frac{-b_w v_v m_{vf} g \cos\theta}{J_w \omega_w^2} \\
A(3,1) & = 0 & A(5,6) & = \frac{b_w m_{vf} g \cos\theta}{J_w \omega_w} \\
A(3,2) & = \frac{1}{J_t+J_p+J_s R_{cvt}^2} & A(6,1..4) & = 0 \\
A(3,3) & = 0 & A(6,5) & = \frac{R_w b_w v_v m_{vf} g \cos\theta}{(m_v R_w^2 + J_w)\omega_w^2} \\
A(3,4) & = \frac{-R_{cvt} R_d}{J_t+J_p+J_s R_{cvt}^2} & A(6,6) & = -\frac{R_w b_w m_{vf} g \cos\theta + 2 c_v R_w^2 v_v \omega_w}{(m_v R_w^2 + J_w)\omega_w} \\
A(3,5) & = 0 & B(1,1) & = \frac{1}{J_e+J_l} \\
A(3,6) & = 0 & A(1,2..6) & = 0
\end{array}$$

Table A.2: Contents matrices A and B

The transfer function can be determined departing from formula A.28:

$$\dot{\tilde{x}} = A\tilde{x} + B\tilde{u} \longrightarrow Laplacetransformation \longrightarrow sX(s) = AX(s) + BU(s)$$

$$(sI - A)X(s) = BU(s)$$

$$H(s) = \frac{X(s)}{U(s)} = (sI - A)^{-1}B \longrightarrow H(j\omega) = \frac{X(j\omega)}{U(j\omega)} = (j\omega I - A)^{-1}B \tag{A.29}$$

Column $H(j\omega)$ consists of the transfer functions that describe the transfer from the input to the different states. Now $H(j\omega)$ is known, it's easy to determine the amplitude ratio and phase shift:

$$Amplitude\ ratio = abs(H(j\omega)) \tag{A.30}$$

$$Phase\ shift = arg(H(j\omega)) \tag{A.31}$$

When using the transfer functions, only T_t (torque in torque converter) and T_d (torque on the front wheels) can be determined. The torque on the transmission and variator acts somewhere between. Inside the transmission, the inertia's are connected rigidly. The torque acting on the separate inertia's can be determined by splitting the inertia's (figure A.10). The inertia's rotate with the same speed because they are connected by a massless rigid body.

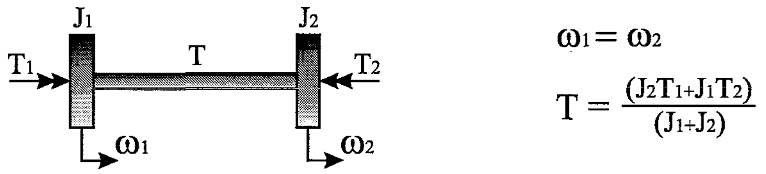

Figure A.10: Inertia split, determining the torque between to inertia's

Using the formula shown in the figure results in:

$$T_{trm} = \frac{(J_t + J_p + J_s R_{cvt}^2 - J_{turb})T_t + J_{turb} T_d R_d R_{cvt}}{J_t + J_p + J_s R_{cvt}^2} \tag{A.32}$$

$J_{turb} = 0.01$ $[kgm^2]$ and represents the turbine part of the torque converter. In the same way, the transfer function can be determined:

$$H_{trm(j\omega)} = \frac{(J_t + J_p + J_s R_{cvt}^2 - J_{turb})H_{2(j\omega)} + J_{turb} H_{4(j\omega)} R_d R_{cvt}}{J_t + J_p + J_s R_{cvt}^2} \tag{A.33}$$

The transfer to the variator (primary variator) $H_{pp(j\omega)}$:

$$H_{pp(j\omega)} = \frac{(J_{pp} + J_s R_{cvt}^2)H_{2(j\omega)} + (J_t + J_p - J_{pp})H_{4(j\omega)} R_d R_{cvt}}{(J_t + J_p + J_s R_{cvt}^2)} \tag{A.34}$$

$J_{pp} = 0.015$ $[kgm^2]$ and represents the inertia of the primary pulley.

stationary point

The transfer functions calculated by using formula A.29 are valid at one situation only: the stationary point. A stationary situation is reached if all states are stationary: equation A.11, A.24, A.15, A.16, A.17 and A.20 are 0. Some variables have to be prescribed and are assumed not to change: cvt ratio R_{cvt}, engine speed ω_e (vehicle speed v_v, air drag F_d and speeds of rotation can be determined) and gradient (hill climbing resistance F_g and normal force on wheels and torque on the drive shaft can be calculated). For all other situations, the stationary situation is different; the matrices have to be determined again.

A.1.3 Connecting the engine model and powertrain transfer

The formulas that describe the gas pressure torque and inertia torque on the crankshaft (A.7 and A.10) consist of different sine and cosine terms. The result of these torques on the transmission and variator depends on the amplitude ratio and phase shift (prescribed by the powertrain transfer function) of the sine and cosine. Figure A.11 shows the Bode plot of the calculated transfer to the transmission. The engine is running at 1000 $[rpm] = 16.7$ $[Hz]$. The crosses represent the gas pressure torque terms, the squares the inertia torque terms. The transfer magnitude shows an eigenfrequency at about 20 $[Hz]$. For higher frequencies, the magnitude decreases fast. It is clear that there is not much left of the amplitudes when the dynamic engine torque reaches the transmission and variator.

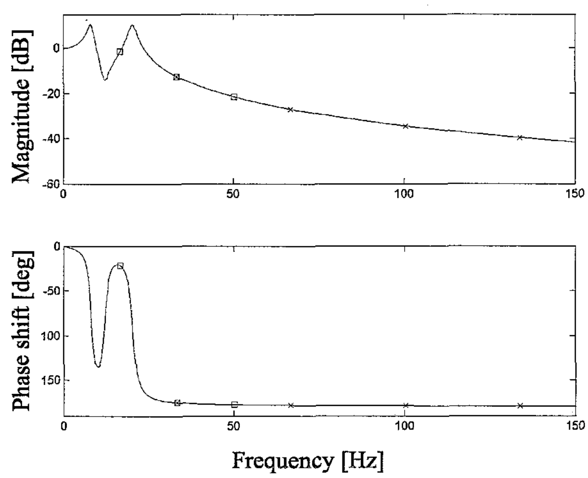

Figure A.11: Bode plot powertrain transfer

A.2 MatLab model

Because doing the preceding calculations by hand is very difficult and time consuming, a Matlab program has been made. Figure A.12 shows a schematic representation of the Matlab program operating procedure. The figure summarizes appendix A. The program is also able to calculate the engine torque in case of different engines configuration (different number of cylinders and 2-4 stroke).

The left side of the figure presents the input variables. These are: slope θ, cvt ratio R_{cvt}, engine speed ω_e, number of cylinders N_c and number of cycles. The stationary situation will

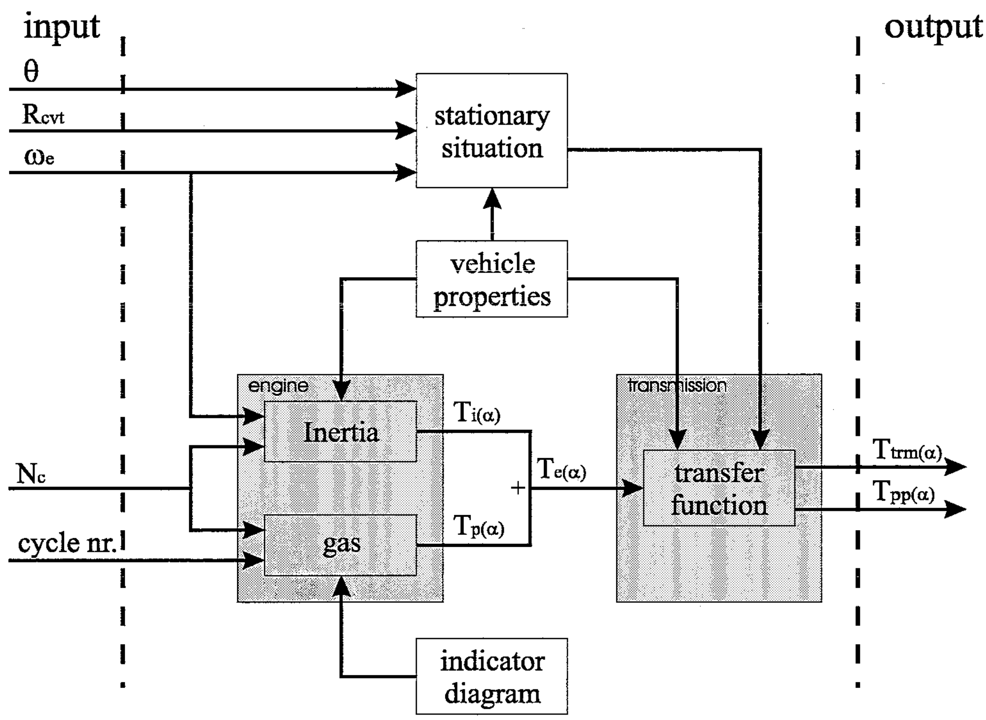

Figure A.12: Schematic representation of the MatLab model

be determined by using the three first input variables and the vehicle properties. The torque on the crankshaft ($T_p + T_i$) depends on the vehicle properties, the last three input variables and the indicator diagram. When the stationary situation is know, the transfer functions can be calculated. Finally, the MatLab program determines the torque on the transmission and variator.

A.3 Model results

Now a Matlab model is available, the torque acting on the transmission and variator can be determined in all occurring situations. The test rig has to be able to simulate the calculated torque pattern. When using the model, investigating the influence of the variables is easy:

CVT-ratio: High ratio causes high transfer magnitudes.

Engine speed: High speeds cause high inertia torque amplitudes and the low transfer magnitudes. The transfer magnitude shows an eigenfrequency at about 20 $[Hz]$

Nominal engine torque: High torques cause high gas pressure torque amplitudes. The highest engine torque (155 $[Nm]$) is reached at 3800 $[rpm]$.

Location in transmission: The transfer magnitude is for the transmission higher than for the variator.

Simulating high torque amplitudes and high frequencies are most demanding for the rig. Now it becomes clear what situations are most difficult to simulate. These situations determine the specifications of the rig.

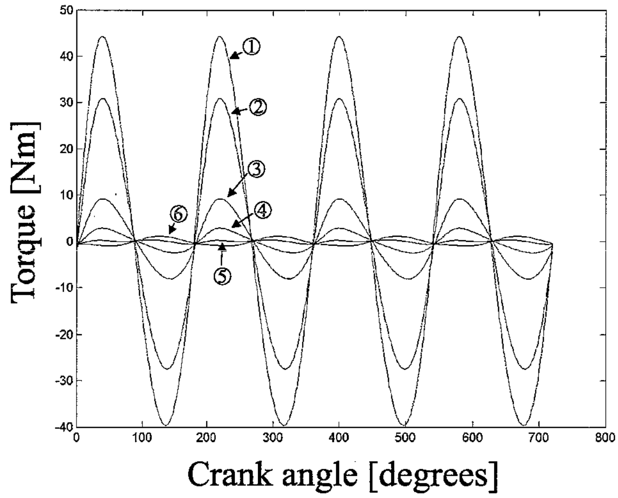

Figure A.13: Dynamic torque acting on the transmission at several speeds and maximum torque

Due to the influence of the different variables (especially nominal torque and motor speed), it is difficult to specify the demands concerning the dynamic torque behaviour. The most demanding situations occur if the transmission ratio is maximum (overdrive = 2.15) and the nominal engine torque is maximum. Figure A.13 shows the calculated dynamic part of the engine torque acting on the transmission at several speeds and maximum engine torque. Only the dynamic part is shown, the nominal torque is omitted. The operating conditions can be found in table A.3.

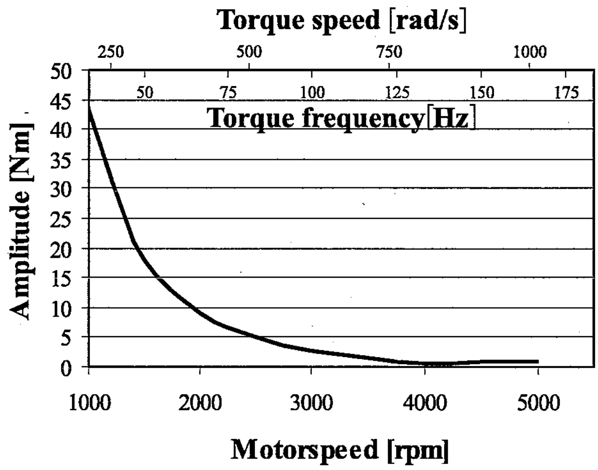

Figure A.14: Dynamic torque amplitudes.

Figure A.14 shows the dynamic torque amplitude depending on the engine speed (the corresponding torque frequency and speed are shown as well). The torque frequency is twice the engine frequency. Because the maximum engine speed is 6000 [rpm], the maximum torque frequency is 200 [Hz]. Figure A.14 is the starting point for designing the dynamic transmission test rig. The hydraulic motor has to be able to generate these torque amplitudes and corresponding frequencies.

Number	*Speed* $[rpm]$	*Nominal Torque* $[Nm]$	*Torque frequency* $[Hz]$	*Torque amplitude* $[Nm]$
1	1000	100	33	44
2	1194	115	40	31
3	2000	135	67	9
4	3000	150	100	2.8
5	4000	150	133	0.6
6	5000	145	167	1

Table A.3: Operating conditions of figure A.13 and A.14.

Appendix B

Introduction hydraulics

The basic fluid power system consists of a generator, a conductive and a motor part (figure B.1). The generator part (pump) transforms mechanical energy (translating or rotating) in hydraulic energy (flow with a certain pressure). The conductive part transports (pipes) and controls (e.g. valves) the hydraulic energy. The motor part converts the hydraulic energy in mechanical energy. A hydraulic medium is necessary for transporting the energy from the generator to the motor part. All parts together represent the hydraulic system. Sometimes, generator components can also be used as motor component and vice versa. For example a hydraulic cylinder can convert translating mechanical energy into hydraulic energy and hydraulic energy into translating mechanical energy. Figure B.1 shows a rotating pump and motor.

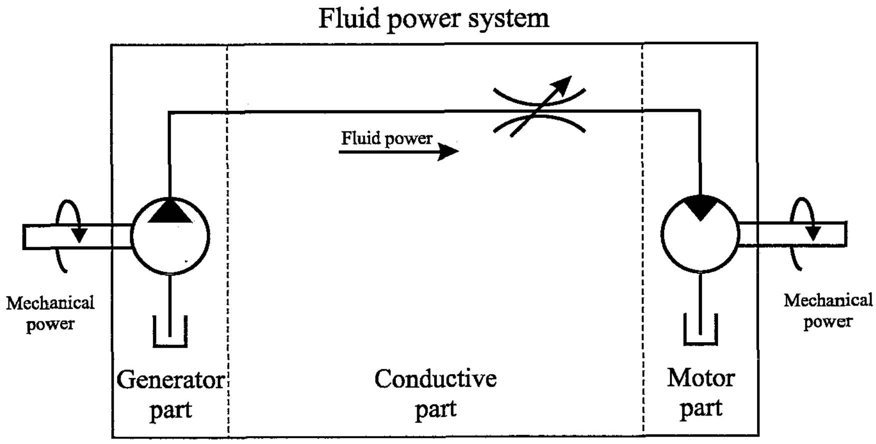

Figure B.1: Schematic representation fluid power system [21]

The generative part is already present in the fluid power laboratory. It consists of a several pumps. If necessary, some pumps can be combined for increasing the flow. For the motor part one of the available rotating fixed displacement motors will be taken. The used medium in the hydraulic system is oil. The oil flow corresponds to the motor speed, the pressure the motor torque. Appendix C shows the available pumps and motors in the Fluid Power Laboratory of the TU/e.

The operating point (pressure-flow combination) depends on the load characteristic and pump characteristic. The intersection between the characteristics (figure B.2) is the operating point of the hydraulic system. The maximum allowable pressure and flow are visualized by the gray area in figure. The pump characteristic can be changed. The pressure can be decreased by setting a pressure relief valve under the maximum allowable pump pressure (horizontal dotted line). The maximum flow can be decreased by changing the swash plate angle of the pump (vertical dotted line). The load characteristic line represents the pressure-flow relationship of the system. The characteristic depends on the system resistance R. More about changing the load characteristic in subsection 3.2.2. The dot in the figure represents the operating point.

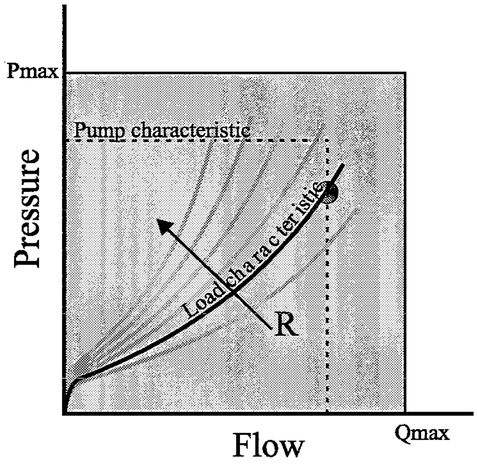

Figure B.2: Operating point prescribed by the pump and load characteristic

Appendix C

Hydraulic pumps and motors

Pump	*Maximum flow* $[L/min]$	*Maximum pressure* $[Bar]$	*Maximum power* $[Kw]$
A	55	350	32.1
B	90	210	31.5
C	90	210	31.5
D	100	10	1.7
F/G/H	30	210	10.5

Table C.1: Properties of pumps available at the power supply unit of the Fluid Power Laboratory of the TU/e

Motor type		*F11-10*	*F11-19*	*F11-39*	*F11-58*	*F11-110*	*F11-150*
Speed max.	$[rpm]$	10000	7500	5200	4500	3300	3000
Speed max. cont.	$[rpm]$	6800	5400	4200	3600	2800	2600
Speed max. feasible with pump B+C	$[rpm]$	10000	7500	4650	3090	1636	1200
Torque at 100 $[Bar]$	$[Nm]$	15.7	30.2	61.6	92.5	175	239
Torque max. feasible with pump B+C	$[Nm]$	32.9	63	129	194	367	501
Inertia $\cdot 10^{-4}$	$[kgm^2]$	4.4	12	45.1	59.1	160	400
TI-ratio $\cdot 10^4$	$[rad/s^2]$	7.4	5.3	2.9	3.3	2.3	1.25

Table C.2: Properties of motors available at the Fluid Power Laboratory of the TU/e

Appendix D

Bosch proportional directional valve

Datasheet of Bosch proportional directional control valve NG6, $[q_{nom}] = 4\ [L/min]$. From [24].

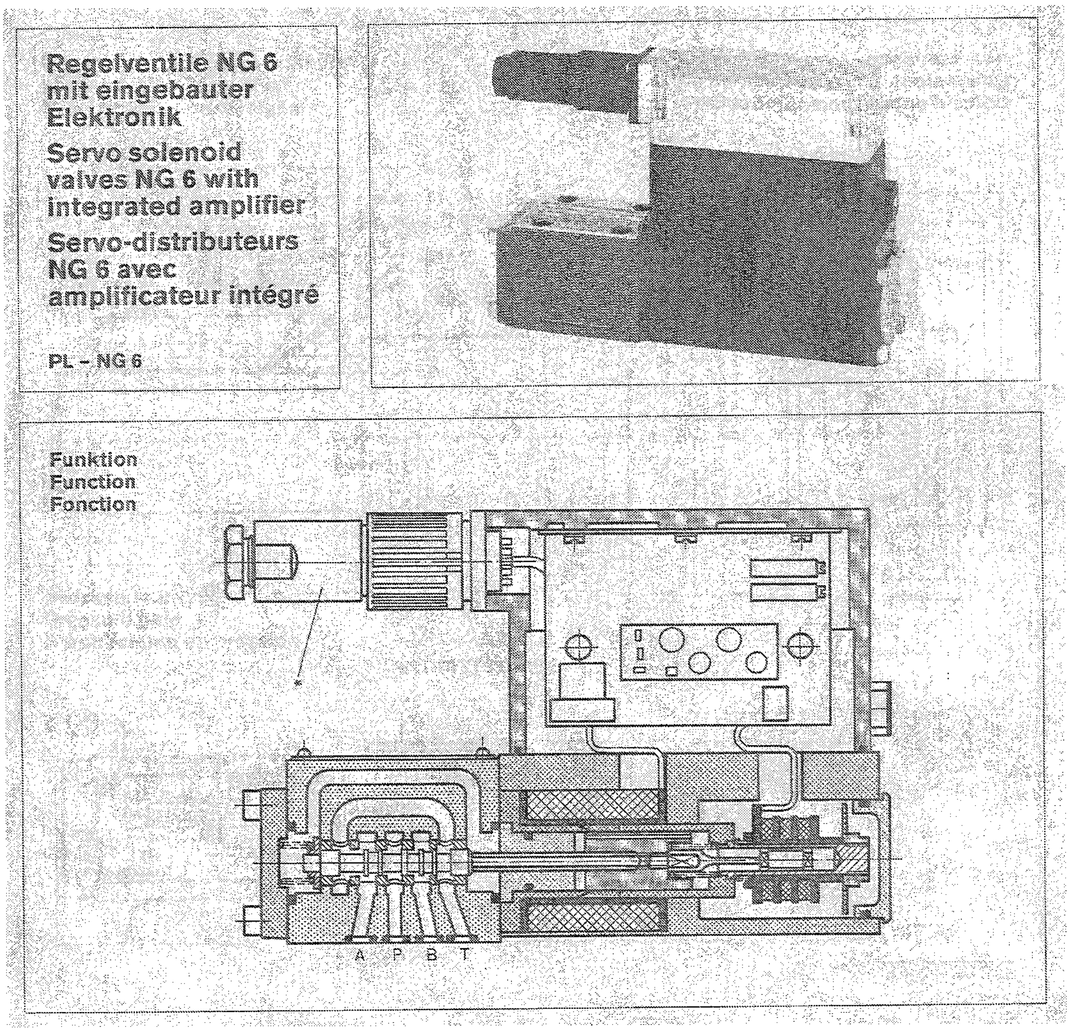

Fail-safe-position

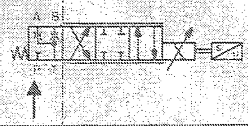	Lecköl Leakage ≈ Fuites internes	bei / at /pour 100 bar P–A 50 cm³/min P–B 70 cm³/min
	Durchfluß Flow-debit ≈ Débit	bei / at / pour Δp = 35 bar A–T 10 … 20 l/min B–T 7 … 20 l/min
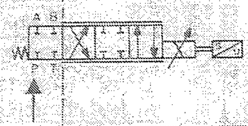	Lecköl Leakage ≈ Fuites internes	bei / at /pour 100 bar P–A 50 cm³/min P–B 70 cm³/min A–T 70 cm³/min B–T 50 cm³/min
Fail-safe	p = 0 bar → 7 m sec p = 100 bar → 10 m sec	Freigabe aus / Enable off / Deblocage arret $U_B \leq 18\,V=$

Characteristics				
General				
Construction	Spool valve, operated directly, with steel sleeve			
Actuation	Proportional solenoid with position control and position control of main stage with integrated amplifier			
Type of mounting	Subplate, hole pattern (ISO 4401)			
Assembly position	optional			
Ambient temperature	−20 … +50 °C			
Vibration Test condition	max. 25 g shaken in 3 dimensions (24 h)			
Hydraulic				
Pressure medium	Hydraulic oil as per DIN 51 524 … 535 Other fluids subject to approval			
Viscosity, recommended max. permitted	20 … 100 mm²/s 10 … 800 mm²/s			
Pressure medium temp.	−20 … +80 °C			
Filtration	Permissible contamination class of pressure medium as per NAS 1638		Achieved with filter βx = 75	
In line with operational reliability and service life	7		X = 5	
	8		10	
	9		15	
Flow direction	see symbol			
max. operating pressure (static) Ports P, A, B:	315 bar			
T:	250 bar			
Nominal flow [l/min] at Δp = 35 bar per notch*	4	12	24	40
Operating limits Δp [bar]	315	315	315	160
	315	315	250	100
Leakage [cm³/min] 100 bar	180	350	700	1100
Static/Dynamic				
Hysteresis	< 0.2 %			
Range of inversion	< 0.1 %			
Response time for signal change 0 … 100 %	< 10 ms			
Thermal drift	< 1 %, at ΔT = 40 °C			
Electrical characteristics	see page 65			

* Flow rate for other valves of Δp

$$Q_x = Q_{Nom} \cdot \sqrt{\frac{\Delta p_x}{35}}$$

Sinnbild Symbol Symbole	NG	Q_{nom} [l/min]		Funktion Function Fonction	P [VA]	[kg]	⊖
18 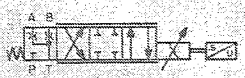	6	4	$\Delta p = 35$ bar	4/4-	30	2,7	0811404600
		12					0811404601
		24					0811404602
		40					0811404603
01 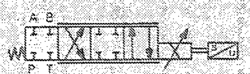		4					0811404610
		12					0811404611
		24					0811404612
		40					0811404613

Volumenstrom - Signalfunktion
Flow rate/signal function
Débit en fonction du signal

$Q = f(U_{D-E})$

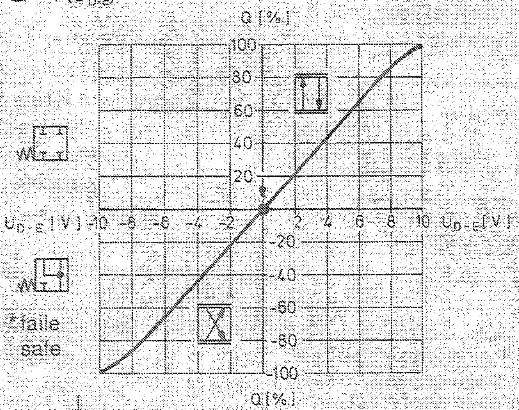

● kalibriert / calibrated / tarage ± 1%

*Fail safe:
Wenn Freigabe gesperrt
When enabling is not released
En cas de blocage

Bode-Diagramm
Bode diagram
Diagramme de Bode

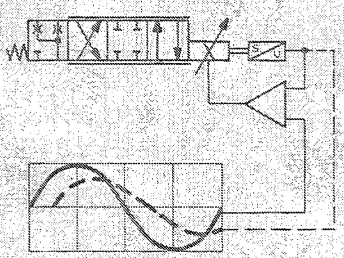

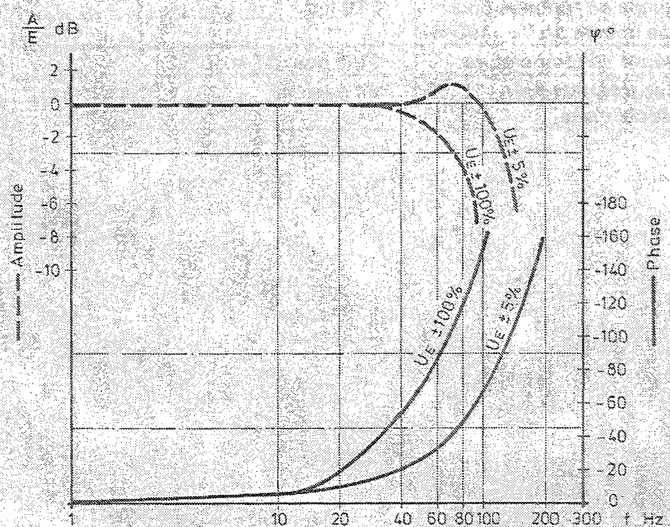

Appendix E

Simulink model

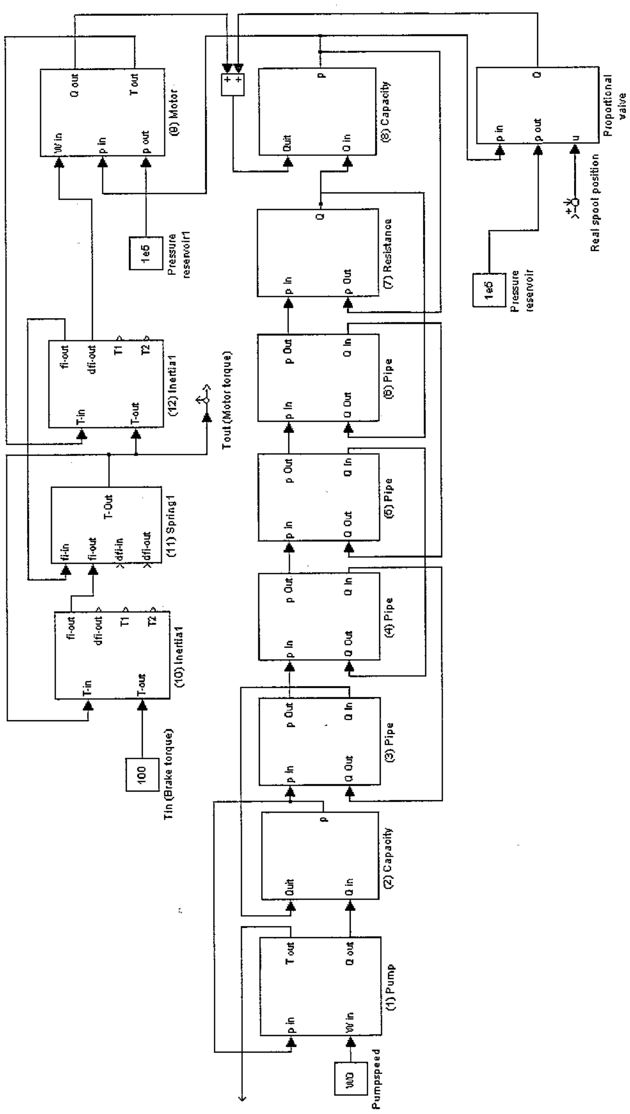

Figure E.1: Schematic overview of the data acquisition system

Appendix F

Data acquisition and control system

The data acquisition and control system has to be able to measure and log different variables. Furthermore, the system has to present the desired spool position to the valve electronics. Actually, the designed system is not a control system! It is an open loop system that prescribes the desired valve spool position to the valve electronics. The valve electronics control the spool position (feedback).

The complete data acquisition and control system consists of the following parts:

Sensors: The following variables will be measured by the sensors:

- Motor torque
- Oil pressure at the supply side of the motor
- Motor speed
- Valve spool position

Actuator: In this case, the spool position is the only actuated variable. Motorspeed and load will be adjusted manually.

TU/e DACS/1: The DACS (**D**ata **A**cquisition and **C**ontrol **S**ystem) acts as the interface between the digital laptop and the analog sensors / actuator. Only the a analog - digital converters are used.

Voltage dividers / amplifiers: The input / output voltages of sensor, actuators and the TU/e DACS system use specific ranges. Because the ranges don't always correspond, some voltages have to be decreased by voltage dividers, others have to increased by amplifiers.

Laptop with Simulink software: The heart of the data acquisition system is the laptop, equipped with Simulink Matlab 6.1 software.

Figure F.1 shows a schematic representation of complete system. This appendix first describes the measured and controlled variables and the used sensors and actuators. Then is discussed what system is used for processing the data.

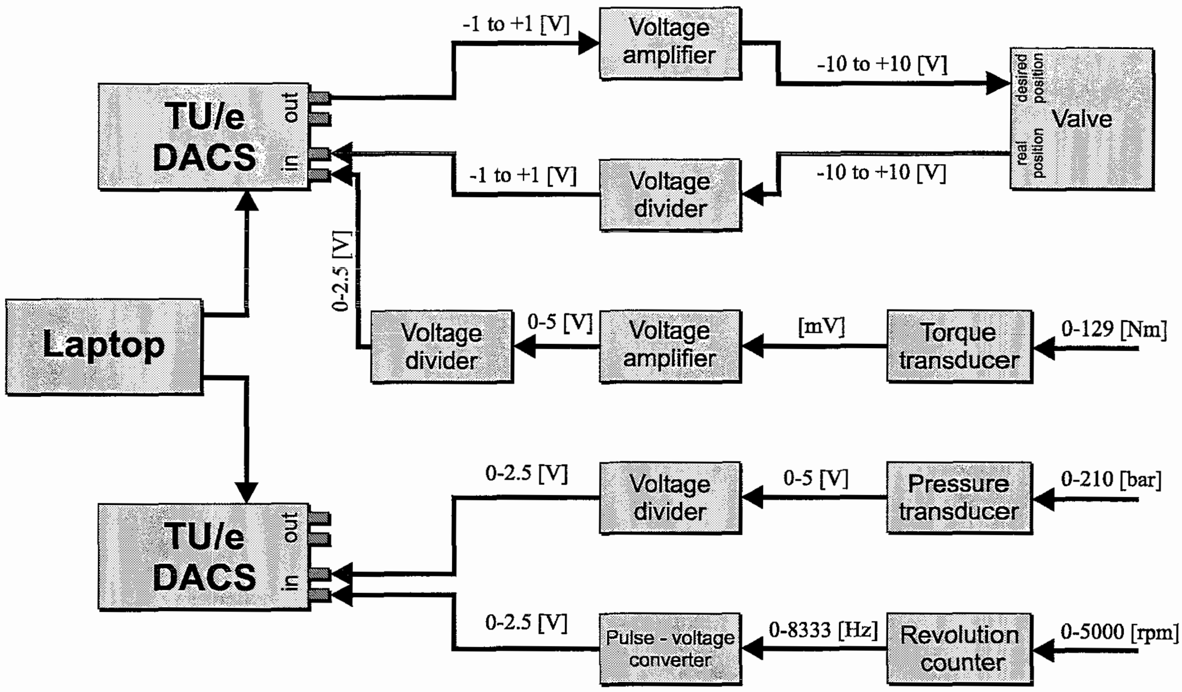

Figure F.1: Schematic overview of the data acquisition system

F.0.1 Measured and controlled parameters

The sensors and actuator will be connected to the TU/e DACS system. This system is able to measure input signals and deliver output signals in a range of - 2.5 $[V]$ and + 2.5 $[V]$.

Torque

The torque to be delivered by the hydraulic motor is an important variable of the test rig. The rig is developed particularly for generating dynamic torques. For measurement, a torque transducer is used. The transducer consists of a shaft that is mounted between the motor and the flywheel. The transducer is a rotating, torque transmitting part of the rig. The actual measuring part consists strain gauges mounted on the shaft. The resistance is related to the torsion, and so to the torque acting on the shaft. The change of resistance is measured by using a full Wheatstone bridge. The signal is transmitted to the fixed world using slide contacts. Because of the voltages differences in the Wheatstone bridge being so small, an amplifier is necessary. A voltage divider decreases the presented voltage range so it can be presented to the TU/e DACS (maximum 2.5 $[V]$). Some transducer properties:

Type:	HBM Torque transducer T1A	
Nominal torque:	500	$[Nm]$
Limit load	750	$[Nm]$
Max. speed of rotation:	6000	$[rpm]$
Inertia:	0.001	$[kgm^2]$
Torsional stiffness:	2.76x10^4	$[Nm/rad]$

The data sheet of the torque transducer can be found in appendix H. The nominal torque of the transducer is 500 $[Nm]$. A transducer of the same type with a nominal torque of 200 $[Nm]$ was available as well. Although the maximum motor torque is 129 $[Nm]$, the 500 $[Nm]$ version has been chosen instead of the 200 $[Nm]$ version. Reason for this choice is the presence of the flywheel, resulting in a large amount of energy stored in the test rig. In case of malfunctioning, it might be possible that the flywheel overloads the torque transducer. In order to prevent overload, a larger transducer has been chosen.

The data acquisition system has to convert the measured voltage to the corresponding torque. The voltage-torque relationship had to be determined first. The torque transducer had to be calibrated. The output voltage of the amplifier were measured at several set values of the torque. The left picture of figure F.2 shows the result of this calibration.

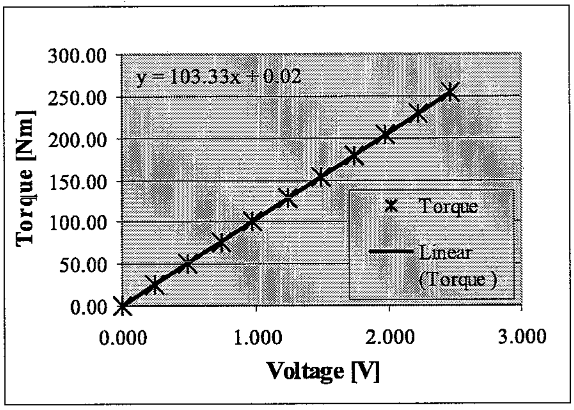

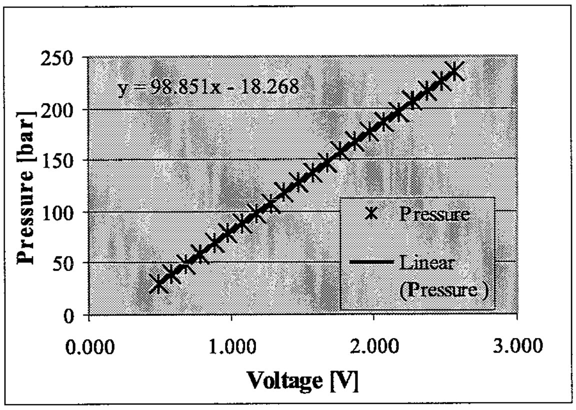

Figure F.2: Calibration. Left: torque transducer Right: pressure transducer

The crosses in the graph represent the measured values, the thick line is the best fit line through the measured values. The calibration was started measuring the lowest torque and was ended with the highest torque. Because the crosses are very close to the line, the voltage is assumed linear with the torque. The data acquisition system uses the next formula for determining the torque:

$$T = 103.33V + 0.02 \tag{F.1}$$

where V $[Volt]$ represents the measured voltage and T $[Nm]$ is the corresponding torque on the transducer. Another calibration was done starting with the highest torque, ending with the lowest torque. The same linearity as formula F.1 was found so there is no hysteresis.

Pressure

A pressure transducer is mounted on the pipe for measuring the pressure at the supply side of the motor. If necessary the effect of the proportional valve on the pressure, and the effect of the pressure on the torque can be investigated. Furthermore, during the tests the pressure is displayed constantly for having a general overview of the situation.
The pressure transducer contains a membrane that is bend by the oil pressure. This bend is measured by strain gauges. Like the torque transducer, a full Wheatstone bridge is used.

The amplifier is integrated in the transducer. Like the torque transducer, a voltage divider is applied. Some pressure transducer properties:

Type:	Transamerica BHL-3022-05 pressure transducer	
Nominal pressure:	250	$[Bar]$
Proof pressure:	500	$[Bar]$

The transducer was calibrated to determine the relationship between the presented voltage and the measured pressure. The voltage was measured at set values of the pressures. The left picture of figure F.2 shows the result. Again, the relation between the voltage and pressure may be represented by as linear relationship:

$$p = 98.85V - 18.27 \tag{F.2}$$

where V $[Volt]$ represents the resulting voltage and p $[Bar]$ the corresponding pressure.

Motor speed

When testing the performance of the rig, knowledge of the motor speed is not an important issue. Due to the high stiffness of the torque transducer in combination with the high torque frequency the speed will almost be constant. Furthermore, the motorspeed doesn't influence the transfer function. Like the pressure, the motorspeed is displayed constantly by the data acquisition system.

The motor speed is measured by a sensor that uses a light detecting element. The sensor generates a voltage pulse when a light beam reaches the element. The light beam is interrupted by a perforated disc that is mounted on the motor shaft. One pulse represents 1/100 rotation of the shaft so 1 $[Hz]$ = 0.6 $[rpm]$. Because the data acquisition system can only measure voltages, a converter is used to convert the frequency to a voltage. The converter ratio is 3333.3 $[Hz/V]$ = 2000 $[rpm/V]$. Because the maximum input voltage for the data acquisition system is 2.5 $[V]$, the maximum measurable speed is 5000 $[rpm]$.

Spool position

The spool position of the proportional valve is an important parameter because the valve generates the dynamic torque. The valve electronics have an input and an output. On the input, the desired spool position is presented by the data acquisition / control system. The output presents the real spool position measured by the internal measuring system. For the valve input and output, the voltage range -10 to +10 $[V]$ corresponds to the spool position $[u]$ range -1 to +1 [-]. Because the data acquisition / control system can only measure and present voltages between -2.5 and +2.5 $[V]$, a voltage amplifier (10x) and a divider (1/10) are applied. Now, presented voltage from and to the data acquisition / control system (-1 to +1 $[V]$) correspond to the spool position (u = -1 to +1 $[-]$).

F.0.2 Data processing

Two TU/e-DACS/1 systems and a laptop were used for data processing.

TU/e DACS system

The DACS (**D**ata **A**cquisition and **C**ontrol **S**ystem) systems acts as the interface between the laptop and the sensors / actuator. Each of them contains two AD- and two DA-converters. The AD-converters digitize the analogous signal and present it to the computer. The digital signal presented by the laptop prescribing the desired spool position is converted by the DACS system into an analogue signal. The voltage range of the analogue in- and output signals is bipolar (-2.5 to +2.5 $[V]$). Because four sensor signals had to be logged and one actuator had to be activated, two DACS systems were necessary. These systems were connected to the laptop by means of PCMCIA connections.

All input signals of a single DACS system are sampled at the same moment. However, it is not sure that both DACS systems measure exactly at the same time. That's why it is important that sensors of which the signals have to be compared (e.g. for the purpose of determining phase shift) are connected to the same DACS system.

Laptop

The laptop is the heart of the data acquisition / control system. A special Matlab Simulink program was developed. This program is able to log the four sensor signals and display them real-time. The desired valve spool position can be a logged, displayed and adjusted real time as well. All kind of signals can be presented to the input of the proportional valve electronics (e.g. sine or block shaped functions). Figure F.3 shows the Simulink program for real time operation.
The sample rate and measuring time are the most important adjustable parameters. The maximum sample rate depends on the laptop performance and not on the DACS system. The laptop is able to operate at a maximum frequency of 1600 $[Hz]$. The maximum sine frequency to be presented and to be measured is 200 $[Hz]$. In combination with the maximum sample rate this results in 8 samples per sinus. When performing a Fourier analysis, frequencies up to 800 $[Hz]$ can be analyzed. The measuring system isn't oversized but should suffice.

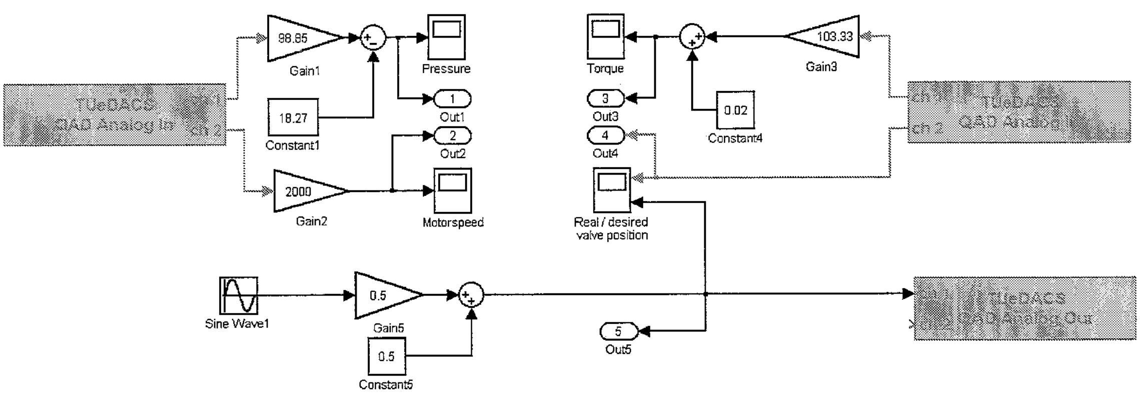

Figure F.3: Simulink model for operating the rig

Appendix G

Dynamic modeling of elementary hydraulic components

Hydraulic systems can be considered as a collection of interconnected basic elements. Section 3.2.3 describes the basic way of modeling hydraulic systems. For better understanding, the elements should be described in the $j\omega$ domain in stead of the time domain in case of dynamic systems. The behaviour of the elements depends on the frequency. The basic relationship between the pressure and flow rate is:

$$p = X \cdot q \tag{G.1}$$

X represents the impedance of the hydraulic system. The impedance can be a composite term of resistance, capacity and inductance. The hydraulic system will present a different impedance value for each frequency of excitation. The dynamic relationships of the basic elements can be obtained by replacing the operator $\frac{d}{dt}$ by $j\omega$ in the hydraulic relationships (formula 3.5, 3.6 and 3.7).

Fluid inductance $\mathbf{X}_I$: The fluid inductance is a measure of inertia forces developed when a fluid is accelerated in a pipe. The impedance relationship of the inductance:

$$p = I\frac{dq}{dt}$$

under dynamic conditions:

$$p = Ij\omega q = X_I q \tag{G.2}$$

$X_I = Ij\omega$ is called the impedance of the inductance. Due to the imaginary impedance, the flow lags the pressure 90^o.

Fluid capacity $\mathbf{X}_C$: The hydraulic capacity is a measure of energy storage. The storage can take the form of compression of the liquid or elasticity of piping walls. The impedance relationship of the capacity:

$$q = C\frac{dp}{dt}$$

under dynamic conditions:

$$q = Cj\omega p$$

in the general form:

$$p = \frac{1}{Cj\omega}q = X_C q \tag{G.3}$$

Where $X_C = \frac{1}{Cj\omega} = \frac{-j}{C\omega}$ is called the impedance of the capacity. Due to the imaginary impedance, the pressure lags the flow 90^o.

Fluid resistance $\mathbf{X}_R$: The fluid resistance will only exhibit linear characteristics under laminar flow conditions.

$$p = Rq$$

under dynamic conditions:

$$p = X_R q \tag{G.4}$$

X_R is called the impedance of the resistance. In contrast with the impedance of the inductance and capacity, the impedance of the resistance is not complex and consequently independent of the frequency.

The individual fluid elements have distinct impedance / frequency characteristics as summarized in figure G.1.

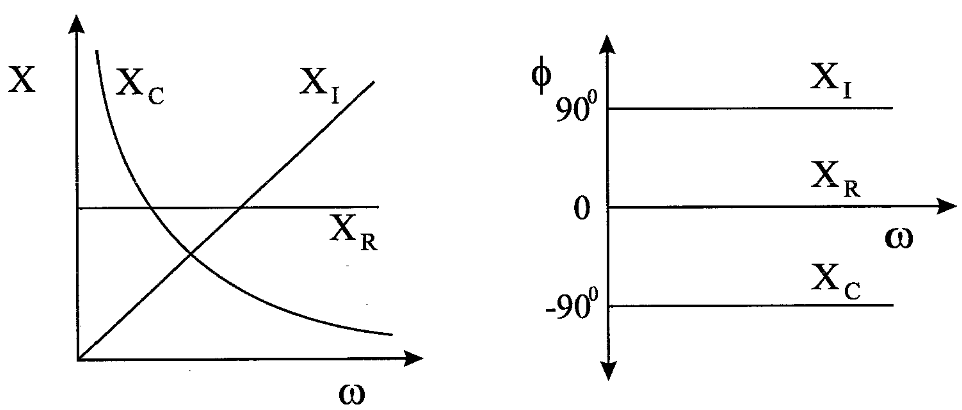

Figure G.1: Impedance characteristics of basic elements [16]

Appendix H

HBM Torque transducer T1A

Datasheet of HBM torque transducer T1A. Nominal torque = 500 $[Nm]$. From [23].

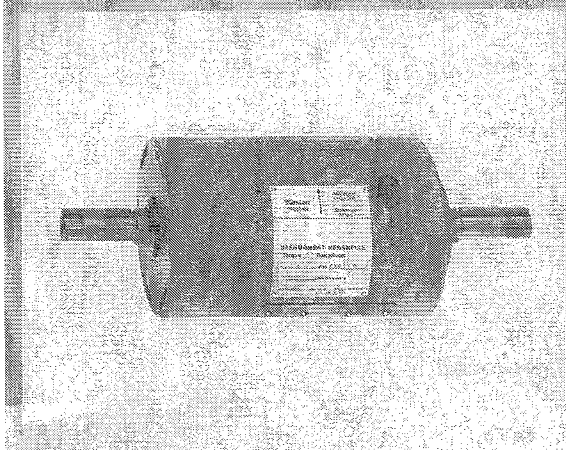

- Measurements without friction due to bearings and slip-rings
- Torque transfer via stub shafts with keys
- Slip-ring brushes which can be raised prevent brush abrasion and wear in the intervals between measurements
- EEx ib IIC T4 version available
- Can be used on rotating and stationary objects
- 0.1 accuracy class
- Curved-tooth couplings available, tried and tested for the torque transducers.

Mechanical values

Nominal torque	Limit load [Nm]	Breakage limit load [Nm]	Max. vibration amplitude 3) (peak - peak)	Max. permissible: Speed of rotation [rpm]	Max. permissible: bending moment 2) [Nm]	Max. permissible: lateral force 2) [kN]	Max. permissible: axial force 2) [kN]	Mass moment of inertia [kgm²]	Torsion angle at M_N [Degrees]	Torsional stiffness C_T [Nm/rad]
50 Nm	75	150	35 Nm	6000	55	0.17	9.8	0.0006	0.9	3.30×10^3
100 Nm	150	300	70 Nm	6000	45	0.14	8.2	0.0006	0.7	8.66×10^3
200 Nm	300	600	140 Nm	6000	20	0.08	9	0.001	1	1.18×10^4
500 Nm	750	1500	350 Nm	6000	55	0.21	16.5	0.001	1.1	2.76×10^4
1 kNm	1500	3000	0.7 kNm	6000	105	0.38	25	0.0022	0.9	6.75×10^4
2 kNm	3000	6000	1.4 kNm	6000	220	0.7	42	0.0037	1.1	1.10×10^5
5 kNm	7500	15000	3.5 kNm	4000	550	1.4	88	0.018	0.9	3.31×10^5

2) Each of the extraneous loadings (bending moment, lateral or longitudinal forces, exeeding of the nominal torque) is only permissible up to the stated limit when none of the others can arise. Otherwise the limits must be reduced. (If 30% each of the bending moment and the lateral force limits araise, then only up to 40% of the longitudinal force limit is permissible with the nominal torque not being exceeded). Loads of this nature can have an effect on the measurement results equivalent to <1% of the nominal torque.

3) The nominal torque must not be exceeded.

Dimensions (in mm, 1mm = 0.03937inches)

Technical Data

Type		T1A
Accuracy class		0.1
Nominal torque (M_N)	Nm kNm	50; 100; 200; 500 1; 2; 5
Nominal sensitivity (nominal output signal at nominal tor-que)	mV/V	1.5
Sensitivity tolerance (deviation of the actual frequency range from the nominal signal range at M_N)	%	≤±0.1
Temperature effect on the sensitivity per 10K at nominal temperature range, related to the actual value	%	≤±0.1
Temperature effect on zero signal per 10K at nominal temp. range, related to the nom. sensitivity	%	≤±0.05
Linearity deviation including hysteresis related, to the nominal sensitivity	%	≤±0.1
Relative standard deviation of reproducibility according to DIN 1319	%	≤±0.05
Nominal range of excitation voltage	V	0.5...12
Maximum permissible excitation voltage	V	18
Input resistance at reference temperature (between connections 2 and 3)	Ω	350±2
Output resistance at reference temperatur (between connections 1 and 4)	Ω	350±1.5
Mechanical shock, degree of precision to IEC 68-2-27-1987		
Number		1000
Duration	ms	3
Acceleration	m/s^2	500
Vibration stress test, degree of precision to IEC 68-2-6-1982		
Frequency range	Hz	5...65
Duration	h	1.5
Acceleration	m/s^2	50
Reference temperature	°C [°F]	+23 [+73]
Nominal temperature range[1)]	°C [°F]	+10...+60 [+50...+140]
Service temperature range[1)]	°C [°F]	-10...+60 [+14...+140]
Storage temperature range	°C [°F]	-50...+70 [-58...+158]

[1)] In continuous operation the bearings warm up due to friction. This bearing heating must be taken into account when considering the ambient temperature and determined as follows:

For torque transducers with a nominal speed of
4000 rpm: 60 – speed in rpm x 0.005 = max. ambient temperature in °C
6000 rpm: 60 – speed in rpm x 0.0033 = max. ambient temperature in °C

Appendix I

Moog servovalve D765

Moog servovalve D765. Nominal flow = 38 [L/min]. From [22].